MAINTAINENCE OF PRIMARY HUMAN HEPATOCYTE FUNCTION *IN VITRO* BY EXTRACELLULAR MATRIX SCAFFOLDS

by

Tiffany L. Sellaro

Bachelor of Science in Mechanical Engineering, The George Washington University, 1999

Master of Science in Bioengineering, University of Pittsburgh, 2003

Submitted to the Graduate Faculty of the

Swanson School of Engineering in partial fulfillment

of the requirements for the degree of

Doctor of Philosophy

University of Pittsburgh

2008

UNIVERSITY OF PITTSBURGH

SWANSON SCHOOL OF ENGINEERING

This dissertation was presented

by

Tiffany L. Sellaro

It was defended on

April 30, 2008

and approved by

Donna Beer-Stolz, PhD, Department of Cell Biology and Physiology

Jorge Gerlach, MD, PhD, Department of Bioengineering

Stephen Strom, PhD, Department of Pathology

John F. Patzer II, PhD, Department of Bioengineering

Dissertation Director: Stephen F. Badylak, DVM, MD, PhD, Department of Surgery

MAINTAINENCE OF PRIMARY HUMAN HEPATOCYTE FUNCTIONS *IN VITRO* BY EXTRACELLULAR MATRIX SCAFFOLDS

Tiffany L. Sellaro, Ph.D.

University of Pittsburgh, 2008

Liver disease is a leading cause of mortality in the United States. Tissue engineering and regenerative medicine (TE&RM) approaches to treating liver disease have the potential to provide temporary support with biohybrid liver-assist devices or long term therapy by replacing the diseased liver with functional constructs. A rate-limiting step for TE&RM strategies has been the loss of hepatocyte-specific functions after hepatocytes are isolated from their highly specialized *in vivo* microenvironment and placed in *in vitro* culture systems. The identification of a biologic substrate that can maintain a functional hepatocyte differentiation profile during *in vitro* culture would advance potential TE&RM therapeutic strategies.

The present study is predicated upon the hypothesis that the substrate upon which hepatocytes are seeded is a critical determinant of cell phenotype and function. Biologic scaffolds composed of extracellular matrix (ECM) derived from mammalian organs have been used to maintain cell phenotype *in vitro*. Two studies were performed to evaluate the ability of ECM scaffolds to maintain primary human hepatocyte (PHH) phenotype *in vitro*. The first study evaluated the effect of ECM scaffolds derived from porcine liver (PLECM) and human liver (HLECM) upon maintainence of PHH specific functions *in vitro*. Cytochrome P450 activity and albumin secretion were used as indicators of hepatocyte functionality. No differences in hepatoycte-specific functions were measured when comparing PHH cultured with PLECM and HLECM. From a clinical perspective, the results are appealing because of the limited

availability of human liver tissue compared to porcine liver tissue for the manufacture of ECM scaffolds.

The second study cultured PHH between two layers of PLECM and compared with Matrigel double gel cultures and adsorbed type-1 collagen. Albumin secretion, hepatic transport activity and ammonia metabolism were used as markers of hepatocyte functionality. PHH cultured between two layers of porcine liver ECM had significantly higher levels of albumin secretion, hepatic transport activity, and ammonia metabolism compared to PHH cultured on collagen.

TABLE OF CONTENTS

LIST OF TABLES

LIST OF FIGURES

PREFACE

I am grateful to countless individuals for their support during the completion of my Dissertation. To Dr. Badylak, I am forever grateful for sharing your vision and mentorship in the field of tissue engineering and regenerative medicine. Dr. Badylak provided a world class laboratory that enabled endless opportunities for those willing to take the challenge.

The completion of my dissertation would not have been possible without the generosity of Dr. Strom and his laboratory. I was blessed to work closely with such a talented and amazing group of researchers. My heartfelt gratitude goes out to Dr. Strom and the members of his laboratory: Ken Dorko, Dr. Ewa Ellis, Dr. Fabio Marongiu, Dr. Aarati Ranade, and Dr. Roberto Gramignoli. Thank you for your support and mentorship and most importantly, your friendship. Thank you for filling my days at the bench with much laughter and sunshine.

A huge thank you goes out to my other committee members Dr. Beer-Stolz, Dr. Gerlach and Dr. Patzer. I appreciate all of your time and efforts on behalf of this dissertation. I have benefitted from your instruction and comments and each of you have provided a unique perspective for my work.

I would like to thank Dr. Harvey Borovetz for his guidance and support. The Department of Bioengineering could not want a better chairperson who truly cares for each student. A huge thank you is in order for other members of the Department of Bioengineering, including Joan Williamson and Lynette Spataro.

To all the members of the Badylak Laboratory – past and present – who I have had the privilege of working with: thank you for all of your help and support. Thank you to Janet Reing for your mentorship and friendship. Thank you to Renee Atkinson for your friendship and perpetually smiling face.

Thank you to all of my amazing friends, who have touched my life and fed my spirit during difficult times: Dr. Joie Marhefka, Dr. Susan Moore, Dr. Helder Marcal and Caroline Evans.

I could not have completed this work without the love, intellectual encouragement, and support of my family: Carole, Lou and Ashley. Thank you for believing that I could achieve anything that I set my mind to. To my mother and father, who taught me to never stop trying to connect with my dreams.

ACRONYMS

6β-(OH)	6β-Hydroxylase
BAL	Biohybrid Artificial Liver
b-FGF	Basic Fibroblast Growth Factor
β-NF	β-Napthaflavone
BSEP	Bile Salt Export Pump
Cx32	Connexin 32
CYP	Cytochrome P450
DMSO	Dimethylsulfoxide
ECM	Extracellular Matrix
EGF	Epidermal Growth Factor
EROD	Ethoxyresorufin-O-Deethylation
HGF	Hepatocyte Growth Factor
HLECM	Human-derived Liver Extracellular Matrix
HMM	Hepatocyte Maintainence Media
LBLM	Human Liver-Derived Basement Membrane Matrix
MG	Matrigel™
NPC	Non-Parenchymal Cells
NTCP	Sodium Taurocholate Cotransporting Polypeptide

PHH	Primary Human Hepatocytes
PLECM	Porcine-derived Liver Extracellular Matrix
RIF	Rifampicin
RT-PCR	Reverse Transcriptase Polymerase Chain Reaction
SEC	Sinusoidal Endothelial Cell
SEM	Scanning Electron Microscopy
SIS-ECM	Small Intestinal Submucosa Extracellular Matrix Scaffold
TE	Testosterone
TC	Taurocholate
TGF-β	Transforming Growth Factor
UBM-ECM	Urinary Bladder Extracellular Matrix Scaffold
VEGF	Vascular Endothelial Growth Factor

1.0 INTRODUCTION

1.1 THE MAMMALIAN LIVER

The liver is the largest internal organ and is responsible for over 500 functions essential for life. Hepatocytes are the major cells of the liver. The non-parenchymal cells of the liver include sinusoidal endothelial cells, stellate cells, Ito cells, and Kuppfer cells. The NPCs work in concert with hepatocytes to maintain many life-essential functions, including the following: synthesizing of a myriad of proteins essential for the blood coagulation cascade and the immune response; regulating the levels of many chemicals found in the bloodstream; storing and catabolizing glycogen; metabolizing drugs, toxins, hemoglobin, and ammonia; aiding the body in fat digestion by production of bile; storing reserves of vitamins, minerals, and nutrients; and detoxifying blood of poisons and wastes.

1.2 HEPATOCYTES

Hepatocytes are the parenchymal cells of the liver and account for approximately 80% of all liver cells [1, 2]. Hepatocytes perform hundreds of functions essential for liver function, which include but are not limited to:

- Metabolize drugs and steroids by cytochrome P450s. CYP3A4 & CYP1A comprise 60-90% of the total CYP proteins in human liver and measurement of basal and induced levels of drug metabolizing enzymes indicate maintainence of hepatocyte functionality
- Synthesize many important proteins, including albumin
- Detoxify ammonia from the blood by metabolizing ammonia into urea for excretion
- Production of bile salts (sodium taurocholate)

1.3 HEPATIC EXTRACELLULAR MATRIX

ECM proteins are distributed in varying amounts throughout the normal liver. ECM proteins in the liver include the collagens (mainly type-I collagen and minor quantities of types III, IV, V, and VI), fibronectin, vitronectin, tenascin, elastin, proteoglycans, ECM-bound growth factors, and small amounts of laminin [3].

1.4 LIVER DISEASE

Liver disease is the eleventh leading cause of mortality and results in approximately 30,000 deaths per year in the United States [4]. Approximately 17,000 patients are on the liver transplant waiting list, and about 10,000 patients are added to the list each year, with ~2,500 deaths per year [5]. Chronic liver diseases include metabolic liver disease, alcoholic liver disease, hepatitis, portal hypertension, hemachromatosis, cholestasis, steatosis, Gaucher disease, liver cancer, and primary biliary cirrhosis. Chronic liver diseases account for approximately 80% of the deaths because the patients are too ill to tolerate liver transplantation. Acute liver failure due to ischemia/reperfusion injury, idiosyncratic drug reaction, acetaminophen poisoning, alcohol poisoning, and viral hepatitis represents the remaining 20% of the deaths [6].

1.5 LIVER DISEASE THERAPIES

Allogeneic liver transplantation is the “gold standard” treatment of choice for patients with end-stage liver disease but is limited by its high cost and the severe donor organ shortage. Both xenotransplantation and hepatocyte transplantation represent alternative therapies but the technologies have had limited clinical success [7, 8]. Xenotransplantation could provide a limitless supply of donor organs; however, previous attempts have resulted in hyperacute rejection and death [9]. Hepatocyte transplantation offers much promise for correcting non-emergency conditions such as genetic defects of the liver [10, 11] but several stumbling blocks have limited its clinical success. Low efficiency of engraftment, long-term immunosuppression from the use of allogeneic cells, and a lag time of 48 hours for the transplanted hepatocytes to

become functional *in vivo*, which is too long in a rapidly deteriorating patient, have hindered the advancement of hepatocyte transplantation.

Biohybrid artificial liver (BAL) provides temporary support for patients waiting for an allogeneic liver transplant and since the liver can regenerate, the temporary support provided by BAL may allow time for the liver to regenerate. However, the lack of reliable cell source combined with the inability of BAL to maintain the functionality of hepatocytes for long periods of time have hindered its clinical success.

2.0 TISSUE ENGINEERING AND REGENERATIVE MEDICINE

Tissue engineering and regenerative medicine approaches to treating liver disease may alleviate the crisis by providing temporary liver support with biohybrid artificial liver-assist devices or by replacing the function of the diseased liver with tissue-engineered constructs utilizing a combination of cells, scaffolds and bioactive factors that are implanted into the body [12, 13]. Additionally, tissue engineered scaffolds that maintain hepatocyte functionality *in vitro* could be used to develop *in vitro* models to study drug metabolism or the pathophysiology of liver disease [14, 15]

A common regenerative medicine strategy for tissue and organ reconstruction involves the seeding of a scaffold with cells harvested from the tissues or organs of interest, followed by eventual placement of the cell-scaffold combination to the intended *in vivo* location. Cells that are isolated from their native microenvironment dedifferentiate and the rate of dedifferentiation is dependent on the microenvironment, of which the substrate or scaffold is of paramount importance [16, 17]. Loss of *in vivo* microenvironmental signals such as paracrine interactions (cell-cell), physical-chemical factors (i.e. oxygen tension, metabolites), mechanical stimuli (blood flow), and cell-extracellular matrix interactions result in dedifferentiation and the effects of dedifferentiation following seeding upon various scaffolds of the constructs are largely unknown but logically would detract from optimal function [18].

The development of therapies to treat liver disease is an intense area of research that has spanned several decades but the progress has been limited. The success of tissue engineering and regenerative medicine therapies depend upon the ability to provide a microenvironment that supports the viability of hepatocytes with maintainence of liver-specific functions both *in vitro* and *in vivo*. As the field of tissue engineering and regenerative medicine moves toward the replacement of more complex tissues and three-dimensional organs, such as the liver or heart, it is likely that more specialized scaffolds will be needed to support multiple, functional cell phenotypes in site-specific, unique three-dimensional arrangements.

A myriad of scaffolds have been used to culture hepatocytes *in vitro* with the ultimate goal of maintaining the functionality and viability of a large mass of isolated hepatocytes for more than several weeks. Substrates used for hepatoycte culture range from synthetic polymers (e.g. polylactic acid, polyglycolic acid, and poly(ethylene glycol) (PEG) hydrogels) [13, 14, 19-21] to naturally-derived materials (e.g. collagen, alginate, chitosan) [22-25] and complex extracellular matrix (ECM) substrata (e.g. Matrigel (MG) or ECM derived from rat or porcine liver) [26-28]. The ideal scaffold upon which the cells are seeded or to which they are recruited must sustain the biological processes of the cells, including cell attachment, migration, differentiation, and self-assembly of groups of cells. Further, the scaffold material must have physical and material properties that will support clinical utility (e.g., surgical manipulation, suture retention strength, and local tissue mechanical forces) and ideally would degrade at an appropriate rate while new matrix is deposited and tissue remodeling occurs.

2.1 USE OF BIOLOGIC EXTRACELLULAR MATRIX SCAFFOLDS FOR TISSUE ENGINEERING AND REGENERATIVE MEDICINE APPLICATIONS

Biologic ECM scaffolds are typically allogeneic or xenogeneic in origin and are derived from a variety of tissues and organs, including but not limited to the following: pericardium [29], fascia lata [30], dermis [31], small intestine [32, 33], and urinary bladder [32, 33]. ECM scaffolds have been used as for the reconstruction of numerous tissue types in both preclinical animal studies and in human clinical applications [32]. Further, acellular ECM scaffolds have also been evaluated for their ability to maintain cell phenotype *in vitro* [28, 34-37]. Compared to the use of individual components of ECM, such as type-1 collagen or laminin, studies have shown that intact ECM provides a more favorable substrate for the growth and differentiation of various cell types [28, 34, 38-40]. Squamous epithelial, fibroblastic (Swiss 3T3), glandular epithelial (adenocarcinoma), and smooth muscle-like (urinary bladder) cells cultured on SIS-ECM maintained superior expression of tissue-specific phenotype compared to those same cells cultured on plastic, Vitrogen, or Matrigel [39]. In a study that utilized human islets, SIS enhanced the functions of the islets *in vitro* compared to islets cultured on standard islet substrates [40]. Lin et. al., recently compared hepatocytes cultured on LECM to the well characterized hepatocyte culture models, double gel ("sandwich") cultures and adsorbed type-1 collagen [28]. Hepatocytes survived up to 45 days on LECM and several liver-specific functions such as albumin synthesis, urea production, and P-450 IA1 activity were significantly greater compared to the growth and metabolism of cells cultured on collagen.

Our laboratory recently showed the origin or anatomic location from which the ECM scaffold is derived can affect cell phenotype after only 24 hours [34]. Hepatic sinusoidal endothelial cells (SEC) maintained their differentiated state the longest when cultured on ECM

derived from the liver compared to ECM derived from either the urinary bladder (UBM-ECM) or the small intestine (SIS-ECM). The SEC maintained fenestrations and expression of SE-1, a marker specific to differentiated hepatic SEC, longer than SEC cultured on UBM-ECM or SIS-ECM. The results of the study suggested that the liver-derived ECM provides a unique set of tissue-specific signals that contribute to the maintenance of a site-specific, fenestrated phenotype for SEC [34].

2.2 COMPOSITION OF EXTRACELLULAR MATRIX SCAFFOLDS

The ECM consists of a complex mixture of structural and functional proteins that provide signals for cell growth, migration, proliferation, and differentiation. ECM is tissue and species-specific and reflects the structural and functional requirements of the tissue or organ [41-43].

ECM scaffolds are produced by subjecting the tissue of interest to a series of chemical, enzymatic, and/or mechanical treatments that remove the cellular components of the tissue, leaving the ECM framework intact. The ECM scaffolds were prepared using methods that preserved as much of the native composition and ultrastructure as well as the inherent structural and functional proteins of the liver, which may explain the retained bioactivity [44, 45].

Since the ECM composition of tissues and organs vary throughout the body, the resulting ECM biologic scaffolds also vary in composition. ECM scaffolds have been shown to be composed of type I collagen with minor amounts of collagen types III, IV, V, VI and VII [44, 46]. ECM scaffolds have also been shown to retain a variety of glycosaminoglycans including heparin, heparan sulfate, chondroitin sulfate A&B, and hyaluronic acid [47], and adhesion

molecules such as fibronectin and laminin [44 , 47]. ECM scaffolds have been shown to retain transforming growth factor (TGF-β) [39, 48], b-FGF [39, 49], vascular endothelial growth factor (VEGF) [49], epidermal growth factor (EGF) and hepatocyte growth factor (HGF) (unpublished data from Badylak Laboratory). Several of these growth factors have been shown to retain bioactivity even after terminal sterilization and long-term storage [48, 49]. Differential proteomics profiling of LECM confirmed the presence of the ECM proteins listed above (unpublished data from collaboration with University of New South Wales Proteomics Facility, Sydney, AU).

3.0 MAINTAINENCE OF HEPATOCYTE-SPECIFIC FUNCTIONS *IN VITRO*

Complex inter-relations of cellular and non-cellular elements in the liver modulate hepatoycte functions. The maintenance of hepatocyte phenotype is dependent on microenvironmental signals such as paracrine interactions (cell-cell), physical-chemical factors (i.e. oxygen tension, metabolites), mechanical stimuli (blood flow), and cell-extracellular matrix interactions [41, 50-54]. Strategies commonly utilized to maintain long-term hepatocyte functions *in vitro* include: (1) using hormonally defined media containing soluble factors; (2) restoring cell-cell contacts by culturing PHH with other cells (either nonparenchymal liver cells or nonhepatic cells); and (3) reestablishing cell-ECM contacts by culturing PHH with individual ECM components or complex ECM substrata. A brief discussion of the effects of cell-cell contacts and cell-ECM contacts upon maintainence of hepatocyte-specific functions is discussed below.

3.1 CO-CULTURE WITH NON-PARENCHYMAL CELLS

Hepatocytes are the parenchymal cells of the liver and account for approximately 80% of all liver cells [1, 2]. Hepatocytes perform most of the functions of the liver and work in concert with a number of other cell types to perform the functions essential for survival of the individual. The non-parenchymal cells (NPC) of the liver include: sinusoidal endothelial cells, Kupffer cells

and stellate cells. Cocultivation of PHH with other cells types can maintain liver-specific functions for several weeks *in vitro* [55]. Liver-derived NPCs [56-61] as well as non-hepatic endothelial cells [60], epithelial cells, [62] and fibroblasts [60, 63, 64] have been cocultured with hepatocytes to maintain hepatocyte morphology and a variety of synthetic, metabolic, and detoxification functions of the liver. Bhatia et al, have provided an extensive summary of studies used to preserve hepatoycte-specific functions *in vitro* through coculture with other cells [55].

3.2 CULTURE ON EXTRACELLULAR MATRIX SUBSTRATES

Individual ECM components or combinations of desired ECM components have been used as substrates for hepatoycte culture systems for several decades [35, 65, 66]. While cell culture substrates composed of individual ECM proteins such as type-1 collagen, laminin and fibronectin have facilitated primary rat hepatocyte attachment and maintainence of a few liver-specific functions and established hepatocyte polarity and morphology for short periods of culture, these systems are far from physiologically relevant [67-70]. The lack of an intact ECM that is composed of multiple ECM proteins specific to the native liver, affects cell-cell interaction, cell-ECM interaction, physical-chemical influences, and mechanical stimuli. As a result, the cells in culture eventually lose their functional cell phenotype [17].

Conventional culture models for hepatocytes include the use of type-I collagen and Matrigel^{TM} (MG) [71]. The sandwich configuration, where hepatocytes are cultured between two layers of either type-I collagen or MG, is a commonly used hepatocyte culture model [26, 66, 72, 73]. Sandwich culture of rat hepatocytes maintains hepatoycte polarity and morphology better than hepatocytes cultured on a single layer of type-I collagen or MG [35, 69, 74]. Further,

hepatocyte-specific functions, such as cytochrome-P450 (CYP450) activity and responsiveness [26, 66, 75, 76], albumin secretion [73], and urea synthesis, are enhanced when the sandwich culture model is used.

Several investigators have cultured primary human hepatocytes (PHH) on type-1 collagen with MG overlay [15, 26, 77]. The sandwich configuration facilitates maintenance and induction of xenobiotic metabolizing enzymes, particularly the phenobarbital-mediated responsiveness of cytochrome P450 2B6 [26]. Page et al recently showed that MG overlay enhanced PHH mRNA expression levels for differentiated hepatocyte genes such as the cytochrome P450s, liver-specific markers such as albumin, transferrin, and connexin 32 [78].

The use of complex ECM substrates derived from mammalian tissues for hepatocyte culture began more than two decades ago. Early culture models utilized ECM substrates derived from either rat liver [27, 37] or the Engelbreth-House sarcoma mouse tumor, which is called Matrigel [71]. Rat hepatocytes cultured on type-1 collagen show less cell attachment and survival compared to rat hepatocytes cultured upon a biomatrix derived from solubilized rat liver [27].

More recently, ECM substrates derived from porcine, bovine, or human liver have been used to improve hepatocyte survival, polarity and liver-specific functions *in vitro* (Table 1) [28, 35]. Lin et. al. compared rat hepatocytes cultured on ECM biologic scaffolds derived from porcine liver (PLECM) to well characterized hepatocyte culture models (type-1 collagen sandwich configuration or a single layer of type-1 collagen)[28]. Hepatocytes survived up to 45 days on a sheet form of PLECM and several liver-specific functions such as albumin synthesis, urea production, and P-450 IA1 activity were markedly enhanced compared to the growth and metabolism of cells cultured on a single layer of type-1 collagen.

Zeisburg et al isolated liver-derived basement membrane matrix (LBLM) from human or bovine liver, and used the substrate for culture of human hepatocytes [35]. Human hepatocytes adhered more efficiently to LBLM and expressed lower levels of vimentin and cytokeratin-18, which are markers of hepatocyte dedifferentiation, compared to hepatocytes cultured on MG or type-1 collagen. However, maintainence of liver-specific functions *in vitro* was not reported [35].

Table 1. ECM Substrates Derived from Mammalian Tissues for Hepatocyte Culture

Substrate	Derived From	ECM Composition
Biomatrix Reid et al, 1980	Rat liver	Type-I collagen Type-111 collagen Fibronectin
Matrigel Kleinman et al, 1982	Engelbreth-Holm-swarm mouse sarcoma tumor	Laminin Type IV collagen Entactin Heparin sulfate proteoglycan Chondroiton sulfate proteoglycan ECM-bound growth factors
Basement Membrane Matrix Zeisberg et al, 2006	Bovine or human liver	Type-IV collagen Laminin Entactin Heparin sulfate proteoglycan
ECM Sheet Form Lin et al, 2004	Porcine liver	Type-I collagen Type-VI collagen Type-III collagen Type-IV collagen Type XI collagen Type-XIX collagen Heparin Sulfate Proteoglycan Laminin Biglycan Tenascin Fibronectin ECM-bound growth factors

4.0 MOTIVATION AND SPECIFIC AIMS OF THE PRESENT STUDY

The ability of the liver to regenerate is an important survival mechanism of the body. Up to 75% of the liver mass can be surgically removed or destroyed by disease or chemical insult before it ceases to function [79-81]. To restore the loss of tissue, the remaining liver cells regrow to within 10% of the original mass by compensatory hyperplasia to form a functional tissue replacement. However, when hepatocytes are isolated from their highly specialized microenvironment *in vivo,* they are unable to proliferate *in vitro*. In addition to losing their ability to proliferate *in vitro,* hepatocytes quickly lose their liver-specific functions without cell-cell [55] or cell-ECM contacts [35, 82, 83]. Therapies to treat liver disease, including BAL devices and tissue engineered constructs, have had limited clinical success because of the inability to maintain the liver-specific functions of a large mass of isolated human hepatocytes.

The field of tissue engineering and regenerative medicine strives to restore liver function by recreating the liver *ex vivo* and subsequently implanting the tissue-engineered construct, or to provide a bridge to liver transplantation, utilizing a combination of cells and bioreactors to perform the function of the liver *ex vivo.* The identification of a biologic scaffold that could maintain a functional hepatocyte differentiation profile would represent an advancement toward therapies to treat liver disease.

Studies have also shown that liver-specific functions can be maintained *in vitro* for several weeks when hepatocytes are cultured on complex ECM substrata (MG, biomatrix, LBLM) or

between two layers of MG/type-1 collagen [27, 28, 84]. While the results of these studies are encouraging, the studies have utilized either porcine or rat hepatocytes.

Hepatoycte functions, such as drug metabolism, vary between species [85, 86] and the use of a patient's own cells would preclude the use of long-term immunosuppression. Only a few studies have examined the effects of extracellular matrix substrates on maintainence of primary human hepatocyte-specific functions [15, 26, 66, 75, 86, 87].

The **overall goal** of this project is to determine the ability of naturally-derived liver extracellular matrix (LECM) to support primary human hepatocyte-specific functions *in vitro*. The project is predicated upon the hypothesis that the scaffold or substrate upon which PHH are seeded is a critical determinant of cell phenotype and function.

Bioscaffolds composed of LECM will be used as a substrate for hepatocyte growth and the following variables will be evaluated for their ability to maintain hepatocyte phenotype *in vitro*: (1) the source (i.e. species) of LECM scaffolds, and (2) the LECM geometrical configuration.

Based on the need to develop substrates that support primary human hepatocyte-specific functions *in vitro*, the specific aims of the present study were the following:

1. To compare the effect of liver-derived ECM scaffolds derived from two different species, human and porcine, on human hepatocyte-specific functions. The interaction of hepatocytes with the ECM [88, 89] is essential for the maintainence of hepatocyte-specific functions. While porcine liver is a readily available source for LECM, ECM from human liver (HLECM) may support superior human hepatocyte function since ECM properties are tissue- and species-specific [3, 43].

The specific aim was based on the hypothesis that PHH cultured with HLECM will have enhanced liver-specific functions, compared to PHH cultured with PLECM, Matrigel or type-1

collagen. The latter two are routinely used for hepatocyte culture, so they were also used in this study for comparison. The mRNA levels of connexin 32, albumin, CYP1A1, CYP1A2, and CYP3A4 were measured. Albumin secretion and cytochrome P450 1A1/1A2 and 3A4 activity were used as indicators of hepatocyte functionality.

2. To determine the effect of porcine-derived ECM sandwich configuration upon maintainence of hepatocyte-specific functions. Previous studies have shown that hepatocyte polarity and liver-specific functions, such as albumin production, are stabilized *in vitro* for longer periods of time when hepatocytes are cultured between two layers of a gel [74, 82, 90, 91].

The specific aim was based on the hypothesis that the primary human hepatocytes cultured between two layers of PLECM will maintain hepatocyte-specific functions better than primary human hepatocytes cultured on type-1 collagen alone or between two layers of Matrigel, since PLECM composition is more similar to the native liver ECM composition compared to Matrigel or type-1 collagen. The mRNA levels of connexin 32, albumin, bile salt export pump (BSEP), and sodium taurocholate co transporting polypeptide (NTCP) were measured. Hepatocyte functionality was assessed by albumin secretion, hepatic transport activity, and ammonia metabolism.

5.0 SPECIFIC AIM 1: THE EFFECT OF SPECIES-SPECIFIC ECM SCAFFOLDS ON HEPATOYTE- FUNCTIONS *IN VITRO*

Previous studies have shown that intact ECM derived from mammalian organs provides a more favorable substrate for the growth and differentiation of various cell types compared to the use of individual components of ECM, such as type-1 collagen or fibronectin [28, 34, 36, 38-40]. Further, Sellaro et al showed that ECM scaffolds are tissue-specific [34] by culturing rat sinusoidal endothelial cells (SEC), which are a highly specialized endothelial cell population derived from the liver, on ECM derived from small intestine, urinary bladder, and liver. The SEC maintained their phenotype the longest on ECM scaffolds derived from the liver.

Since Sellaro et al demonstrated that ECM retain their tissue-specificity, the next logical question would examine if ECM scaffolds retain their species-specificity. Would ECM derived from human liver support human hepatocyte functions better than ECM derived from porcine liver since ECM are tissue- and species-specific [3, 43].

To address Specific Aim 1, PHH were cultured on type-1 collagen alone, or cultured on type-1 collagen with either Matrigel, HLECM or PLECM overlay. The mRNA levels of connexin 32, albumin, CYP1A1, CYP1A2, and CYP3A4 were measured. Albumin secretion and cytochrome P450 inducibility and activity (CYP1A1/1A2 and CYP3A4) were used as indicators of hepatocyte functionality.

5.1 METHODS

5.1.1 Reagents

Pepsin, sodium hydroxide, glycerol, dibasic sodium phosphate, monobasic sodium phosphate, dexamethasome, β-napthoflavone (β-NF), rifampicin (RIF), dimethylsulfoxide (DMSO), ethoxyresorufin-O-deethylation (EROD), and EDTA were purchased from Sigma Chemical Co. (St. Louis, MO). Trypsin was purchased from Gibco (Carlsbad, CA). Type-1 collagen was purchased from Becton Dickinson (Franklin Lakes, OR). Quant-iT PicoGreen Assay was obtained from Invitrogen-Molecular Probes (Eugene, OR). Triton-X 100 and sodium deoxycholic acid were purchased from Spectrum (Gardena, CA). Hepatocyte Maintainence Media (HMM) was purchased from Cambrex (Baltimore, MD). Penicillin, streptomycin and bovine calf serum were purchased from Gibco (Carlsbad, CA). Trizol reagent was purchased from Invitrogen (Carlsbad, CA). Ethidium bromide was purchased from Sigma Chemical Co. (St. Louis, MO). All quantitative real-time RT-PCR reagents were purchased from Applied Biosystems (Foster City, CA). Cyclophilin albumin, CYP3A4, CYP1A1, and CYP1A2 were synthesized by Applied Biosystems with assay identification numbers: cyclophilin (Hs03045993_gH), Cx32 (Hs00702141_s1), albumin (Hs00910222_m1), CYP3A4 (Hs00604506_m1), CYP1A1 (Hs01054796_g1), and CYP1A2 (Hs01070374_m1).

5.1.2 Isolation and Preparation of Liver-derived Extracellular Matrix (LECM) Scaffolds

ECM scaffolds have been isolated from a variety of species, including the following: porcine, canine, ovine, bovine, ratus, murine, and human. Mammalian tissue and organ sources

for ECM scaffolds include but are not limited to the following: brain (unpublished data Badylak Laboratory), lung, pancreas [92], tendon, trachea [93], adrenal [94], amnion [95], peripheral nerve [96], skin [31], small intestine [97], urinary bladder [98, 99], stomach [100], heart [101], pericardium [29], and liver [28]. Combinations of physical, chemical and enzymatic techniques are used to decellularize tissues and organs. Because of the tissue- and species-specificity of tissue and organs, decellularization protocols are tailored for a specific tissue or organ. For instance, the decellularization protocol of small intestine [102] is very different than the decellularization protocol for cardiac tissue [103]. Gilbert, Sellaro, and Badylak recently published an extensive summary of decellularization protocols and techniques [104].

Isolation and Preparation of ECM. The methods used to isolate porcine liver ECM (PLECM) have been previously described [28, 44, 104]. Livers were harvested from market weight pigs (~110-130kg) immediately after euthanasia. The tissues were rinsed with tap water and frozen until used. Each liver lobe was cut into 5 mm thick slices with a rotating blade and subjected to three separate 30 minute washes in deionized water with mechanical agitation on an orbital shaker. The sections were then gently massaged to aid in cell lysis and soaked in 0.02% trypsin/0.05% EDTA at 37° C for one hour. The tissue was rinsed in deionized water and the massaging was repeated followed by mechanical agitation of the liver sections in 3% Triton X-100 for one hour. The rinsing and massaging process was repeated until all visible remnants of cellular material were removed. The tissue sections were then mechanically agitated in 4% sodium deoxycholic acid for one hour followed by rinsing in water a minimal of three times. Tissues were immersed in a solution of 0.1% peracetic acid followed by three rinses in water or phosphate buffered saline at pH 7.4 [105]. The resulting decellularized connective tissue matrix was referred to as PLECM [28].

Human liver tissue was obtained from donor livers that had not been used for transplantation. The same protocol delineated above was followed for the decellularization of human liver tissue, with the following modifications. After sectioning of the liver tissue into 5 mm thick slices, each tissue slice was transferred into individual mesh bags that were subsequently sealed. The encasement of liver slices within mesh bags prevented tearing of the tissue, since human liver tissue tore more easily than porcine liver tissue. The holes in the mesh bag facilitated transfer of solutions to the tissues. Prior to placing the human liver tissue on the mechanical orbital shakers for the first time, the human liver tissue was stored in deionized water at 4° C for 72 hours. The deionized water was changed daily. A small amount (0.001 g per flask) of sodium azide was added to the solution to prevent contamination. Tissues were immersed in a solution of 0.1% peracetic acid followed by three rinses in water or phosphate buffered saline at pH 7.4 [105]. Following decellularization, the resulting acellular connective tissue matrix was referred to as HLECM (Figures 1A&B).

DAPI and hematoxylin and eosin staining were performed on random samples to assess degree of decellularization of human and porcine liver tissues. Figure 2 shows the H&E and DAPI staining for native human liver (Figures 2A&B) and decellularized human liver (Figures 2C&D).

5.1.3 Preparation of ECM Digests

The method used to prepare a digest of harvested ECM has been previously described [99]. The protocol was adapted to produce a digest from porcine and human liver. A powdered form of LECM was produced from sheets of LECM. The hydrated, sheet form of the disinfected ECM was lyophilized overnight. Lyophilized sheets of LECM were cut into small pieces, and

then placed in a rotary knife mill (Wiley Mill) to create a particulate form of the ECM. Particles less than 250 micron were collected by sieve through a #60 mesh screen.

One gram of lyophilized LECM powder and 100 mg of pepsin (2000-3000 U/mg) were mixed in 100 mL of 0.01 M HCl and stirred for ~72 hours at room temperature (25ºC). The final viscous solution of digested LECM or pre-gel solution had a pH of approximately 3.0 - 4.0. Inactivation of pepsin activity occurred when the pH was raised to 7.4.

5.1.4 Isolation and Culture of Primary Human Hepatocytes.

Hepatocytes were isolated from either donor livers that were not used for transplantation or from areas of hepatic tissue that were not involved in tumor from tissue resections for cancer. All human subject protocols were reviewed and approved by the University of Pittsburgh Institutional Review Boards. Hepatocytes in this study were isolated from six human donors of different age groups, genders and medical histories (Table 2). Significant amounts of steatosis (fat) were not observed in any of the livers. Viability of the hepatocytes at the time of plating was greater than 70%, as measured by trypan blue exclusion.

Table 2. Donor Information for Human Hepatocyte Preparations For Specific Aim 1.

Donor HH#	Age	Sex[a]	Race[b]	Tissue Resection or Organ Donor	Drug History	Cause of Death	Viability
HH1332	37	M	ND	Resection	NK	NA	83%
HH1338	54	M	ND	Resection	Chemotherapy	NA	73%
HH1344	44	F	C	Organ Donor	None	Intercranial Bleed	82%
HH1356	25	F	C	Organ Donor	None	Non-heart beating donor	70%
HH1367	72	M	C	Resection	NK	NA	91%
HH1369	61	F	C	Organ Donor	Omeprozole, Celebrex, Glimpride, Trazadone, Effexor, Zetia, Detrol, Actus, Accupril	Intercranial Hemorrhage	91%

ND, data not provided; NK, no known chronic drug treatment; NA, not applicable
[a]M, male; F, female; [b]C, Caucasion

PHH were isolated by a three-step collagenase perfusion of human liver [106] and plated in 6-well plates precoated with adsorbed type-1 collagen at a seeding density of $1.5x10^6$ cells per well. HMM supplemented with 10^{-7} M dexamethasome, 10^{-7} M insulin, 100 U/mL penicillin, 100 µg/ml streptomycin and 10% bovine calf serum. After 4 hours of culture at 37° C, the media was replaced with serum free HMM with the supplements listed above and changed every 24 hrs. After 24 hrs of culture, unattached PHH were removed by gentle agitation and PHH were overlaid with a solution of HMM containing either 0.222 mg/ml of MG, HLECM digest or

PLECM digest (Figure 3). The HMM-ECM solutions formed a semi-solid layer over the cells. Media was changed daily.

5.1.5 Light Microscopy of Primary Human Hepatocytes

PHH were maintained in HMM media for seven days under different extracellular matrix (ECM) conditions. On day five, PHH cultured on type- 1 collagen alone, or on type-1 collagen with either MG, HLECM, or PLECM overlay were imaged at 100x with a light microscope.

5.1.6 Measurement of DNA Content

Using a cell scraper, cells were harvested on ice in 150 µl cell harvest buffer containing: dibasic sodium phosphate (11.5 g/L), monobasic sodium phosphate (2.6 g/L), EDTA (0.033 g/L), and 20% glycerol. The cell lysates were produced by sonication and stored at –20° C. Total DNA was quantified using the commercially available Quant-iT Picogreen dsDNA Kit according to the manufacturer's instructions. For each group, a minimum of two samples were used to determine total DNA and each samples was measured in triplicate.

5.1.7 RNA Isolation and Quantitative real time RT-PCR Methods

Total RNA was isolated using Trizol Reagent as described by the manufacturer's instructions. RNA concentration was determined by spectrophotometer (µQuant Microplate

Spectrophotometer, Biotek Instruments, Winooski, VT) at 260 nm. The purity of RNA was determined by spectrophotometry at 280 nm and the integrity checked by agarose gel electrophoresis stained with ethidium bromide. RNA was stored at −80° until further use.

mRNA expression levels of albumin, BSEP, and NTCP were determined using TaqMan quantitative reverse-transcriptase polymerase chain (TaqMan QRT–PCR) assays. From each group, 2 µg of total RNA was incubated with 5 U RQ DNase, 5 µL 10 x RQ buffer in a total volume of 10 µL at 37°C for 30 min. The samples were then incubated with 1 µL RQ DNase Stop Solution at 65°C for 10 min. The DNAse treated RNA was then incubated with 1 µL of random hexamer primers (100 ng/ L) at 70°C for 5 min for cDNA synthesis. cDNA generation continued with incubation at 37°C for 60 min with the following reagents: 1 µL dNTP (10 mmol/L of each), 5 µL MMLV 5x, and 1 µL MMLV RT for a total volume of 12 µL.

Cyclophilin, albumin, CYP1A1, CYP1A2, CYP3A4, and Cx32 specific primers and probe were purchased as a pre-developed gene expression assay and used according to manufacturer's instructions.

TaqMan one-step RT–PCR assays were performed with 4 ng of each RNA sample in a final reaction volume of 72 µL prepared from TaqMan one-step RT–PCR Master Mix Reagents Kit. Assays were performed using an Applied Biosystems' ABI Prism 7900HT sequence detection system. An initial RT step occurred for 30 min at 48° and was subsequently followed by heating to 95° for 10 min followed by 40 cycles of 95° for 15 s, 60° for 1 min.

5.1.8 Measurement of Albumin Secretion

Due to limited availability of cells, conditioned media was collected from donors HH1356, HH1367, and HH1369 on days three, five, and seven, and stored at -20°C until

analysis. PHH secretion of albumin was measured using a commercially available kit (Bethel Laboratories, Texas). At least three samples were collected from each culture condition and each sample was measured in triplicate. All data was normalized to total DNA content.

5.1.9 RIF-Induced CYP3A4 Activity

The concentration of 6β-hydroxytestosterone in the medium was measured by HPLC in five independent PHH preparations (Table 2: HH1338-HH1369) as previously described [107], with the following modifications. PHH were induced with 10 μM RIF for 72 hours. At day five, culture media was changed and PHH were incubated with HMM containing 0.25 mmol/L testosterone for 30 minutes at 37°C. From each group, 500 μL of medium were collected from three samples and were diluted with an equal volume of methanol and centrifuged at 13,000 r.p.m. for five minutes. One hundred microliters of the conditioned media with methanol solution was injected into a LiChristopher 100 RP-18 column (4.6 x 250 mm, 5 μm). 6β-hydroxytestosterone was eluted with a mobile phase of methanol/water (60:40, v/v) at a flow rate of 1.2 ml/min and the eluents were monitored at 242 nm. The concentration of the 6β-(OH) TE metabolite was determined by comparing the peak areas in samples to a standard curve containing a known amount of the metabolite. All data was normalized to total DNA content of each sample.

5.1.10 β-NF-Induced CYP1A1/1A2 Activity

β-NF-induced CYP1A1/1A2 activity was measured in five independent PHH preparations (Table 2: HH1338-HH1369) on day five using a method previously described [108]. Briefly,

PHH were induced with 10 μM β-NF for 72 hours. On day five, PHH were challenged with 0.25 mmol/L EROD prepared in HMM. CYP1A1/1A2 activity is measured by EROD activity, which is the conversion of EROD to resorufin. After 30 min of incubation with EROD at 37°C, 250 μL of media was collected from each well. EROD activity was measured by a fluorescent spectrometer (LS-50b from Perkin-Elmer). For each group, media was collected from a minimum of three samples and each sample was measured in triplicate. Resorufin formation was measured by comparing the fluorescence to a standard curve of resorufin prepared in HMM. All data was normalized to total DNA content of each sample.

5.1.11 Statistical Analysis.

All values were calculated as mean ± S.D. For statistical analysis, all data was normalized to PHH cultured on type-1 collagen. A one-way analysis of variance with a post-hoc Tukey's multiple comparison procedure was performed. A p value of ≤ 0.05 was considered statistically significant and all calculations were performed using SAS software, version 9.1 (Cary, NC).

5.2 RESULTS

A summary of all techniques used to characterize hepatocyte phenotype is in Figure 4.

5.2.1 Effect of ECM Overlay on Hepatocyte Morphology

The PHH attached to collagen-type 1 showed the typical morphological appearance of PHH as viewed by light microscopy. PHH had polygonal shapes with one or more nuclei per cell. PHH had similar morphologies regardless of the culture conditions (Figures 5A-C).

5.2.2 Effect of ECM Overlay on DNA Contents

Average DNA content of PHH varied between livers. PHH isolated from HH1332 had the highest average DNA content of 3.65±0.14 µg (Figure 6A). PHH isolated from HH1338 had an average DNA content of 1.68±0.24 µg (Figure 6B) and PHH isolated from HH1344 had an average DNA content of 1.55±0.41 µg (Figure 6C). PHH isolated from HH1356 and HH1367 had an average DNA content of 2.85±0.31 µg (Figure 6D) and 1.11±0.28 µg (Figure 6E), respectively. PHH isolated from HH1369 had an average DNA contents of 1.63±0.34 µg (Figure 6F).

Average DNA contents for PHH cultured on type-1 collagen alone was 1.6±0.67 µg, and the DNA content for PHH cultured on type-1 collagen with either MG, HLECM, or PLECM was 1.93±0.51 µg, 2.09±0.93 µg, and 2.11±0.79 µg, respectively (Figure 7). The DNA content of PHH were similar, regardless if an overlay was used.

When data from each group was averaged and normalized to DNA content of PHH cultured on type-1 collagen, no statistical differences were measured between the groups (Figure 8).

5.2.3 Effect of ECM Overlay on Cx32 mRNA Expression

Individual donor Cx32 mRNA expression values are reported in Figure 9. Due to technical difficulties with RNA isolation from HH1367, Cx32 mRNA expression data was not graphed. For HH1338, HH1344, and HH1356, PHH cultured with ECM OL had higher Cx32 mRNA expression levels than PHH cultured on type-1 collagen only. For HH1369, PHH cultured on type-1 collagen alone had the highest Cx32 mRNA expression levels.

Data from each culture condition was averaged and normalized to data from PHH cultured on type-1 collagen only. PHH had similar Cx32 mRNA expression levels, regardless of the culture condition (Figure 10).

5.2.4 Effect of ECM Overlay on Alb mRNA Expression

Albumin mRNA expression was measured in PHH isolated from donors HH1356, HH1367, and HH1369 because albumin secretion was measured in PHH isolated from these livers. Figure 11 shows the albumin mRNA expression from each liver. For HH1344, PHH cultured with MG overlay had the highest albumin mRNA expression levels (Figure 11A). For HH1356, PHH cultured with HLECM overlay had the highest albumin mRNA expression levels (Figure 11B) while in HH1369, PHH cultured on type-1 collagen had the highest albumin mRNA expression levels (Figure 11C).

Data from each culture condition was averaged and normalized to PHH cultured on type-1 collagen only. PHH had similar albumin mRNA expression levels, regardless of the culture condition (Figure 12).

5.2.5 Effect of ECM Overlay on Albumin Secretion

Albumin secretion was measured on days three, five and seven in the following donor cases: HH1356, HH1367, and HH1369.

Figure 13 shows the albumin concentrations in conditioned media of PHH isolated from each liver and cultured on type-1 collagen alone (Figure 13A), or type-1 collagen with MG (Figure 13B), HLECM gel (Figure 13C), or PLECM gel overlay (Figure 13D). In HH1356, albumin secretion levels were comparable regardless of day or presence of ECM overlay. In HH1367, PHH cultured with MG overlay had higher levels of albumin secretion than PHH cultured on type-1 collagen on all days. PHH cultured with HLECM overlay had comparable levels of albumin secretion to PHH cultured with type-1 collagen alone at day three and seven. PHH cultured with PLECM overlay had higher levels of albumin secretion on day three and seven compared to PHH cultured on type-1 collagen alone. In HH1369, PHH cultured with MG overlay had higher levels of albumin secretion on all days compared to PHH cultured on type-1 collagen alone. PHH cultured with HLECM overlay had higher levels of albumin secretion on day seven compared to PHH cultured on type-1 collagen alone. PHH cultured with PLECM overlay had higher levels of albumin secretion on day five and seven compared to PHH cultured on type-1 collagen only.

Albumin secretion data from each culture condition was averaged and normalized to the albumin secretion data from PHH cultured on type-1 collagen at day three. PHH had comparable levels of albumin secretion of days three, five and seven regardless of culture condition (Figure 14).

Albumin secretion was calculated as the average amount of secretion per day (Figure 15) Due to large variability in albumin secretion values from donor to donor, average albumin secretion values were not different between the groups (Figure 15).

5.2.6 Effect of ECM Overlay on CYP3A4 mRNA Expression

Non-RIF induced and RIF-induced CYP3A4 mRNA expression levels of each donor are shown in Figure 16. Due to a technical difficulty with the RNA of HH1367, only mRNA values for PHH cultured with either HLECM or PLECM overlay were shown. In all cases, RIF induction of PHH increased the CYP3A4 mRNA expression levels compared to the controls (non-RIF induced).

When the CYP3A4 mRNA expression data from each culture condition was averaged and normalized to the data from PHH cultured on type-1 collagen only, no differences in CYP3A4 expression levels were measured (Figure 17).

5.2.7 Effect of ECM Overlay on RIF-Induced CYP3A4 Activity

RIF is an inducer of CYP3A4 activity. CYP3A4 metabolizes TE and a metabolite is 6β(OH)-TE. Each experiment had RIF-induced PHH and non-RIF induced PHH (controls). RIF-induced PHH were incubated with RIF for 72 hours prior to addition of TE. RIF-induced PHH had increased levels of 6β(OH)-TE formation compared to controls (non-RIF induced PHH).

PHH isolated from HH1332 were cultured on type-1 collagen with either a MG or HLECM overlay. PHH cultured with MG overlay had an 8.0 ±0.4-fold increase in the formation

rate of 6β(OH)-TE compared to control. PHH cultured with HLECM overlay had a 14.5±0.7-fold increase in the formation rate of 6β(OH)-TE compared to control (Figure 18A).

PHH isolated from HH1338 were cultured on either type-1 collagen, or type-1 collagen with either MG or HLECM overlay. RIF induced PHH cultured on type-1 collagen had a 9.1±5.8-fold increase in formation of 6β(OH)-TE compared to control. PHH cultured with MG overlay had an 8.5±1.1-fold increase in the formation rate of 6β(OH)-TE compared to control. PHH cultured with HLECM overlay had a 24.3±7.1-fold increase in the formation rate of 6β(OH)-TE compared to control (Figure 18B).

PHH isolated from HH1344, HH1356, and HH1367 were cultured on either type-1 collagen, or type-1 collagen with either a MG, HLECM or PLECM overlay. For HH1344, RIF induced PHH cultured on type-1 collagen produced 4.3±1.3-fold higher 6β(OH)-TE formation rate compared to control. PHH cultured with MG overlay increased 6β(OH)-TE formation by 6.9±1.3-fold compared to control. PHH cultured with HLECM overlay had a 5.2±2.5-fold increase in the formation rate of 6β(OH)-TE compared to control. PHH cultured with PLECM had a 3.4±0.6-fold increase in the formation rate of 6β(OH)-TE compared to control (Figure 18C).

For HH1356, RIF induced PHH cultured on type-1 collagen only had a 3.1±0.3-fold higher 6β(OH)-TE formation rate compared to control. PHH cultured with MG overlay had an 34.3±4.3-fold increase in the formation rate of 6β(OH)-TE compared to control. PHH cultured with HLECM overlay had a 35.3±1.4-fold increase in the formation rate of 6β(OH)-TE compared to control. PHH cultured with PLECM had a 40.8±0.9-fold increase in the formation rate of 6β(OH)-TE compared to control (Figure 18D).

For HH1367, PHH in all culture conditions had comparable levels 6β(OH)-TE formation rate. RIF induced PHH cultured on type-1 collagen had a 9.6±1.9-fold higher 6β(OH)-TE formation rate compared to control. PHH cultured with MG overlay had an 10.9±3.7-fold increase in the formation rate of 6β(OH)-TE compared to control. PHH cultured with HLECM overlay had a 8.8±2.0-fold increase in the formation rate of 6β(OH)-TE compared to control (Figure). PHH cultured with PLECM had a 11.1±3.0-fold increase in the formation rate of 6β(OH)-TE compared to control (Figure 18E).

For HH1369, PHH in all culture conditions had comparable levels 6β(OH)-TE formation rate. RIF induced PHH cultured on type-1 collagen had a 2.0±0.3-fold higher 6β(OH)-TE formation rate compared to control. PHH cultured with MG overlay had an 2.3±0.6-fold increase in the formation rate of 6β(OH)-TE compared to control. PHH cultured with HLECM overlay had a 2.9±0.1-fold increase in the formation rate of 6β(OH)-TE compared to control. PHH cultured with PLECM had a 3.8±2.7-fold increase in the formation rate of 6β(OH)-TE compared to control (Fig 18F).

6β(OH)-TE formation data from each culture condition was averaged and normalized to the 6β(OH)-TE concentrations of RIF-induced PHH cultured on type-1 collagen. Due to large variability in 6β(OH)-TE formation in RIF-induced PHH from donor to donor, 6β(OH)-TE formation values were not different between the groups (Figure 19).

5.2.8 Effect of ECM Overlay on CYP1A1 mRNA Expression

CYP1A1 mRNA expression values are shown in Figure 20. In all cases, β-NF induction of PHH increased the CYP1A1 mRNA expression levels compared to the controls (non- β-NF induced).

For HH1338 and HH1356, PHH had similar levels of CYP1A1 mRNA expression (Figures 20 B & D). In HH1344, PHH cultured on type-1 collagen alone had the highest CYP1A1 mRNA expression (Figure 20C). For HH1367, there were technical difficulties with MG control RNA so the control mRNA expression was not plotted. For HH1367, PHH cultured with either MG or PLECM overlay had the highest CYP1A1 mRNA expression (Figure 20E). For HH1369, PHH cultured with PLECM overlay had the highest levels of CYP1A1 mRNA expression (Figure 20F).

When CYP1A1 mRNA data from each culture condition was averaged and normalized to the data of PHH cultured on type-1 collagen, PHH had similar CYP1A1 mRNA expression levels (Figure 21).

5.2.9 Effect of ECM Overlay on CYP1A2 mRNA Expression

Individual donor CYP1A2 mRNA expression values are shown in Figures 22 A-F. In all cases, β-NF induction of PHH increased the CYP1A2 mRNA expression levels compared to the controls (non- β-NF induced). In HH1332, HH1338, and HH1367, PHH cultured with HLECM overlay had the highest CYP1A2 mRNA expression levels (Figures 22A-B, E). In HH1344, PHH cultured on type-1 collagen alone had the highest CYP1A2 mRNA expression levels (Figure 22C). For HH1356, PHH cultured with PLECM overlay had the highest CYP1A2 mRNA expression levels (Figure 22D) while in HH1369, PHH cultured with MG overlay had the highest CYP1A2 mRNA expression levels (Figure 22E).

When CYP1A2 mRNA data from each culture condition was averaged and normalized to the data of PHH cultured on type-1 collagen, PHH had similar CYP1A2 mRNA expression levels (Figure 23).

5.2.10 Effect of ECM Overlay on β-NF-Induced CYP1A1/1A2 Activity

β-NF upregulates CYP1A1/1A2 activity. CYP1A1/1A2 metabolizes EROD and a metabolite is resorufin. Each experiment had β-NF-induced PHH and controls (non- β-NF induced PHH). β-NF-mediated CYP1A1/1A2 activity increased in PHH for all donors compared to controls (Figure 24).

PHH isolated from HH1332 were cultured on type-1 collagen with either a MG or HLECM overlay. β-NF-induced PHH cultured with either MG or HLECM overlay had comparable levels of fold increase resorufin formation over control, 15.3±0.4-and 15.7±0.4-fold increase, respectively (Figure 24A).

PHH isolated from HH1338 were cultured on either type-1 collagen, or type-1 collagen with either MG or HLECM overlay. β-NF induced PHH cultured on type-1 collagen produced 7.5±0.8-fold higher resorufin formation compared to control. PHH cultured with MG overlay had a 3.8±0.1-fold increase in the resorufin formation compared to control, while PHH cultured with HLECM overlay had a 4.9±0.4-fold increase in the resorufin formation (Figure 24B).

PHH isolated from HH1344, HH1356, HH1367, and HH1369 were cultured on either type-1 collagen, or type-1 collagen with either a MG, HLECM or PLECM overlay. For HH1344, β-NF induced PHH cultured on type-1 collagen alone produced 8.67±0.7-fold higher resorufin formation compared to control. PHH cultured with MG overlay had a 6.8±0.7-fold increase in the resorufin formation compared to control. PHH cultured with HLECM overlay had an 11.4±2.4-fold increase in the resorufin formation compared to control. PHH cultured with PLECM had a 8.1±0.1-fold increase in the resorufin formation compared to control (Figure 24C). For HH1356, β-NF induced PHH cultured on type-1 collagen had a 42.2±9.7-fold increase in resorufin formation compared to control. PHH cultured with MG overlay had a 56.2±4.5-fold

increase in resorufin formation compared to control. PHH cultured with HLECM overlay had a 41.8±2.7-fold increase in resorufin formation compared to control. PHH cultured with PLECM had a 41.2±0.5-fold increase in resorufin formation compared to control (Figure 24D). For HH1367, β-NF induced PHH cultured on type-1 collagen had a 4.1±0.7-fold increase in resorufin formation compared to control. PHH cultured with MG overlay had a 10.9±1.5-fold increase in resorufin formation compared to control. PHH cultured with HLECM overlay had a 15.1±0.5-fold increase in the resorufin formation compared to control. PHH cultured with PLECM had a 8.9±0.2-fold increase in resorufin formation compared to control (Figure 24E). For HH1369, β-NF induced PHH cultured on type-1 collagen had a 15.1±0.7-fold increase in resorufin formation compared to control. PHH cultured with MG overlay had a 15.0±2.3-fold increase in resorufin formation compared to control. PHH cultured with HLECM overlay had a 13.0±1.6-fold increase in the resorufin formation compared to control. PHH cultured with PLECM overlay had a 12.6±2.0-fold increase in resorufin formation compared to control (Figure 24F).

When the resorufin formation of β-NF-induced PHH from group was averaged and normalized to the resorufin formations of β-NF-induced PHH cultured on type-1 collagen, no differences were measured (Figure 25).

5.3 DISCUSSION

PHH in all culture configurations had robust RIF-induced CYP3A4 activity and robust β-NF induced CYP1A1/1A2 activity. However, a pronounced ECM-dependent induction response was not observed in PHH treated with RIF or β-NF: ECM overlays did not correlate to higher levels of induced CYP3A4 or CYP1A1/1A2 activity. Other studies have also shown that the

presence of a complex ECM substrate or overlay does not affect the inducibility of PHH. Silva et al. cultured PHH on either type-1 collagen or MG [75] and showed that PHH had similar levels of RIF-induced CYP3A4 activity, regardless of the substrate. Hamilton et al. showed that MG overlays had no significant effect of RIF-induced CYP3A4 and β-NF-induced CYP1A1/1A2 activity [66].

In contrast, Gross-Steinmeyer et al. demonstrated a 2.1 fold increase in phenobarbital-mediated CYP1A1/1A2 activity in PHH cultured with a MG overlay compared to PHH cultured on type-1 collagen. Phenobarbital-mediated CYP2B6 activity had a 1.8 fold increase in PHH cultured with MG overlay compared to PHH cultured on type-1 collagen.

Previous studies have shown that the culture of rat hepatocytes on type-1 collagen precipitates the rapid decline of liver-specific functions [28, 73]. However, when rat hepatocytes were cultured in between two layers of type-1 collagen or ECM such as MG, albumin secretion increased as compared to hepatocytes on type-1 collagen only [28, 73]. Extrapolation of experimental data from one species to another is difficult because of the species-specificity of hepatocytes [109, 110]. In the present study, albumin secretion does not increase significantly in PHH that are cultured with an ECM overlay. Jasmund et. al. compared albumin secretion of PHH cultured on type-1 collagen alone or on type-1 collagen with a biomatrix overlay (derived from porcine liver) overlay. PHH secreted similar levels of albumin, regardless of the presence of a biomatrix overlay, which supports the findings from the present study [86].

5.4 CONCLUSIONS

This study was one of the first set of experiments that evaluated the ability of ECM derived from porcine and human liver to maintain PHH functions *in vitro*. In this study, PHH has similar functional profiles regardless of the presence of an ECM overlay. The lack of differences in several functional assays, including albumin secretion and CYP450 inducibility, suggest that PHH cultured with PLECM overlay will perform as well as PHH cultured with HLECM overlay. Regarding production of ECM scaffolds for clinical applications, these findings are attractive because porcine liver tissues are readily available compared to human liver tissues.

5.5 LIMITATIONS

In this study, albumin secretion and RIF- and β-NF-induced CYP450 activity were used to assess hepatocyte functionality. Other measurements of hepatocyte functionality, such as urea synthesis and hepatic transport activity, would be useful.

Hepatocyte functionality was measured for only seven days. Tissue engineered liver constructs may need to maintain the functionality and viability of a large mass of isolated PHH for longer periods of time, even up to six weeks. Future studies should measure hepatoycte functionality for longer periods.

The biochemical composition of HLECM and PLECM digests are unknown. A biochemical profile detailing the structural and functional proteins present in HLECM and PLECM digests

would be useful, and should include the types of collagen, glycosaminoglycans, and growth factors present.

Due to large variability from donor to donor, no statistical significances were measured in any of the hepatocyte functionality assays. However, trends in some of the donor cases indicated increased hepatocyte functionality of PHH cultured with PLECM and HLECM overlays compared to PHH cultured on type-1 collagen. If more patient samples were added to the study, the data may become statistically significant. However, the availability of human liver tissues for PHH isolation is limited and very costly.

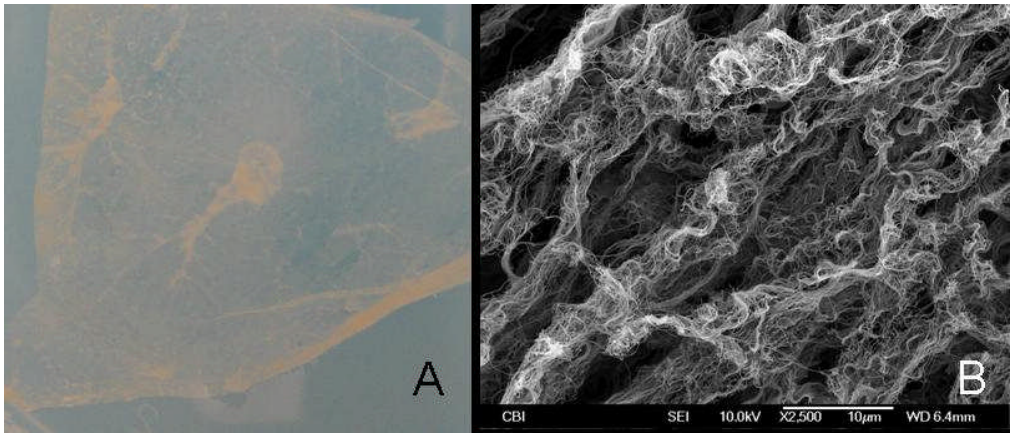

Figure 1. Macroscopic image of the sheet form of (A) HLECM and (B) SEM of HLECM (2500x).

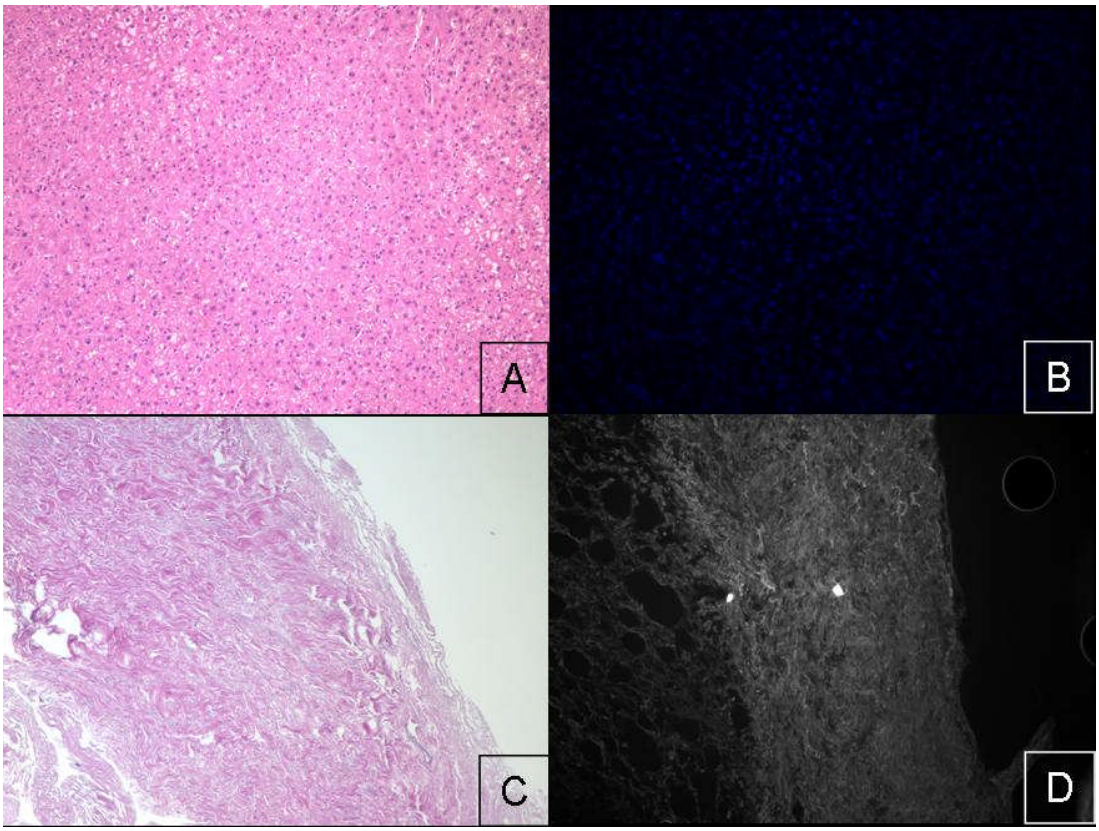

Figure 2. Native human liver and decellularized human liver ECM (100x). (A) Hematoxylin and eosin staining of native human liver and (B) DAPI staining of native human liver. (C) Hematoxylin and eosin staining and (D) DAPI staining of HLECM. Note the lack of intact nuclei after decellularization.

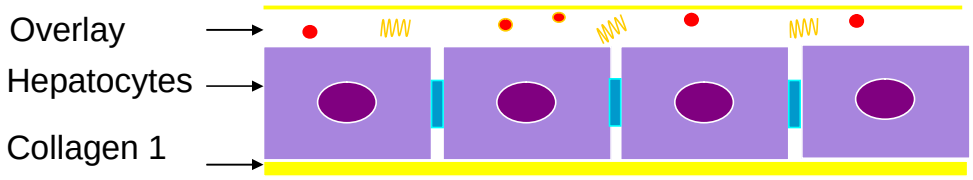

Figure 3. Schematic of experiment. PHH are plated on type-1 collagen. After 24 hours, either a MG, HLECM, or PLECM overlay was added.

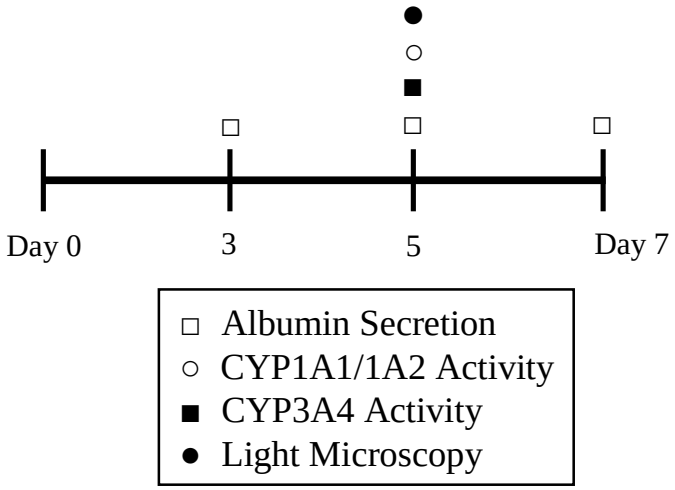

Figure 4. Schematic of techniques and assays used to profile hepatocyte phenotype.

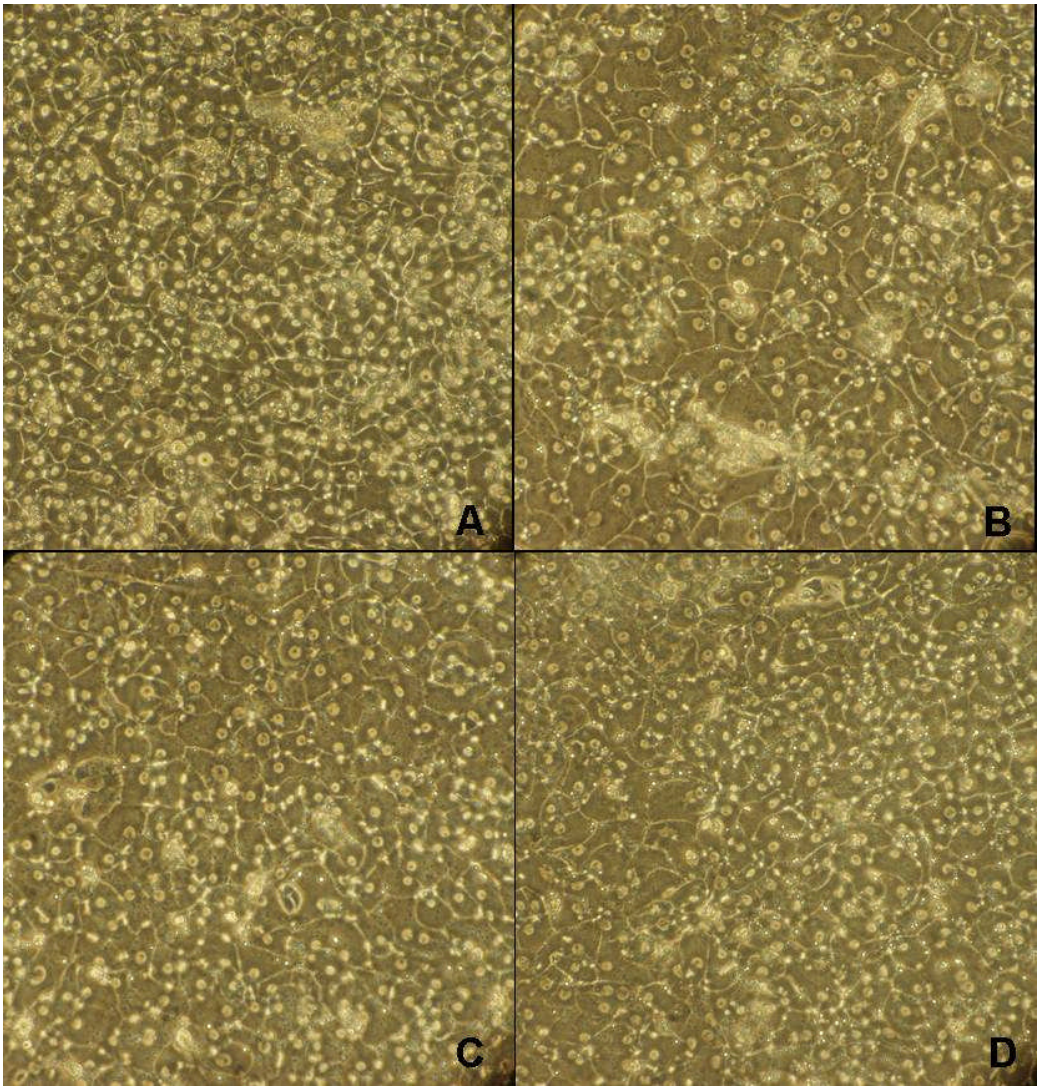

Figure 5. Primary human hepatocyte at day ten. Comparison of morphologic appearance of PHH cultured on (A) type-1 collagen, or (B) type-1 collagen with MG overlay, or (C) with HLECM overlay or (D) PLECM overlay (200x).

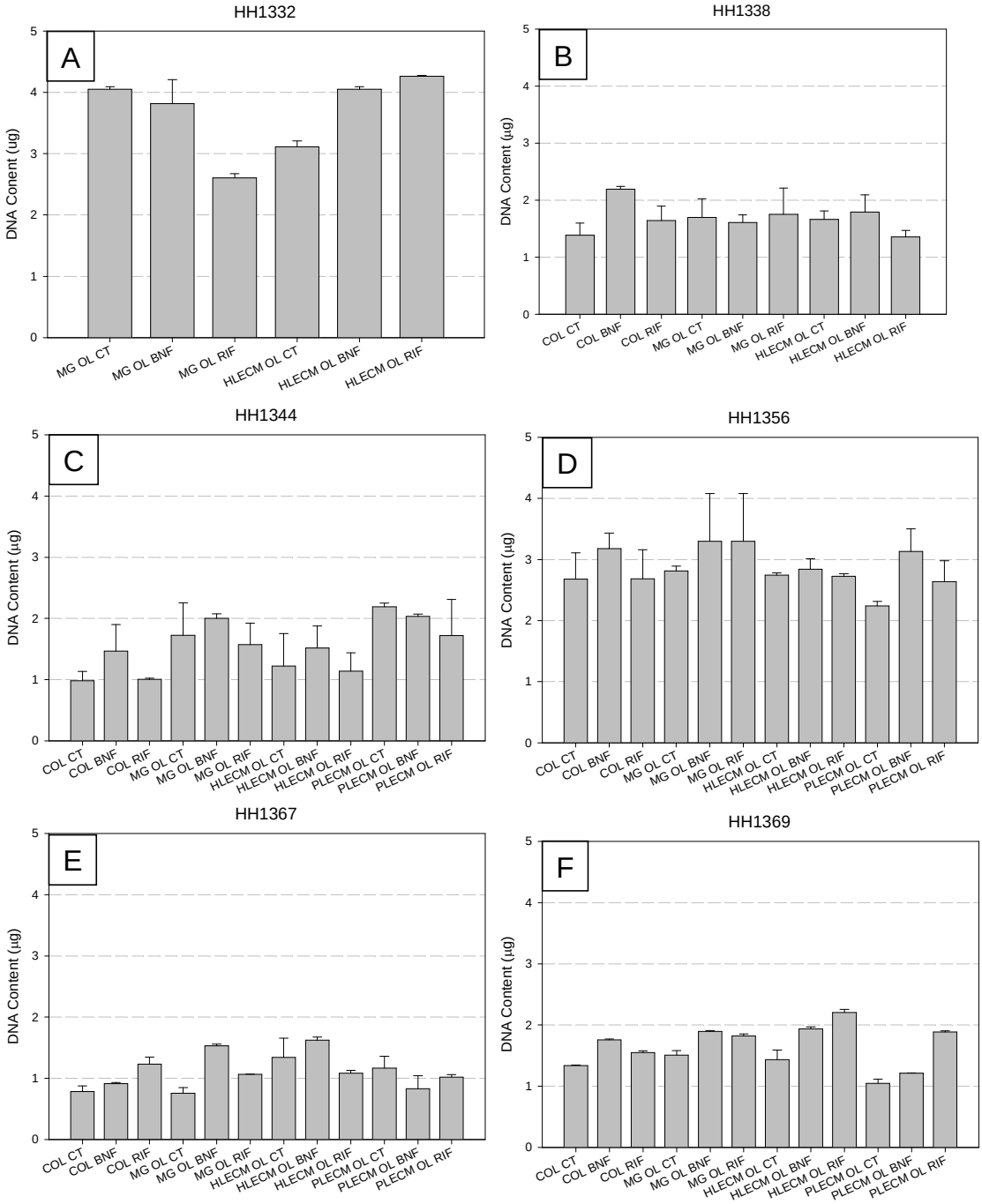

Figure 6. DNA content of PHH derived from different livers. Values are expressed as mean±SD. CT represents control (non-induced PHH), BNF represents BNF-induced PHH, and RIF represents RIF-induced PHH.

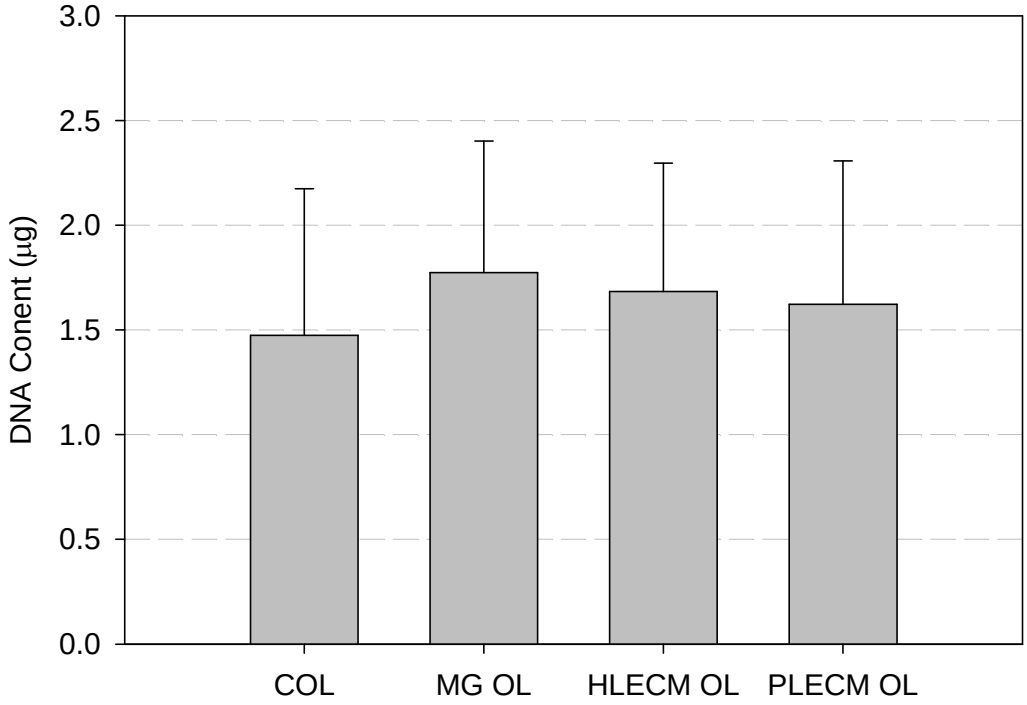

Figure 7. Average DNA content of PHH cultured on type-1 collagen, or on type-1 collagen with either MG, HLECM, or PLECM overlay. Values represent mean±SD of five livers.

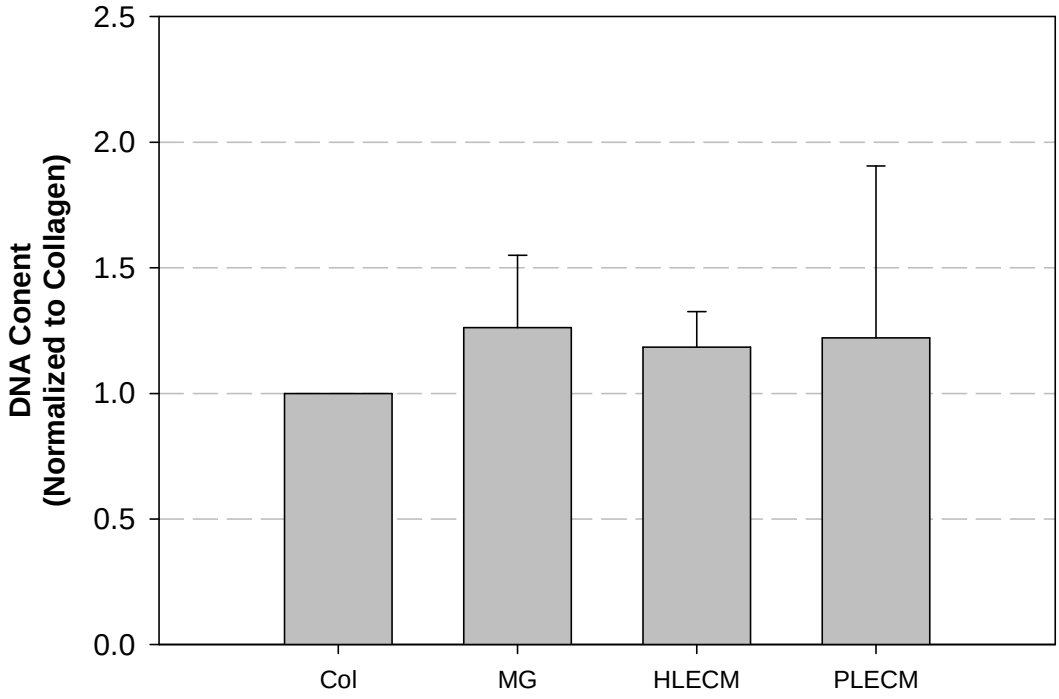

Figure 8. Effect of ECM overlay on DNA Content. Data was normalized to DNA content of PHH cultured on type-1 collagen only. Values represent mean±SD of five livers.

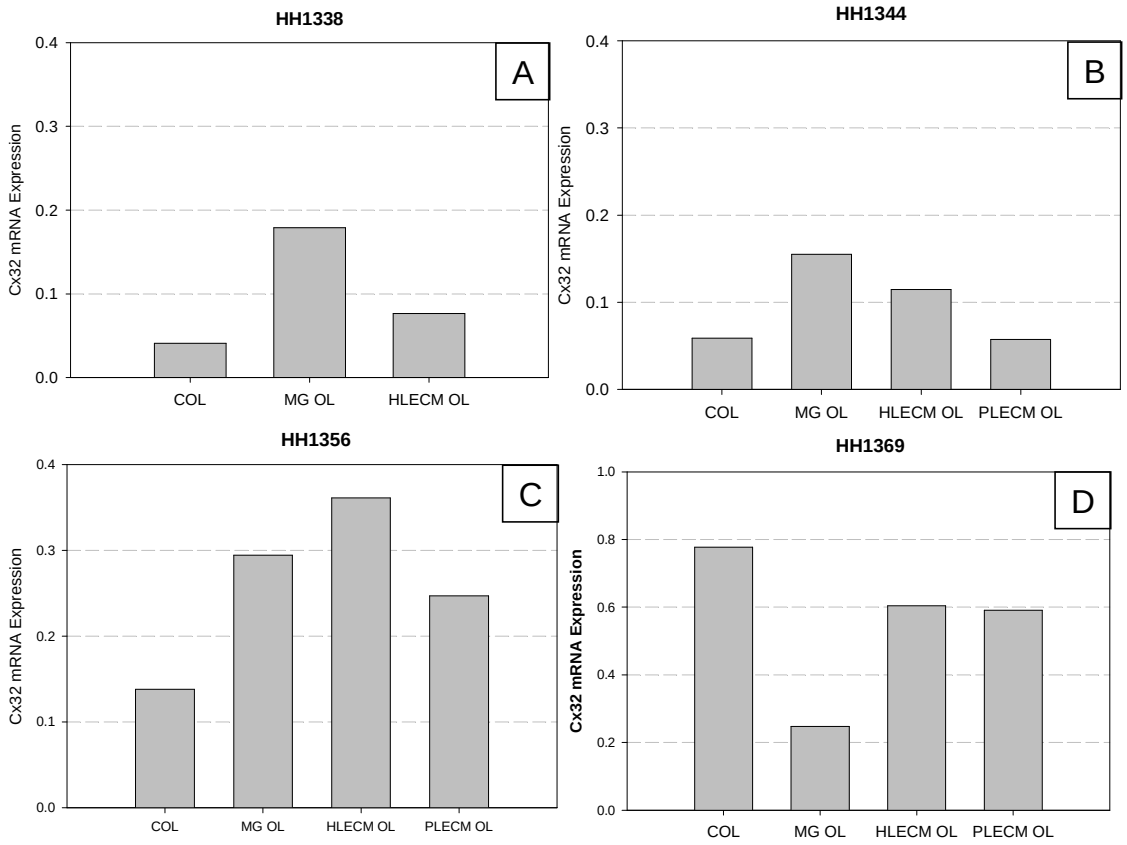

Figure 9. Effect of ECM overlay on Cx32 mRNA expression at day five. PHH were cultured on type-1 collagen or type-1 collagen with either MG, HLECM, or PLECM overlay. All mRNA values are normalized to cyclophilin expression.

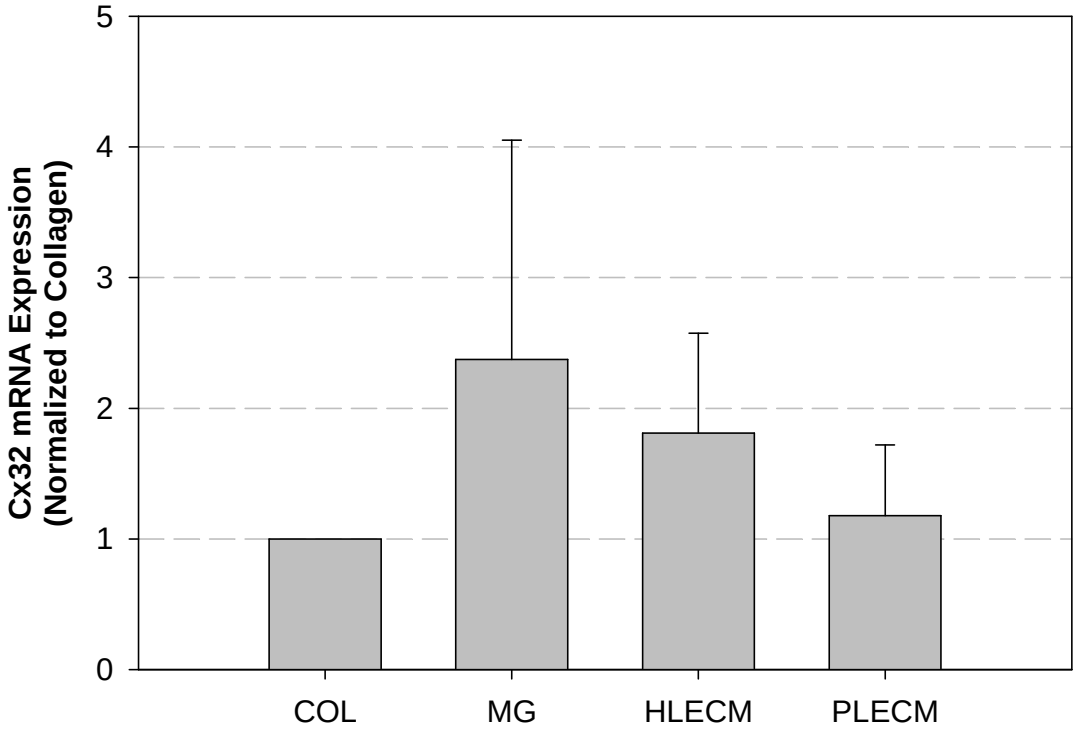

Figure 10. Effect of ECM overlay on average Cx32 mRNA expression at day five. Average Cx32 mRNA expression of PHH cultured on type-1 collagen only or type-1 collagen with either MG, HLECM, or PLECM overlay. Data normalized to Cx32 mRNA expression of PHH cultured on type-1 collagen only. Values represent mean±SD of four livers.

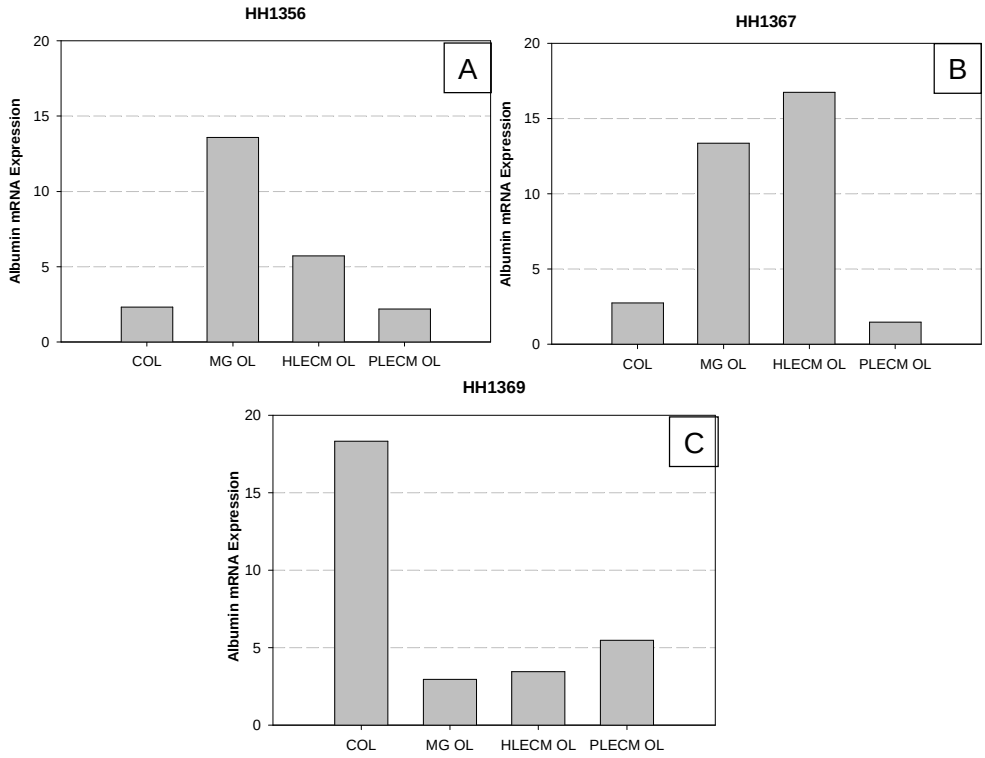

Figure 11. Effect of ECM overlay on albumin mRNA expression of PHH derived from (A) HH1356, (B) HH1367, and (C) HH1369 at day five. All mRNA values are normalized to cyclophilin expression.

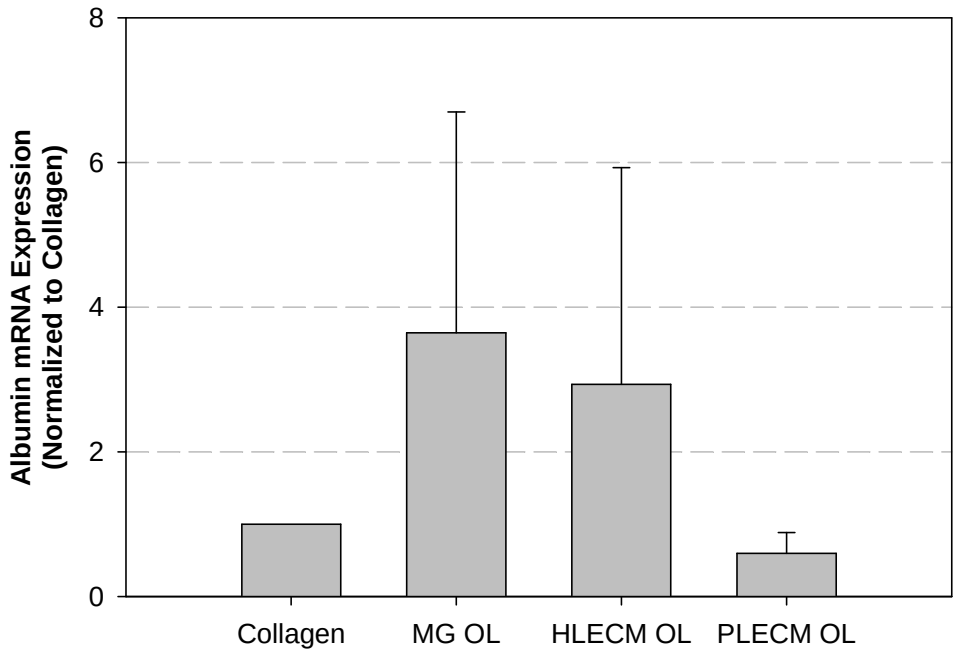

Figure 12. Effect of ECM overlay on average albumin mRNA expression. Average albumin mRNA expression of PHH cultured on type-1 collagen only or type-1 collagen with either MG, HLECM, or PLECM overlay at day five. All data was normalized to albumin mRNA data from PHH cultured on type-1 collagen only. Values represent mean±SD of three livers.

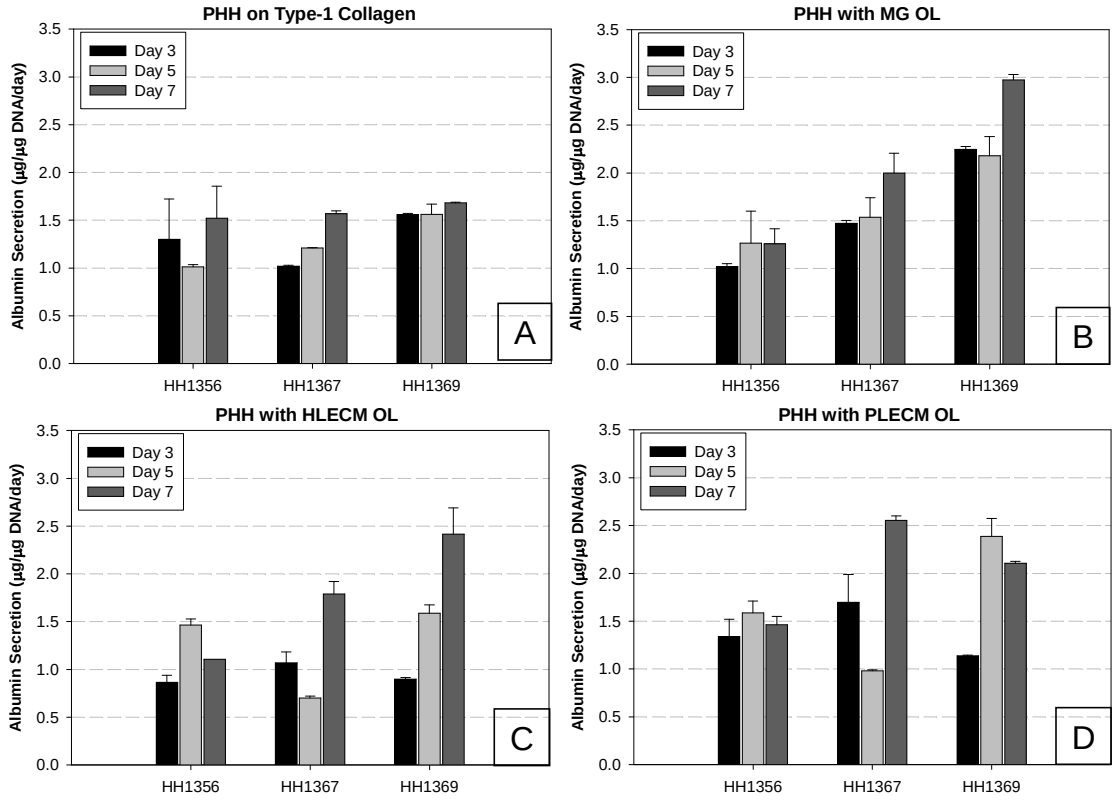

Figure 13. Effect of ECM overlay on albumin secretion of PHH at days three, five, and seven. PHH cultured on (A) type-1 collagen only, or on (B) type-1 collagen with MG, (C) HLECM, or (D) PLECM overlay. Values represent mean±SD.

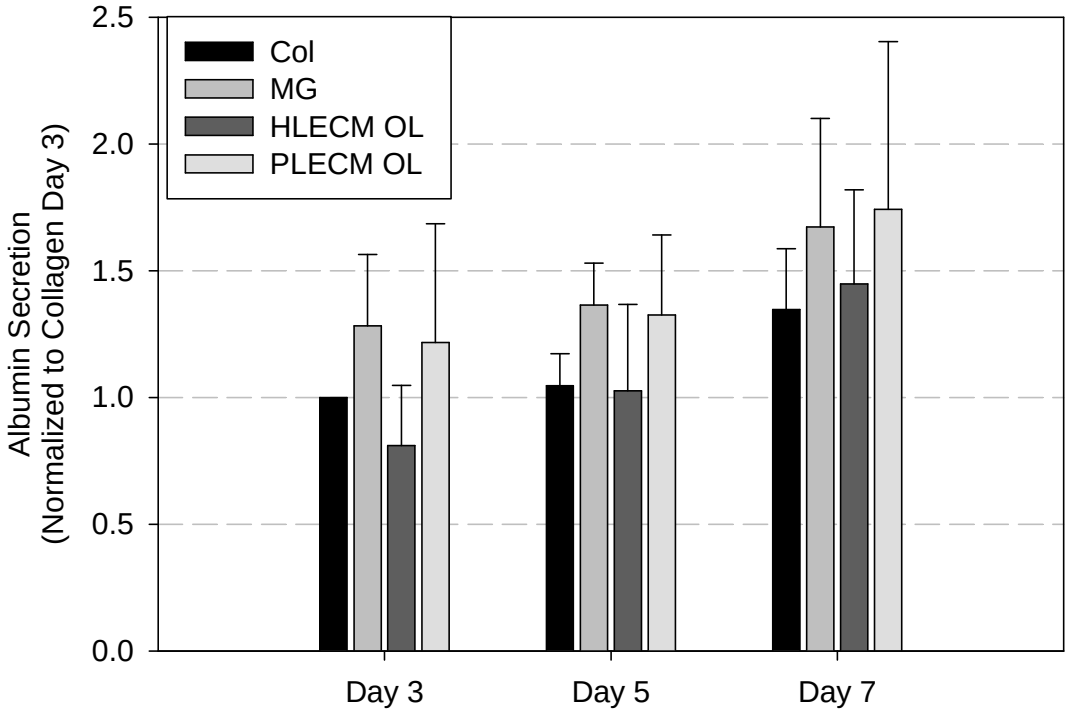

Figure 14. Effect of ECM overlay on average albumin secretion of PHH. Average albumin secretion at days three, five, and seven of PHH cultured on type-1 collagen only or type-1 collagen with either MG, HLECM, or PLECM overlay. All data was normalized to albumin secretion of PHH cultured on type-1 collagen only at day three. Values represent mean±SD of three livers.

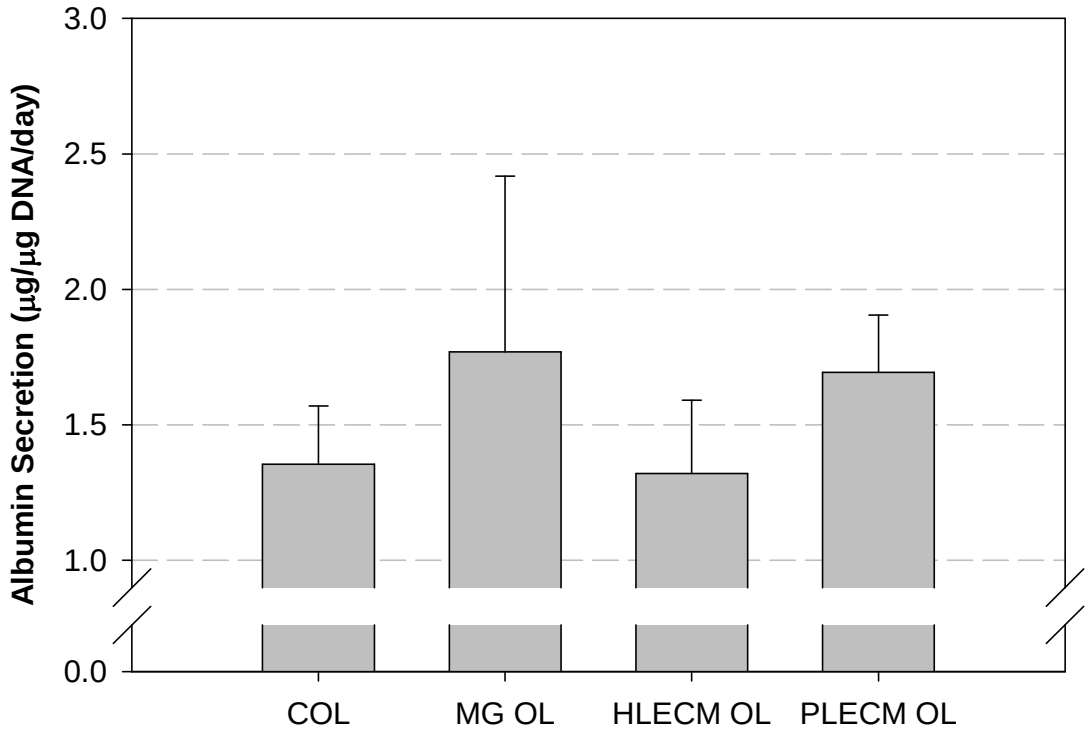

Figure 15. Effect of ECM overlay on average albumin secretion per day of PHH. Average albumin secretion per day of PHH cultured on type-1 collagen only or type-1 collagen with either a MG, HLECM, or PLECM overlay. Values represent mean±SD of three livers.

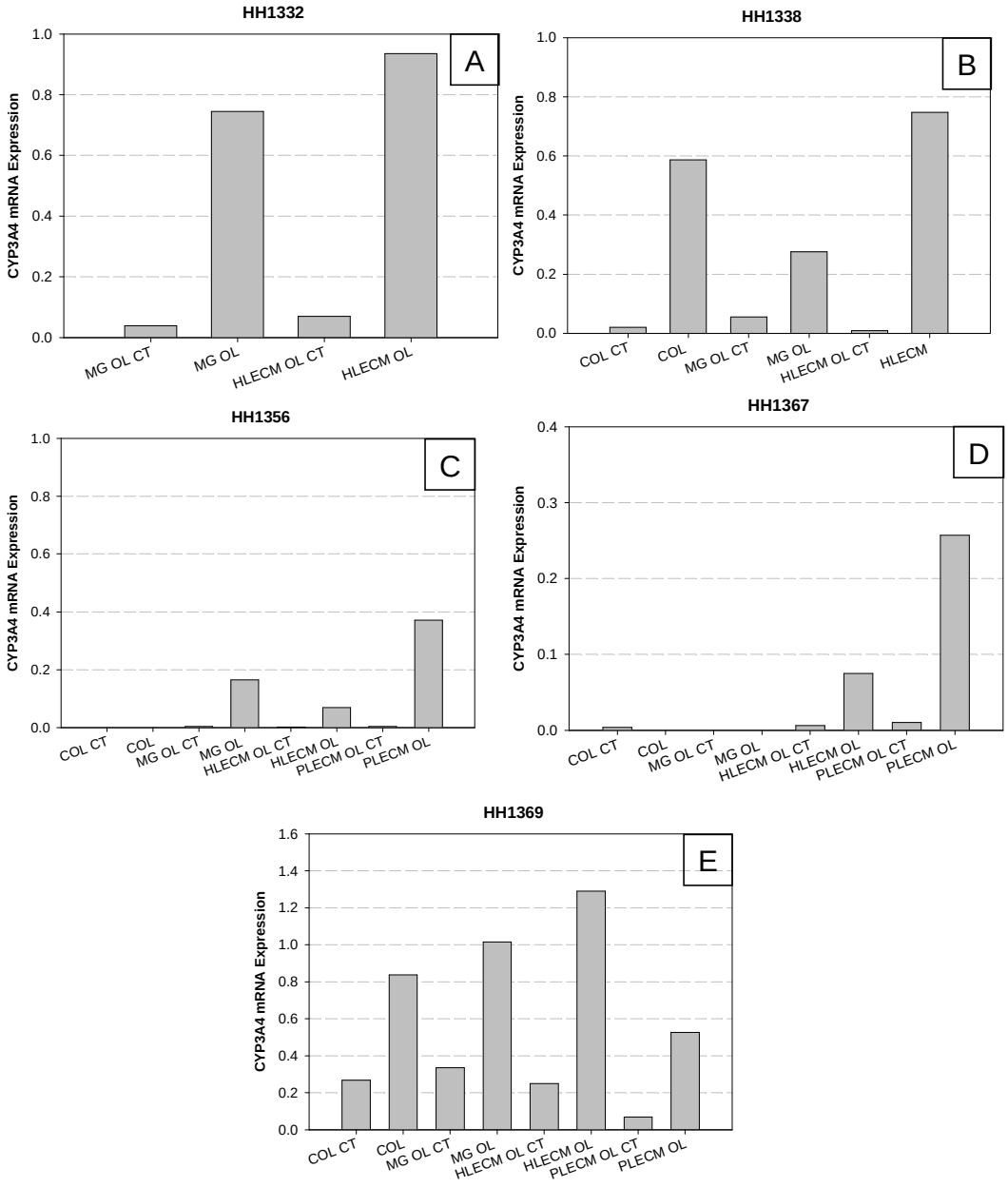

Figure 16. Effect of ECM overlay on CYP3A4 mRNA expression at day five. PHH were cultured on type-1 collagen or type-1 collagen with either MG, HLECM, or PLECM overlay. CT represents control (non-RIF induced PHH). Values represent mean±SD. All data was normalized to cyclophilin expression.

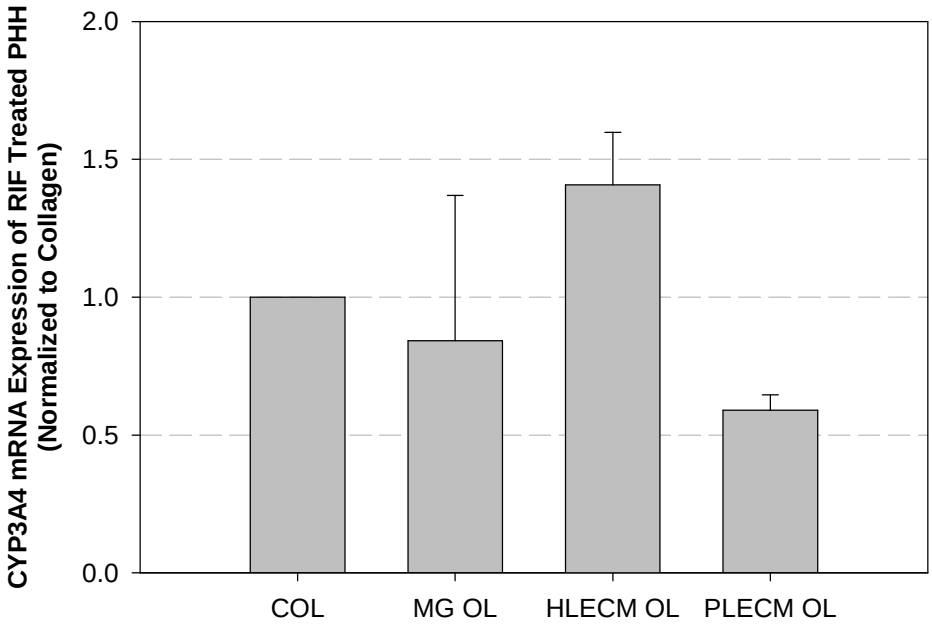

Figure 17. Effect of ECM overlay on average CYP3A4 mRNA expression at day five. PHH were cultured on type-1 collagen or type-1 collagen with either MG, HLECM, or PLECM overlay. Data normalized to CYP3A4 mRNA expression of PHH cultured on type-1 collagen. All data was normalized to cyclophilin expression. Values represent mean±SD. Values represent mean±SD of four livers.

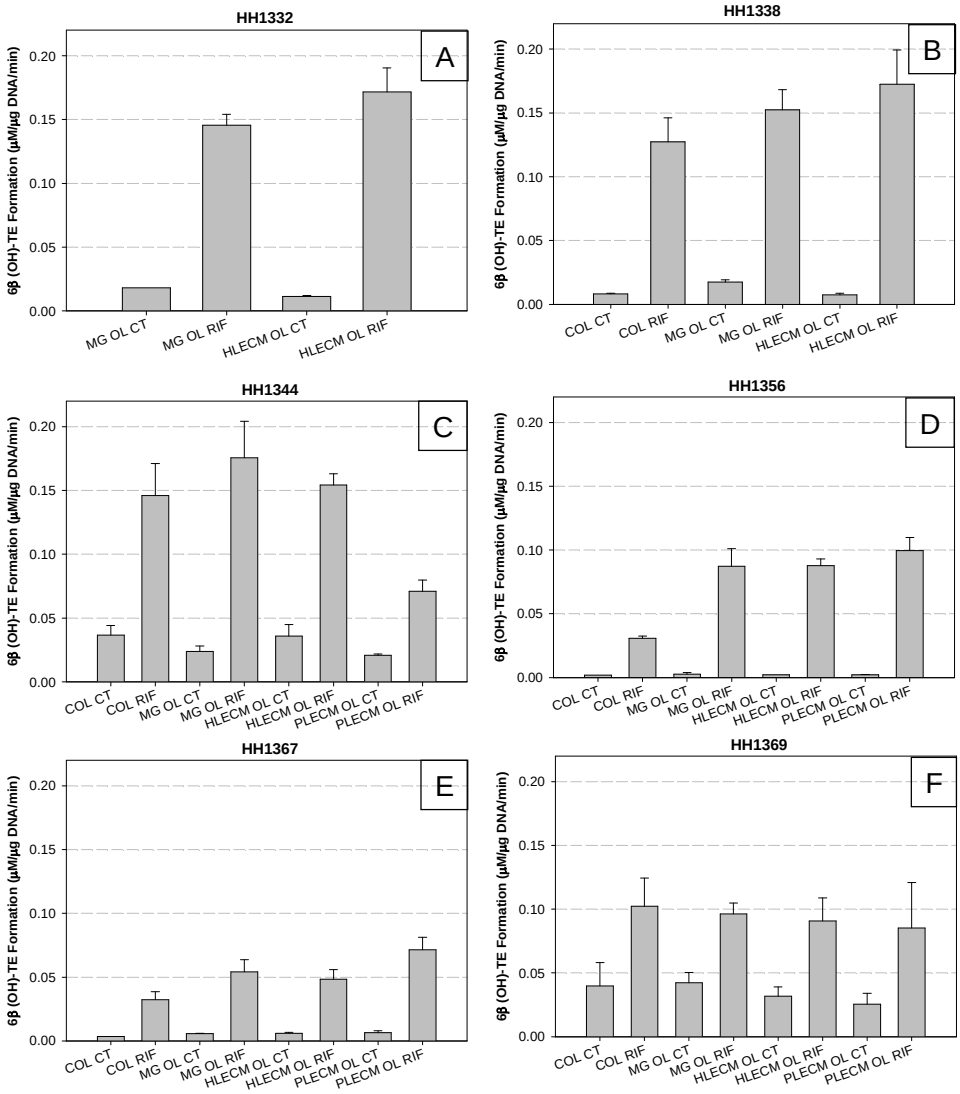

Figure 18. Effect of ECM overlay on CYP3A4 activity (6β(OH)-TE formation) at day five. PHH were cultured on type-1 collagen only or type-1 collagen with either MG, HLECM, or PLECM overlay. Values represent mean±SD. CT represents control (non-induced PHH), BNF represents BNF-induced PHH, and RIF represents RIF-induced PHH.

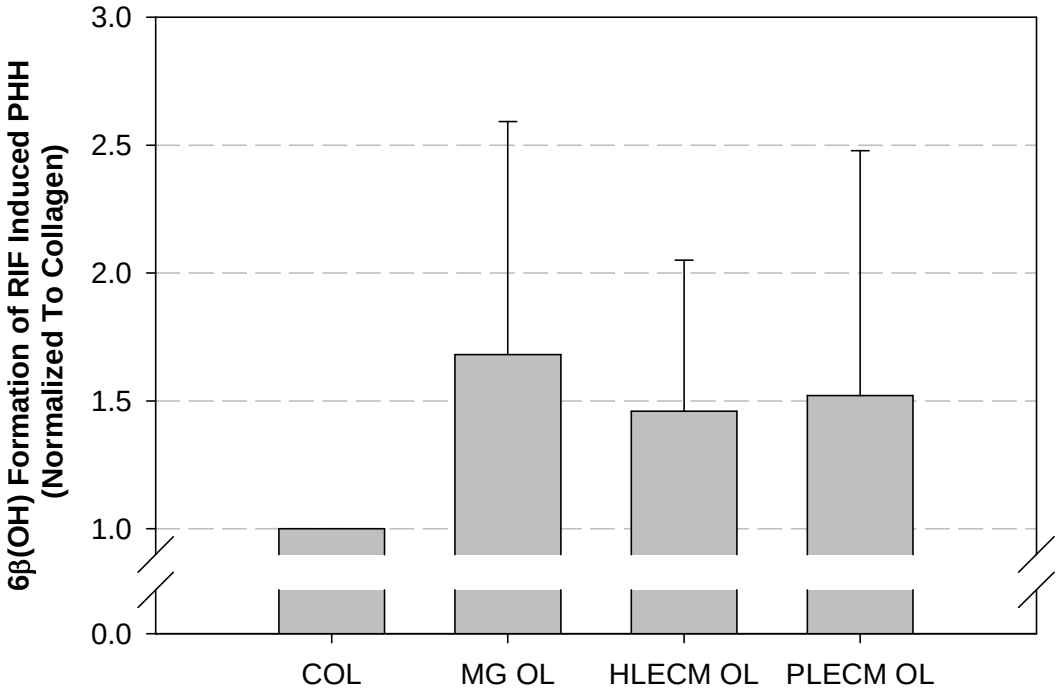

Figure 19. Effect of ECM overlay on RIF-induced CYP3A4 activity of PHH at day five. PHH were cultured on type-1 collagen only or type-1 collagen with either MG, HLECM, or PLECM overlay. All data was normalized to 6β(OH) formation of RIF Induced PHH cultured on type-1 collagen only. Values represent mean±SD of four livers.

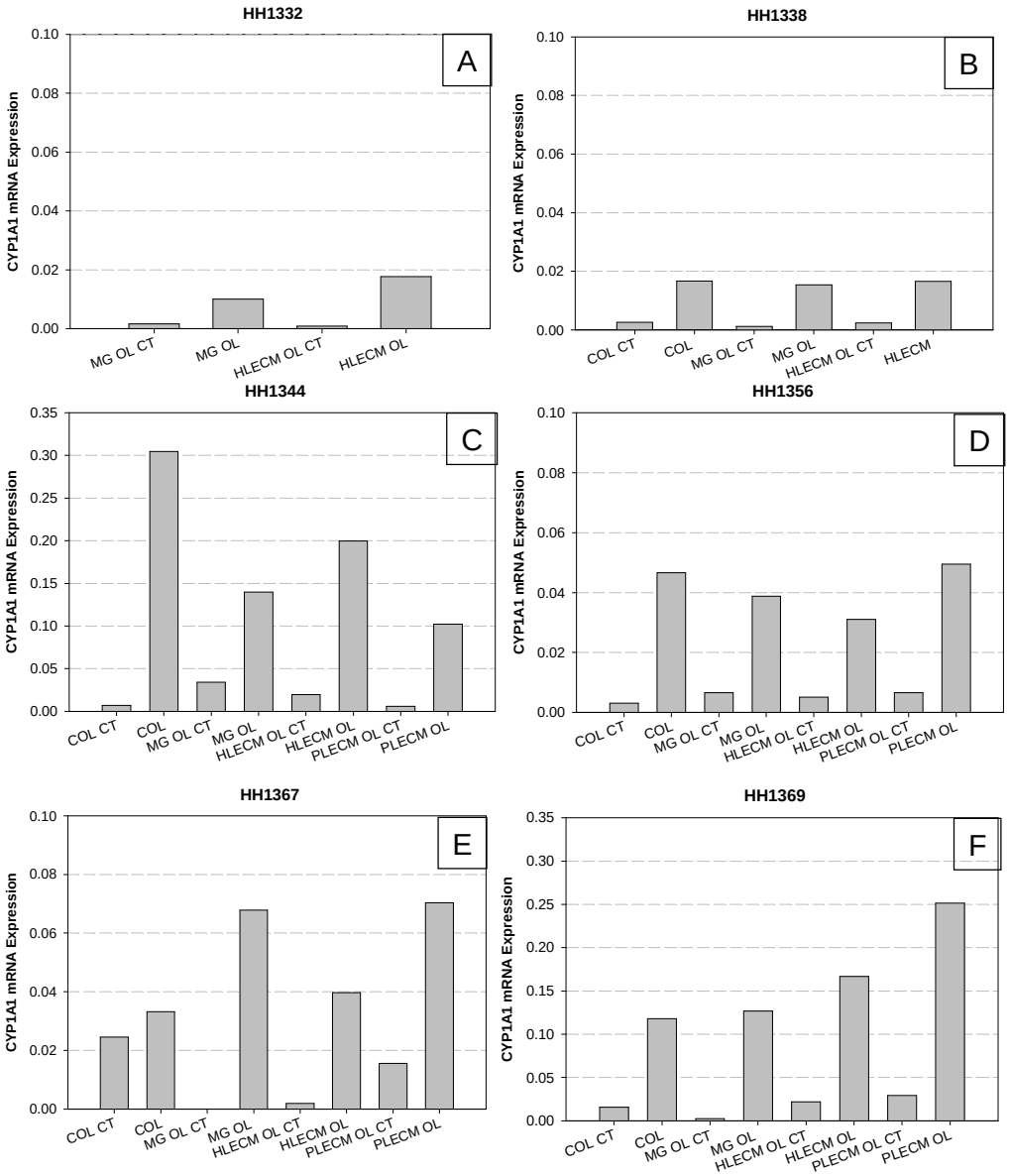

Figure 20. Effect of ECM overlay on CYP1A1 mRNA expression at day five. PHH cultured on type-1 collagen or type-1 collagen with either MG, HLECM, or PLECM overlay. Values represent mean±SD. All data was normalized to cyclophilin expression. CT represents control (non-induced PHH).

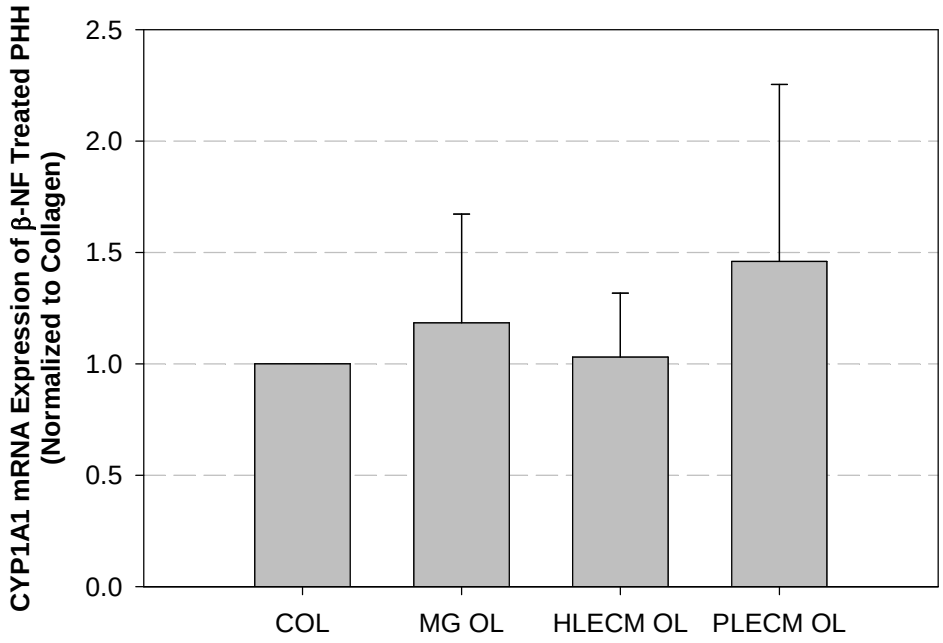

Figure 21. Average CYP1A1 mRNA expression of PHH cultured on type-1 collagen only or type-1 collagen with either MG, HLECM, or PLECM overlay. All data was normalized to CYP1A1 mRNA expression of PHH cultured on type-1 collagen only. Values represent mean±SD of six livers.

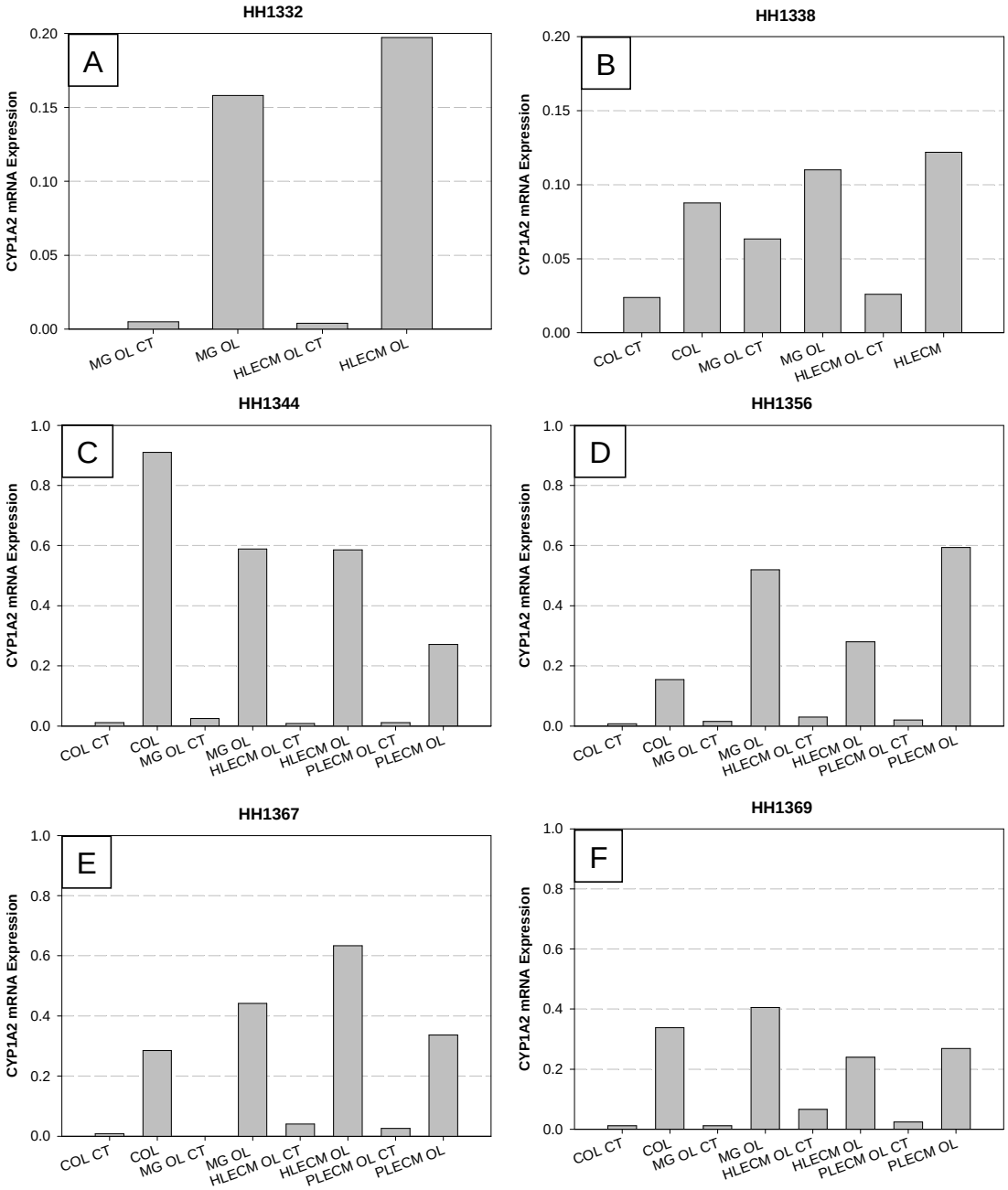

Figure 22. Effect of ECM overlay on CYP1A2 mRNA expression at day five. PHH were cultured on type-1 collagen or type-1 collagen with either MG, HLECM, or PLECM overlay. Values represent mean±SD. All data was normalized to cyclophilin expression. CT represents control (non-induced PHH).

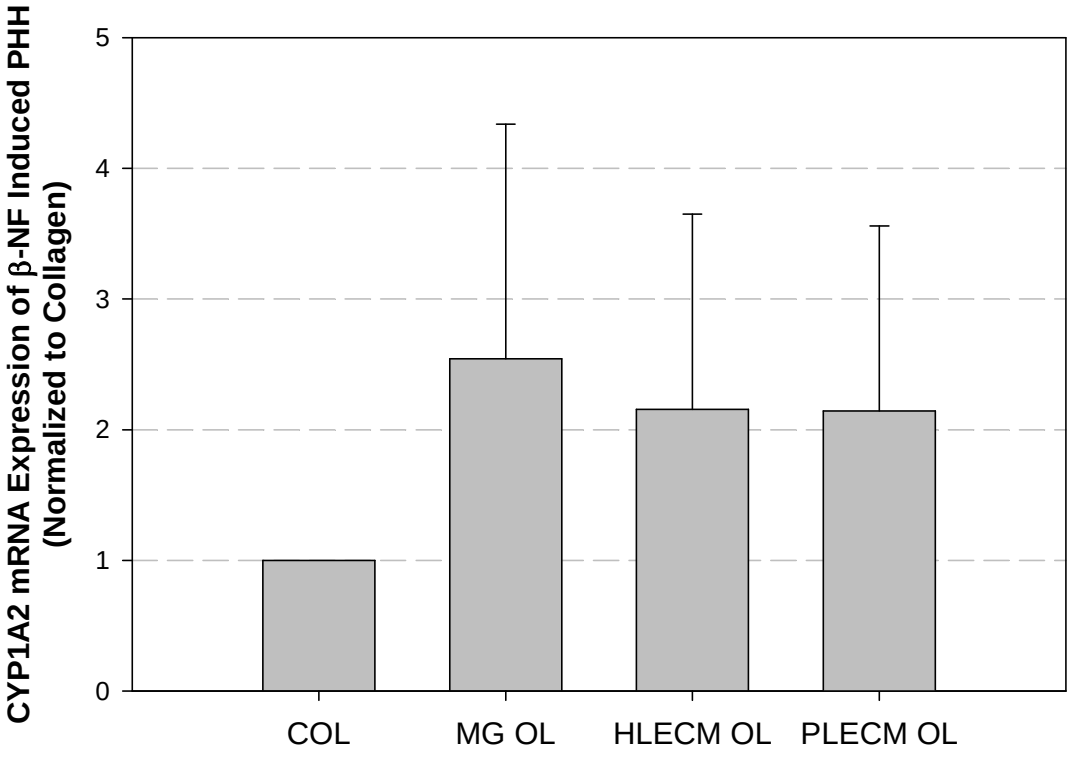

Figure 23. Average CYP1A2 mRNA expression of PHH cultured on type-1 collagen only or type-1 collagen with either MG, HLECM, or PLECM overlay. All data was normalized to CYP1A2 mRNA expression by PHH cultured on type-1 collagen only. Values represent mean±SD of six livers.

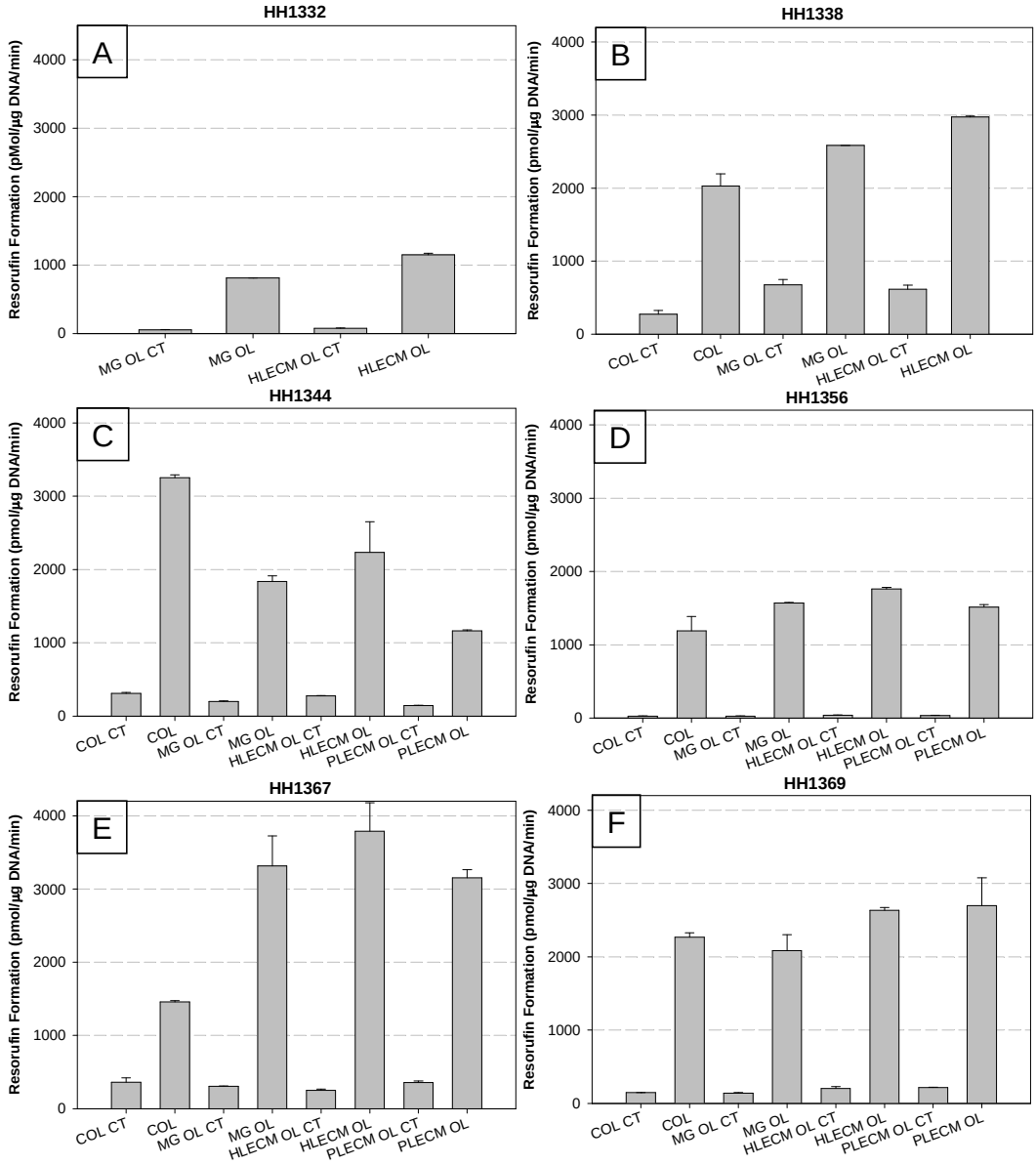

Figure 24. Effect of ECM overlay on βNF-induced CYP1A1/1A2 activity (resorufin formation) of PHH at day five. PHH were cultured on type-1 collagen or type-1 collagen with either MG, HLECM, or PLECM overlay. Values represent mean±SD. CT represents control (non-induced PHH).

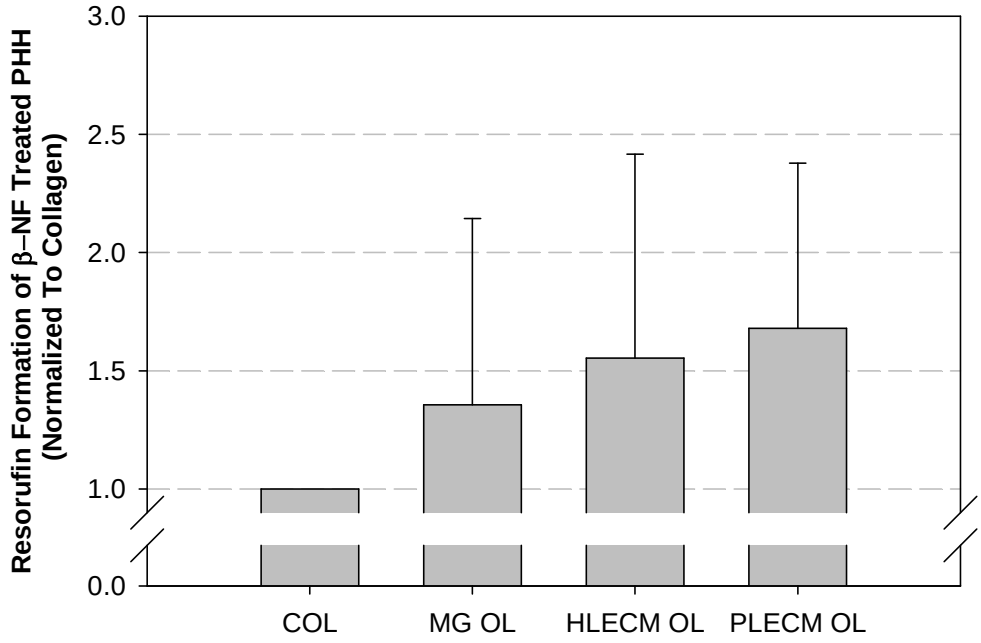

Figure 25. Average βNF-induced CYP1A1/1A2 activity (resorufin formation) of PHH at day five. PHH were cultured on type-1 collagen or type-1 collagen with either MG, HLECM, or PLECM overlay. Data normalized to resorufin formation of β-NF treated PHH on type-1 collagen. Values represent mean±SD of six livers.

6.0 SPECIFIC AIM 2: EFFECT OF PORCINE-DERIVED ECM SANDWICH CONFIGURATION ON HEPATOCYTE SPECIFIC FUNCTION

Liver disease is the eleventh leading cause of mortality and results in over 25, 000 deaths per year in the United States [5]. Allogeneic liver transplantation is the treatment of choice for patients with end-stage liver disease but is limited by both the high cost and severe shortage of donor organs [111]. Both whole organ xenotransplantation and hepatocyte transplantation provide alternative therapies but have had limited clinical success [8]. Tissue engineering and regenerative medicine approaches for the reconstruction of functional liver tissue are being widely investigated and typically involve the use of cells, scaffolds, and bioactive factors [8, 112-114]. The present study is predicated upon the hypothesis that the scaffold or substrate upon which hepatocytes are seeded is a critical determinant of cell phenotype and function.

In vitro culture of hepatocytes is associated with dedifferentiation, decreased hepatocyte-specific functions [71] such as albumin secretion, hepatic transport activity, and ammonia metabolism, and loss of hepatocyte polarity. The identification of a substrate that can maintain a functional hepatocyte differentiation profile would represent an advancement toward development of a tissue engineered liver substitute.

Individual ECM components or combinations of desired ECM components have been used as substrates for hepatoycte culture systems for several decades [37, 65, 66]. While cell culture substrates composed of individual ECM proteins such as type-1 collagen, laminin and

fibronectin have facilitated primary rat hepatocyte attachment and maintainence of selected liver-specific functions and hepatocyte polarity and morphology for short periods of culture, these systems are insufficient to prevent dedifferentiation of hepatocytes [17, 28].

Conventional *in vitro* culture models for hepatocytes include the use of a sandwich configuration in which hepatocytes are placed between two layers of either type-I collagen, Matrigel (MG) or are cultured on type-1 collagen overlaid with MG [26, 66, 72, 73, 76]. Sandwich culture of primary hepatocytes maintains hepatoycte polarity and morphology better than hepatocytes cultured on a single layer of type-I collagen or MG [35, 69, 74]. Further, hepatocyte-specific functions, such as albumin secretion, urea synthesis and cytochrome P450 responsiveness and inducibility are enhanced when the sandwich culture model is used [15, 26, 28, 66, 73, 75, 86, 115].

The present study investigated the ability of extracellular matrix derived from porcine liver (PLECM) to support the following primary human hepatocyte (PHH)-specific functions *in vitro:* albumin secretion, hepatic transport activity and ammonia metabolism. The mRNA expression levels of albumin, bile salt export pump (BSEP), and sodium taurocholate cotransporting polypeptide (NTCP) were also measured.

6.1 OVERVIEW OF EXPERIMENTAL DESIGN

PHH were harvested from six human donor livers of different age groups, genders, and medical histories. PHH viability was determined by trypan blue exclusion (Table 3). PHH were

cultured on either (1) adsorbed type-I collagen, (2) Matrigel™ (MG) overlaid with Matrigel™ (MG sandwich), or (3) on adsorbed PLECM overlaid with PLECM gel (PLECM sandwich). Albumin secretion, hepatic transport activity and ammonia metabolism were evaluated at selected days during a ten day culture period and were used as indicators of hepatocyte functionality (Figure 1). The mRNA levels of albumin, BSEP and NTCP were quantified.

6.2 METHODS

6.2.1 Reagents

Pepsin, sodium hydroxide, glycerol, dibasic sodium phosphate, monobasic sodium phosphate, dexamethasome, EDTA and ethidium bromide were purchased from Sigma Chemical Co. (St. Louis, MO). Trypsin was purchased from Gibco (Carlsbad, CA). Type-1 collagen was purchased from Becton Dickinson (Franklin Lakes, OR). Quant-iT PicoGreen Assay was obtained from Invitrogen-Molecular Probes (Eugene, OR). Triton-X 100 and sodium deoxycholic acid were purchased from Spectrum (Gardena, CA). Hepatocyte Maintainence Media (HMM) was purchased from Cambrex (Baltimore, MD). Penicillin, streptomycin and bovine calf serum were purchased from Gibco (Carlsbad, CA). Trizol reagent was purchased from Invitrogen (Carlsbad, CA). Hanks balanced salt solution (HBSS) was purchased from Lonza (Walkersville, MD). All quantitative real-Time RT PCR reagents were purchased from Applied Biosystems (Foster City, CA). Cyclophilin, albumin, BSEP and NTCP were synthesized by Applied Biosystems and the assay identification numbers are: cyclophilin (Hs03045993_gH), albumin (Hs00910222_m1), BSEP (Hs00184824_m1) and NTCP (Hs00161820_m1).

6.2.2 Isolation and Preparation of PLECM Sheet Form

The methods used to isolate porcine liver ECM (PLECM) have been previously described [28, 44, 104]. Livers were harvested from market weight pigs (~110-130kg) immediately after euthanasia. The tissues were rinsed with tap water and frozen until used. Each liver lobe was cut into 5 mm thick slices with a rotating blade and subjected to three separate 30 minute washes in deionized water with mechanical agitation on an orbital shaker. The sections were then gently massaged to aid in cell lysis and soaked in 0.02% trypsin/0.05% EDTA at 37° C for one hour. The tissue was rinsed in deionized water and the massaging was repeated followed by mechanical agitation of the liver sections in 3% Triton X-100 for 1 hour. The rinsing and massaging process was repeated until all visible remnants of cellular material were removed. The tissue sections were then mechanically agitated in 4% sodium deoxycholic acid for one hour followed by extensive rinsing in water. The remaining decellularized connective tissue matrix was referred to as PLECM [28].

After processing, the PLECM was immersed in a solution of 0.1% peracetic acid followed by repeated rinses in water or phosphate buffered saline at pH 7.4. Complete decellularization was evaluated by hematoxylin & eosin staining, nuclear (DAPI) staining, and measurement of total DNA with Quant-iT Picogreen dsDNA Kit.

6.2.3 Preparation of PLECM Gel Form

The method used to prepare a gel form of harvested ECM has been previously described [99]. The protocol was modified to produce a gel form of porcine-derived liver.

First, a powdered form of PLECM was produced from sheets of PLECM. The hydrated, sheet form of the disinfected PLECM was lyophilized overnight. Lyophilized sheets of PLECM were cut into small pieces, then placed in a rotary knife mill (Wiley Mill) to create a particulate form of the PLECM. Particles less than 250 micron were collected by sieve through a #60 screen.

One gram of lyophilized PLECM powder and 100 mg of pepsin (2000-3000 U/mg) were mixed in 100 mL of 0.01 M HCl and stirred for ~72 hours at room temperature (25ºC). The final viscous solution of digested PLECM or pre-gel solution had a pH of approximately 3.0 - 4.0.

Formation of PLECM gels was initiated by the addition of 0.1 N NaOH (1/10 of the volume of pre-gel solution) and 10X PBS at pH 7.4 (1/9 of the volume of pre-gel solution) at 4°C. Inactivation of pepsin activity occurred when the pH was raised to 7.4. For gelation to occur, the solution was brought to the desired volume/concentration using cold (4°C) 1X PBS at pH 7.4 and was then placed at 37°C.

6.2.4 Preparation of Hepatocyte Culture Dishes

Type-1 collagen (0.3 mg/ml) and PLECM (0.3 mg/ml) were dried overnight to 6-well plates in a laminar flow hood. Plates were sealed in Parafilm and stored at 4°C until use. On the day of the experiment, MG (0.3 mg/ml) was coated onto 6-well plates.

6.2.5 Isolation and Culture of Primary Human Hepatocyte

Hepatocytes were isolated from either donor livers that were not used for transplantation or from areas of hepatic tissue that were not involved in tumor from tissue resections for cancer.

All human subject protocols were reviewed and approved by the University of Pittsburgh Institutional Review Boards. Significant amounts of steatosis (fat) were not observed in any of the livers. Viability of the hepatocytes at the time of plating was greater than 76%, as measured by trypan blue exclusion (Table 3).

PHH were isolated by a three-step collagenase perfusion of human liver [106] and seeded in 12-well plates precoated with either adsorbed type-1 collagen, PLECM or MG at a density of $1.5x10^6$ cells per well. Hepatocytes were seeded in HMM supplemented with 10^{-7} M dexamethasome, 10^{-7} M insulin, 100 U/mL penicillin, 100 µg/ml streptomycin and 10% bovine calf serum. After 4 hours of culture at 37° C, the media was replaced with serum free HMM with the supplements listed above. After 24 hrs of culture in serum free HMM, unattached PHH were removed by gentle agitation and the following overlays were added: MG substrates were overlaid with 0.3 mg/ml of MG, and PLECM substrates were overlaid with 0.3 mg/ml PLECM gel. Media was changed every 24 hours.

6.2.6 Light Microscopy

PHH were maintained in their respective culture conditions for ten days. On day ten, PHH were imaged at 100x with a light microscope (ZEISS Axiovert 40CFL with Axiocam MRc5, Thornwood, NY).

6.2.7 Measurement of DNA Content

Using a cell scraper, cells were harvested on ice in 150 µl cell harvest buffer containing: dibasic sodium phosphate (11.5 g/L), monobasic sodium phosphate (2.6 g/L), EDTA (0.033 g/L), and

20% glycerol. The cell lysates were produced by sonication and stored at –20° C. Total DNA was quantified using the commercially available Quant-iT Picogreen dsDNA Kit according to the manufacturer's instructions. For each group, a minimum of two samples were used to determine total DNA and each samples was measured in triplicate.

6.2.8 RNA Isolation

Total RNA from cell lysates was isolated using Trizol Reagent as described by the manufacturer's instructions. RNA concentration was determined by spectrophotometer at 260 nm. The purity of RNA was determined by spectrophotometry at 280 nm/260 nm ratio, and the integrity checked by agarose gel electrophoresis stained with ethidium bromide. RNA was stored at −80° until further use.

6.2.9 Quantitative Real Time RT-PCR

mRNA expression levels of Cx32 (from all donors), albumin (from donors HH1400, HH1412, HH1423), BSEP (from donors HH1416, HH1417, HH1419, HH1423), and NTCP (from donors HH1416, HH1417, HH1419, HH1423) were determined using TaqMan quantitative reverse-transcriptase polymerase chain (TaqMan QRT–PCR) assays. From each group, 2 µg of total RNA was incubated with 5 U RQ DNase, 5 µL 10 x RQ buffer in a total volume of 10 µL at 37°C for 30 min. The samples were then incubated with 1 µL RQ DNase Stop Solution at 65°C for 10 min. The DNAse treated RNA was then incubated with 1 µL of random hexamer primers (100 ng/ L) at 70°C for 5 min for cDNA synthesis. cDNA generation

continued with incubation at 37°C for 60 min with the following reagents: 1 µL dNTP (10 mmol/L of each), 5 µL MMLV 5x, and 1 µL MMLV RT for a total volume of 12 µL.

TaqMan one-step RT–PCR assays were performed with 4 ng of each RNA sample in a final reaction volume of 72 µL prepared from TaqMan one-step RT–PCR Master Mix Reagents Kit. Assays were performed using an Applied Biosystems' ABI Prism 7900HT sequence detection system. An initial RT step occurred for 30 min at 48° and was subsequently followed by heating to 95° for 10 min followed by 40 cycles of 95° for 15 s, 60° for 1 min.

6.2.10 Measurement of Albumin Secretion

Due to limited availability of cells, conditioned media was collected from donors HH1400, HH1412, and HH1423 on days four, six, eight, and ten, and stored at -20°C until analysis. PHH secretion of albumin was measured using a commercially available kit (Bethel Laboratories, Texas). At least three samples were collected from each culture condition and each sample was measured in triplicate. All data was normalized to total DNA content.

6.2.11 Measurement of Hepatic Transport Activity

Hepatic transport activity was measured for donors HH1416, HH1417, HH1419, and HH1423 as previously described [116]. Briefly, on day five, media was aspirated from PHH and PHH were incubated in Hank's balanced salt solution (HBSS) containing cations (calcium and magnesium) for 20 minutes at 37°C. After this incubation period, the HBSS (with cations) was aspirated and replaced with HBSS (with cations) containing 1 µM [3H]-taurocholate. Following incubation of PHH with 1 µM [3H]-taurocholate for 20 min at 37°C, the solution was aspirated

and the PHH were rinsed three times with ice cold HBSS (with cations). PHH were incubated with either: (1) HBSS containing cations and (2) HBSS without cations for 20 minutes. The media was collected and cells harvested in 1 mL NaOH/SDS solution using a cell scraper. Each sample (0.5 mL) was then counted using a liquid scintillation counter. The harvested cell solution was stored at -80°C until DNA quantification. At least three samples were collected from each culture condition and each sample was measured in triplicate. All data was normalized to total DNA content.

6.2.12 Measurement of Ammonia Metabolism

PHH metabolism of ammonia was measured on day five for donors HH1400, HH1412, HH1419, and HH1423. Media was aspirated and PHH were incubated with 2.5 mM NH_4Cl in HMM for two hours at 37°C. The conditioned media was collected and the concentration of NH_3N was measured using a commercially available kit (Wako Pure Chemical Industries, Tokyo, Japan). At least three samples were collected from each culture condition and each sample was measured in triplicate. All data was normalized to total DNA content.

6.2.13 Statistical Analysis.

All values were calculated as mean ± S.D. All data was normalized to PHH cultured on type-1 collagen. A one-way analysis of variance with a post-hoc Tukey's multiple comparison procedure was performed. A p value of ≤ 0.05 was considered statistically significant and all calculations were performed using SAS software, version 9.1 (Cary, NC)..

6.3 RESULTS

6.3.1 Light Microscopy Images.

Hepatocytes cultured on type-1 collagen without an overlay formed flattened, confluent cell monolayers (Figure 27A). By comparison, hepatocytes cultured in MG (Figure 27B) or PLECM sandwich (Figure 27C) maintained a more three-dimensional-like appearance with characteristic cuboidal shape and formed of chord-like arrays.

6.3.2 DNA Content

PHH cultured on type-1 collagen, or in either MG or PLECM sandwich had similar DNA content (Figure 28A-F). DNA content from each culture condition was normalized to the DNA content of PHH cultured on type-1 collagen (Figure 29).

6.3.3 Effect of ECM Sandwich Configuration on Cx32 mRNA Expression

At day five, PHH derived from donors HH1412 (Figure 30A), HH1416 (Figure 30B), and HH1417 (Figure 30C) and cultured in PLECM sandwich had the highest levels of Cx32 mRNA expression. PHH derived from donors HH1419 (Figure 30D) and HH1423 (Figure 30E) and cultured in MG sandwich had the highest levels of Cx32 mRNA expression at day five.

In HH1419 and HH1423, PHH cultured in MG sandwich had the highest levels of Cx32 mRNA expression on day ten (Figures 31 A & B).

When Cx32 mRNA data of PHH cultured in MG or PLECM sandwich were averaged and normalized to PHH cultured on type-1 collagen, no differences in Cx32 mRNA levels were measured (Figure 32).

6.3.4 Effect of ECM Sandwich Configuration on Alb mRNA Expression Levels

On day five, mRNA levels of albumin were determined for donors HH1400, HH1412, and HH1423 (Figure 33A-C). Albumin mRNA levels from each culture condition were averaged and normalized to albumin mRNA expression of PHH cultured on type-1 collagen. The measured values for albumin mRNA levels of PHH cultured in MG or PLECM sandwich were 1.18±0.96 and 2.01±0.32 fold the value for PHH cultured on type-1 collagen (Figure 34).

6.3.5 Effect of ECM Sandwich Configuration on Albumin Secretion

Albumin secretion by PHH was measured on days four, six, eight, and ten. Due to large variability in albumin secretion values from donor to donor, albumin secretion values were not different between the groups regardless of the day or culture condition (Figure 35).

For donor HH1400, PHH cultured in either MG or PLECM sandwich had comparable levels of albumin secretion at day four, which were higher than the concentration for PHH cultured on type-1 collagen only (Figure 35A). On days six, eight and ten, PHH cultured in PLECM sandwich had the highest levels of albumin secretion (Figure 35A).

For donor HH1412, PHH cultured in either MG or PLECM sandwich had comparable levels of albumin secretion and the concentrations of albumin were higher than PHH cultured on type-1 collagen alone. At days six and eight, PHH had comparable levels of albumin secretion,

regardless of the culture condition. On day ten, PHH cultured PLECM sandwich had the highest levels of albumin secretion (Figure 35B).

For donor HH1423, PHH had comparable levels of albumin secretion regardless of the culture condition at day four. At days six and ten, PHH cultured in PLECM sandwich had the highest levels of albumin secretion. At day eight, PHH cultured in either MG or PLECM sandwich had comparable levels of albumin secretion and the concentrations were higher than PHH cultured on type-1 collagen only (Figure 35C).

When albumin secretion was calculated as the average amount of secretion per day, significant increases were found in the PHH cultured in either MG or PLECM sandwich compared to the PHH cultured on type-1 collagen group. PHH in MG or PLECM sandwich secreted 1.64±0.37 and 2.61±0.70 fold higher amounts of total albumin per day ($p<0.5$) (Figure 36).

6.3.6 Effect of ECM Sandwich Configuration on NTCP mRNA Expression Levels

On day five, NTCP mRNA levels were measured for donors HH1416, HH1417, HH1419, and HH1423 (Figure 37A-D). Data from each culture condition was averaged and normalized to PHH cultured on type-1 collagen only. PHH cultured on type-1 collagen or in either MG or PLECM sandwich had similar NTCP mRNA expression levels (Figure 38).

6.3.7 Effect of ECM Sandwich Configuration on BSEP mRNA Expression Levels

On day five, BSEP mRNA levels were measured for donors HH1416, HH1417, HH1419, and HH1423 (Figure 39 A-D). For donor HH1416, due to a technical difficulty with isolation of RNA from the PLECM group, BSEP mRNA levels were not measured. Data from each culture condition was averaged and normalized to PHH cultured on type-1 collagen only. PHH cultured on type-1 collagen or in either MG or PLECM sandwich had similar BSEP mRNA expression levels (Figure 40).

6.3.8 Effect of ECM Sandwich Configuration on [3H] Taurocholate Uptake

[3H] TC uptake is an indicator of hepatic transport activity and was measured in donors HH1416, HH1417, HH1419, and HH1423 (Figure 41A-D). [3H] TC uptake data from each culture condition was averaged and normalized to the data from PHH cultured on type-1 collagen. The measured values for [3H] TC uptake of PHH cultured in either a MG or PLECM sandwich were 1.34±0.16 and 1.64±0.39 fold the values of PHH cultured on type-1 collagen (Figure 42). Trends indicate that PHH cultured with PLECM sandwich had the highest levels of [3H] Taurocholate uptake but there was no significant difference between the groups (P=0.14).

6.3.9 Effect of ECM Sandwich Configuration on [3H] Taurocholate Efflux

[3H] TC efflux is an indicator of hepatic transport activity and was measured in donors HH1416, HH1417, HH1419, and HH1423 (Figure 43A-D). [3H] TC efflux data from each group

was averaged and normalized to the data from PHH cultured on type-1 collagen. PHH cultured in MG sandwich had 0.66±0.48 fold-lower levels of [3H] TC efflux compared to PHH cultured on type-1 collagen and PHH cultured in PLECM sandwich had 2.00±0.77 fold-higher levels of [3H] TC efflux compared to PHH cultured on type-1 collagen (Figure 44). The PHH cultured in PLECM sandwich had the highest levels of [3H] Taurocholate efflux and the levels were greater than PHH cultured on type-1 collagen or in between two layers of MG ($P<0.5$).

6.3.10 Effect of ECM Sandwich Configuration on Ammonia Metabolism

Ammonia metabolism by PHH was measured in HH1400, HH1412, HH1419, and HH1423 at day five (Figure 45A-D). PHH cultured in either MG or PLECM sandwich had comparable levels of ammonia metabolism in HH1400, HH1412, and HH1423, which were higher than the levels of PHH cultured on type-1 collagen (Figure 45A-B, D). For HH1419, PHH cultured in PLECM had higher levels of ammonia metabolism compared to PHH cultured on type-1 collagen or in MG sandwich (Figure 45C).

Ammonia metabolism data from each culture condition was averaged and normalized to the data from PHH cultured on type-1 collagen. PHH cultured in MG or PLECM sandwich had 1.53±0.03 and 1.64±0.15 fold higher levels of ammonia metabolism compared to PHH cultured on type-1 collagen (Figure 46).

6.4 DISCUSSION

A gel form of ECM derived from porcine liver was shown to support human hepatocyte function *in vitro* at levels equal to or greater than Matrigel or type I collagen. The PLECM gel was prepared by methods designed to maintain as much of the composition of the native liver matrix as possible. Recent studies have suggested that tissue- and organ-specific ECM can promote site appropriate differentiation of progenitor cells [117, 118] and maintain site appropriate phenotype in *in vitro* culture systems [34]. Since the ECM of each tissue and organ is produced by the resident parenchymal cells and logically represents the ideal scaffold or substrate for these cells, it is intuitive that a substrate composed of liver-derived ECM would be favorable for hepatocytes.

It has recently been demonstrated that the biologic ECM scaffolds support tissue-specific cell populations. Hepatic sinusoidal endothelial cells (SEC) maintained their differentiated phenotype the longest when cultured on ECM derived from the liver, as compared to SEC cultured on ECM derived from small intestine or urinary bladder [34]. These results suggest that ECM biologic scaffolds provide a set of unique, tissue-specific signals that is dependent upon the tissue from which an ECM is derived. The tissue-specificity of ECM scaffolds may explain why PHH maintain their phenotype best when cultured on ECM derived from the liver compared to PHH cultured with ECM derived from the Englbreth-Holm-Swarm mouse sarcoma (MG).

Lin et. al. compared rat hepatocytes cultured on PLECM biologic scaffolds to well characterized hepatocyte culture models (type-1 collagen sandwich configuration or a single layer of type-1 collagen) [28]. Hepatocytes survived up to 45 days on a sheet form of PLECM and several liver-specific functions such as albumin synthesis, urea production, and P-450 IA1

activity were markedly enhanced compared to the growth and metabolism of cells cultured on a single layer of type-1 collagen.

Zeisburg et al isolated liver-derived basement membrane matrix (LBLM) from human or bovine liver, and used the substrate for culture of human hepatocytes [35]. Human hepatocytes adhered more efficiently to LBLM and expressed lower levels of vimentin and cytokeratin-18, which are markers of hepatocyte dedifferentiation, compared to hepatocytes cultured on MG or type-1 collagen. However, maintainence of liver-specific functions *in vitro* was not reported [35].

Biologic scaffolds composed of ECM provide a more physiologically relevant culture substrate compared to reconstituted ECM proteins and have unique biochemical profiles that are dependent upon the tissue from which an ECM scaffold is derived. Minimally processed ECM scaffolds and gels, such as PLECM, provide a combination of ECM proteins derived from the liver that are in physiologically relevant amounts (e.g. Type-I, IV, VI, III, XI, XIX, heparin sulfate proteoglycan, ECM-bound growth factors, laminin, biglycan, tenascin, fibronectin) [39, 44, 47].

The enhanced hepatocyte-specific functions of PHH cultured with PLECM compared to PHH cultured with MG may be due to differences in the composition of the respective ECM. MG contains the following ECM proteins: laminin, type IV collagen, entactin, heparan sulfate proteoglycan, chondroiton sulfate proteoglycan, and ECM-bound growth factors [119-121]. Laminin, the most abundant ECM protein in MG, is not a major constituent of adult liver ECM [122, 123]. Further, MG lacks several of ECM proteins found in the liver, such as fibronectin and type-1 collagen. It is not surprising therefore, that an ECM derived from, and produced by the cells of the liver would be a more favorable substrate for hepatocytes *in vitro*. The structural

and functional proteins of an ECM scaffold provide a physical substratum for the attachment and spatial organization of cells [124]. Well known biophysical properties such as 3-dimensional surface topography play important roles in cell phenotype and behavior [125-129]. The 3-dimensional surface topography of an ECM includes variation in pore diameter as well as variation in the distances between the pores [130], surface texture [128], hydrophobicity and/or hydrophilicity [131], and the presence or absence of a basement membrane [44]. Obviously, the three-dimensional surface topography of the gel form of PLECM differs greatly from that of the native liver ECM.

As the field of tissue engineering and regenerative medicine moves toward the replacement of more complex tissues and three-dimensional organs, it is likely that more specialized scaffolds will be needed to support multiple, functional cell phenotypes. The findings of the present study suggest that tissue-specific ECM substrates can help maintain appropriate cell phenotype.

6.5 CONCLUSIONS

PHH cultured in an ECM sandwich retained a more 3-D like morphology compared to the PHH cultured on the type-1 collagen only.

Although no statistically significant mRNA levels were measured, there is a trend towards increased mRNA levels (Cx32, Alb, NTCP, BSEP) in PHH cultured in MG or PLECM sandwich compared to PHH cultured on type-1 collagen. An increased sample size may result in statistical significance.

PHH cultured with PLECM sandwich had the highest concentrations of average albumin secretion and these concentrations were significantly higher than the levels of albumin secreted by PHH cultured on type-1 collagen. PHH cultured in MG sandwich had lower levels of total albumin secretion than PHH secreted in PLECM sandwich, but the concentrations were not statistically significant.

Trends indicate that PHH cultured with PLECM sandwich had the highest levels of [3H] Taurocholate uptake, but the [3H] Taurocholate uptake was not statistically greater than PHH cultured on type-1 collagen or in between two layers of MG. The PHH cultured in between PLECM had the highest levels of [3H] Taurocholate efflux and the levels were statistically significant compared to PHH cultured on type-1 collagen or in between two layers of MG.

PHH cultured with PLECM sandwich had the highest levels of ammonia metabolism, which were significantly higher than the ammonia metabolism of PHH cultured on type-1 collagen. While PHH cultured in PLECM sandwich metabolized higher levels of ammonia than PHH cultured in MG sandwich, the levels were not statistically significant.

6.6 LIMITATIONS

Hepatocyte functionality was measured for only ten days. Tissue engineered liver constructs may need to maintain the functionality and viability of a large mass of isolated PHH for longer periods of time, even up to six weeks. Future studies should measure hepatoycte functionality for longer periods.

The biochemical composition of PLECM gel is unknown. A biochemical profile detailing the structural and functional proteins present in PLECM gel would be useful, and should include the types of collagen, glycosaminoglycans, and growth factors present.

7.0 DISSERTATION SYNOPSIS

7.1 USE OF ECM BIOLOGIC SCAFFOLDS FOR MAINTAINENCE OF HUMAN HEPATOCYTE-SPECIFIC FUNCTIONS IN VITRO

This work represents one of the first attempts to evaluate the maintainence of primary human hepatocyte-specific functions on complex ECM substrates. In Specific Aim 1, no differences in hepatoycte-specific functions were measured when comparing PHH cultured with either MG, PLECM or HLECM overlay. From a clinical perspective, the results are appealing because of the limited availability of human liver tissue compared to porcine liver tissue for the manufacture of ECM scaffolds.

In Specific Aim 2, hepatocytes cultured between two layers of porcine liver ECM had significantly higher levels of albumin secretion, hepatic transport activity, and ammonia metabolism compared to hepatocytes cultured on collagen.

Use of xenogeneic biomaterial derived from porcine tissues does not adversely affect human hepatocyte functions assayed, which include: DNA content, CYP450 inducibility, albumin secretion, hepatic transport activities, and ammonia metabolism. These findings suggest that protein and protein fragments that are leaked out or released from PLECM do not adversely affect human hepatoycte function. Further, even if PHH cultured with PLECM show similar

functional profiles as hepatocytes cultured with MG, PLECM is the preferred substrate because it is derived from the liver and not a tumor cell line.

7.2 USE OF ECM BIOLOGIC SCAFFOLDS FOR HEPATIC TISSUE ENGINEERING APPLICATIONS

Tissue engineering and regenerative medicine (TE&RM) approaches to treating liver disease have the potential to provide temporary support with biohybrid artificial liver-assist devices or long term therapy by replacing the diseased liver with functional tissue-engineered constructs that utilize a combination of cells, scaffolds and bioactive factors.

The limited availability of human hepatocytes impedes advances in hepatic tissue engineering and regenerative medicine technologies. Identification of alternative cell sources for treatment of liver disease is an intense area of research. Proliferation of adult liver stem cells derived from fetal liver tissue [132] or differentiation of embryonic stem cells into hepatocytes [133, 134] are two possible cell sources. However, the alternative cells sources [135] must be cultured in microenvironments conducive for differentiation into hepatocytes [132]. ECM substrates that support differentiation and/or proliferation of stem cells (fetal liver, stem/progenitor or human embryonic stem cells) into hepatocytes would provide an alternative cell source for hepatocytes [134, 136]. Complex ECM substrates could be used alone as substrates or as a coating for stem cell production bioreactors. Cho et al recently showed that the use of collagen facilitated the differentiation of mouse embryonic stem cells into hepatoycte-like cells [134]. Turner et al [132] used hyaluronic acid hydrogels to maintain pluripotent hepatic progenitors derived from human fetal tissue *in vitro*.

Table 3. Donor Information for Primary Human Hepatocyte Preparations for Specific Aim 2.

Donor HH#	Age	Sex[a]	Race[b]	Drug History	Viability
HH1400	21	M	C	NK	87%
HH1412	68	M	C	Chemotherapy	76%
HH1416	79	F	ND	Chemotherapy	83%
HH1417	53	F	ND	None	85%
HH1419	78	M	ND	None	79%
HH1423	51	M	ND	None	81%

ND, data not provided; NK, no known chronic drug treatment; [a]M, male; F, female; [b]C, Caucasion

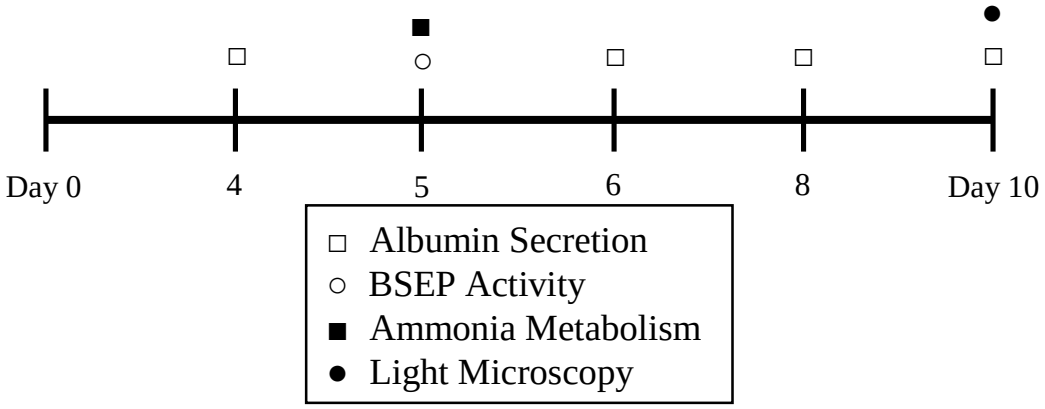

Figure 26. Schematic of assays performed to characterize PHH phenotype.

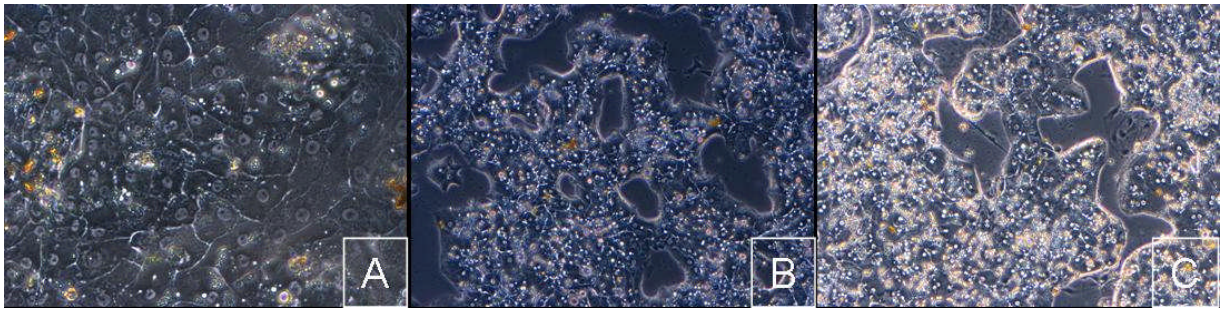

Figure 27. Primary cultures of human hepatocytes (PHH) maintained for ten days under different extracellular matrix (ECM) conditions (100x). PHH were cultured (A) on type-1 collagen; (B) between two layers of Matrigel™; or between (C) two layers of PLECM. Note the differences in cell morphology depending on the ECM conditions.

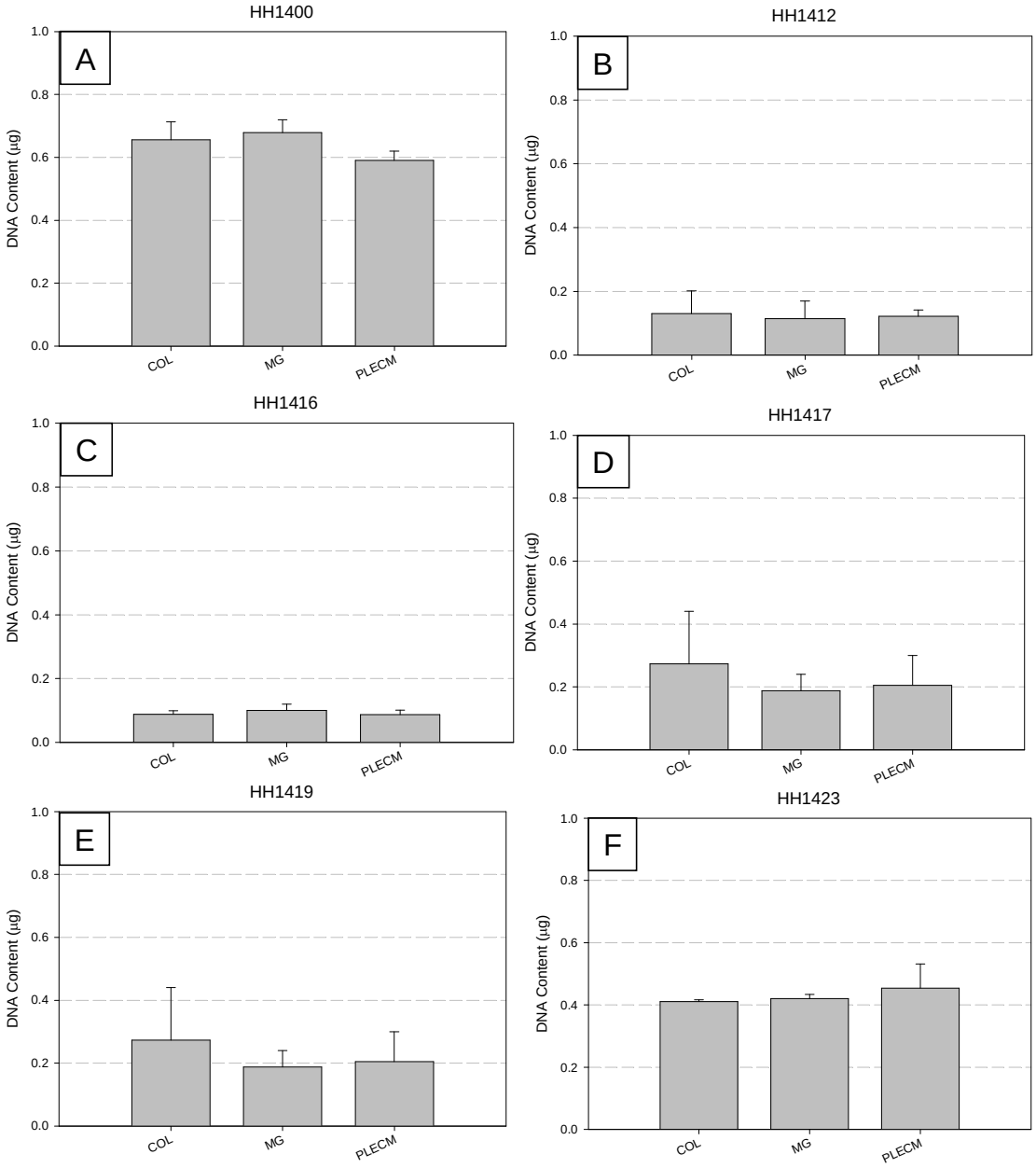

Figure 28. DNA content of PHH cultured on type-1 collagen alone or in MG or PLECM sandwich. Values represent mean±SD.

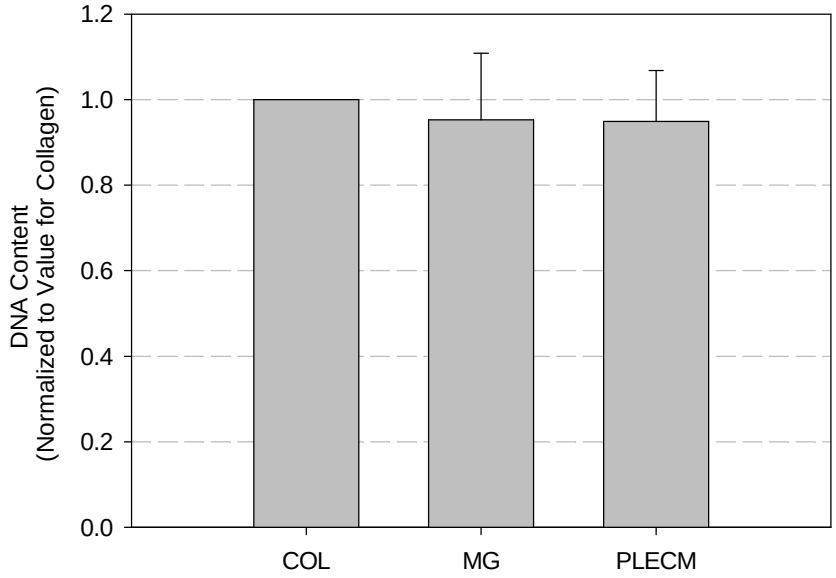

Figure 29. Average DNA content of six livers. Data from each culture condition was normalized to DNA content of PHH cultured on type-1 collagen. Values represent mean±SD of six livers.

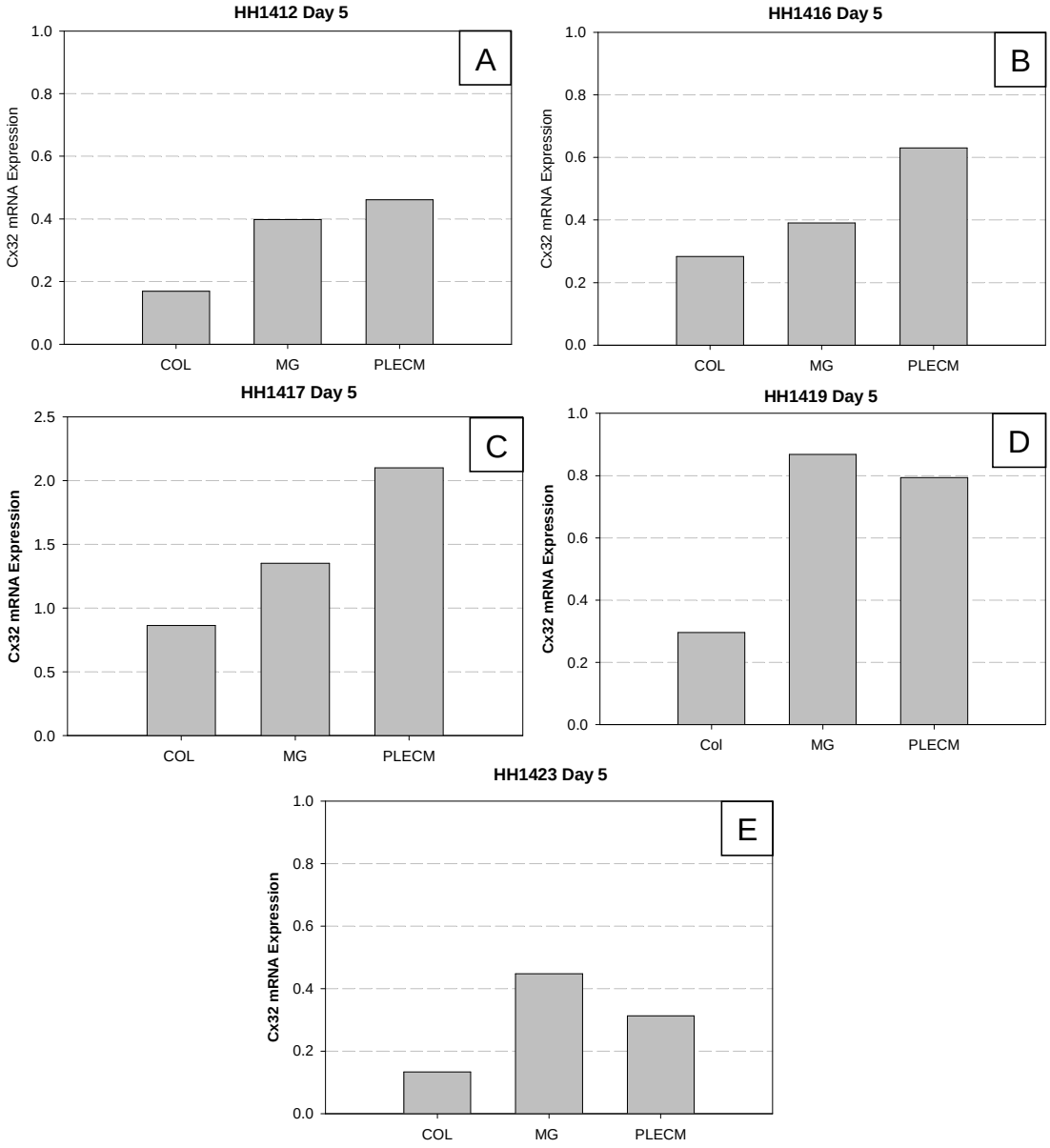

Figure 30. Effect of ECM sandwich configuration on Cx32 mRNA expression at day five. All data normalized to cyclophilin. Values represent mean±SD.

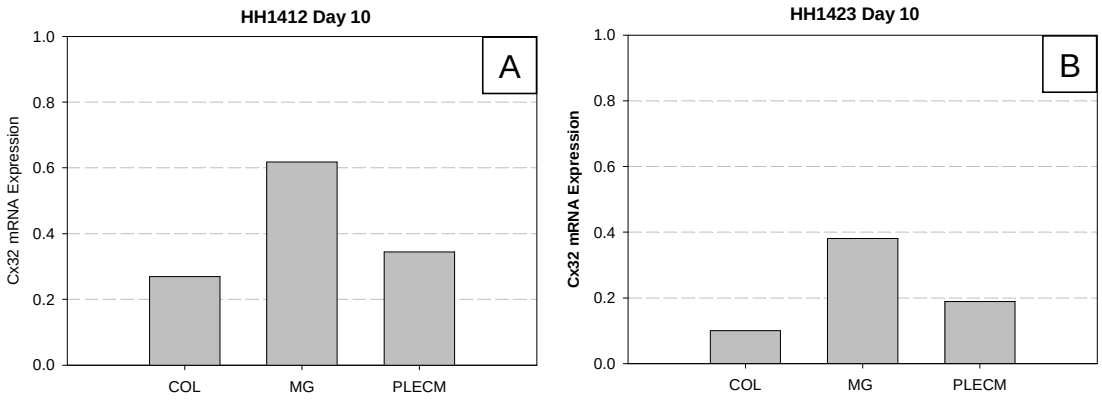

Figure 31. Effect of ECM sandwich configuration on Cx32 mRNA expression at day ten. All data normalized to cyclophilin. Values represent mean±SD.

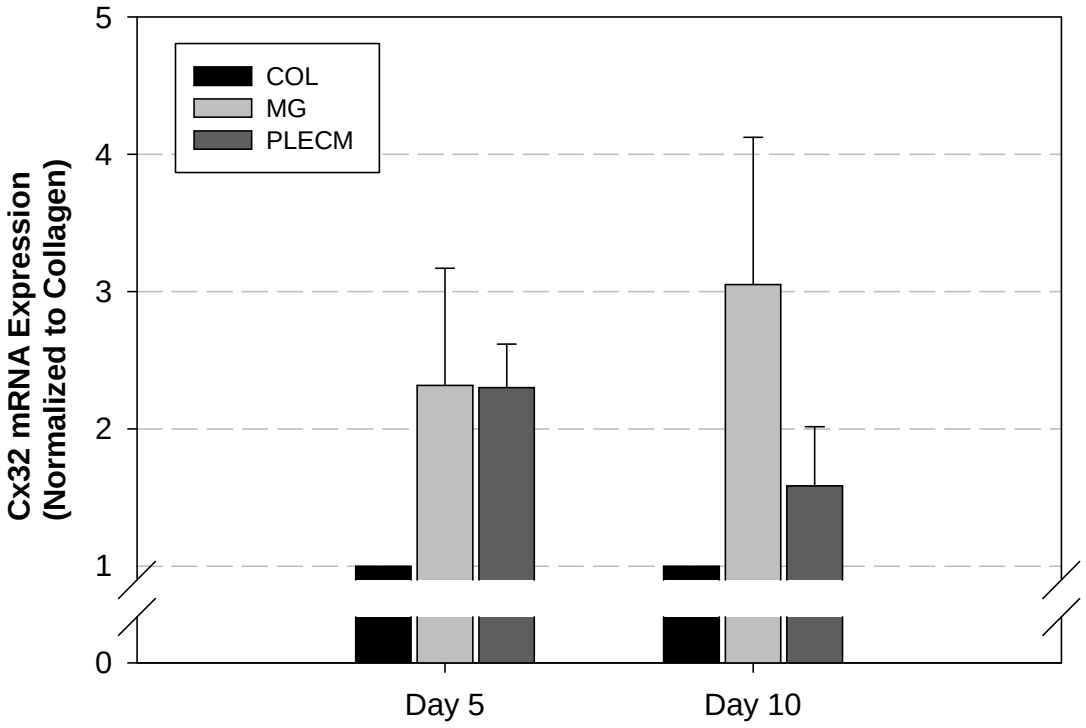

Figure 32. Effect of ECM sandwich configuration on Cx32 mRNA expression at days five and ten. Data normalized to Cx32 mRNA levels of PHH cultured on type-1

collagen at respective timepoint. Values represent mean±SD of n=5 livers for day 5 and n=2 livers for day ten.

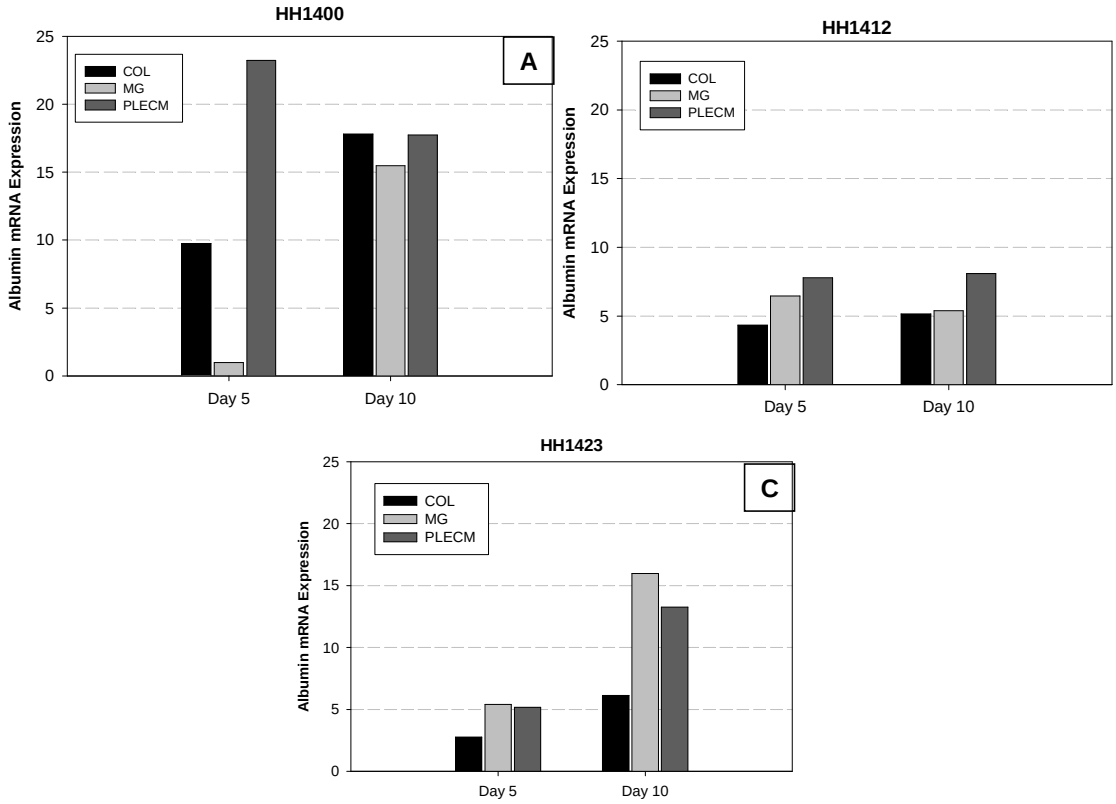

Figure 33. Effect of ECM sandwich configuration on albumin mRNA expression at days five and ten. All data normalized to cyclophilin. Values represent mean±SD.

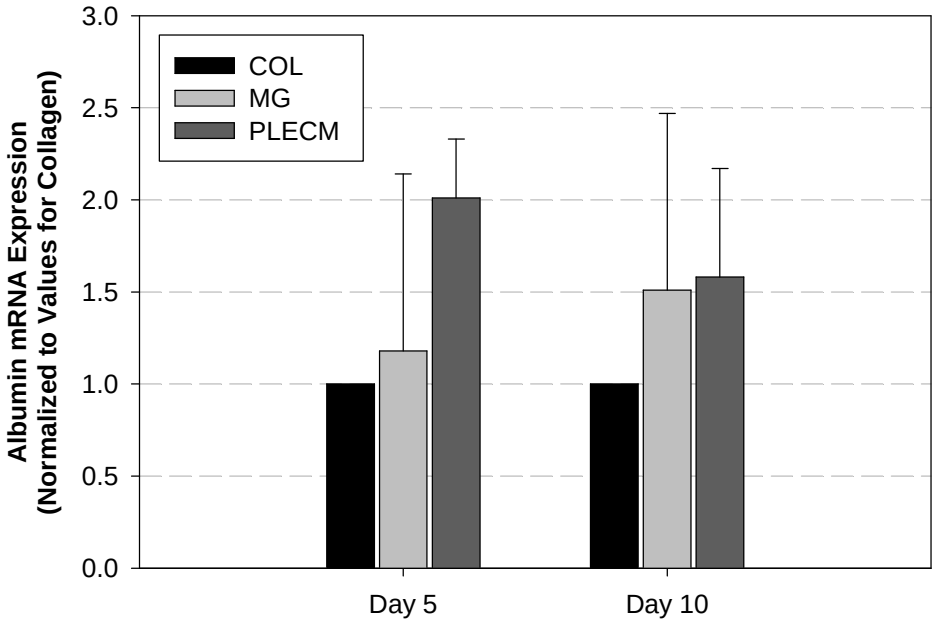

Figure 34. Effect of ECM sandwich configuration on albumin mRNA expression at days five and ten. Data from each culture condition was normalized to albumin mRNA of PHH cultured on type-1 collagen. Values represent mean±SD of three livers.

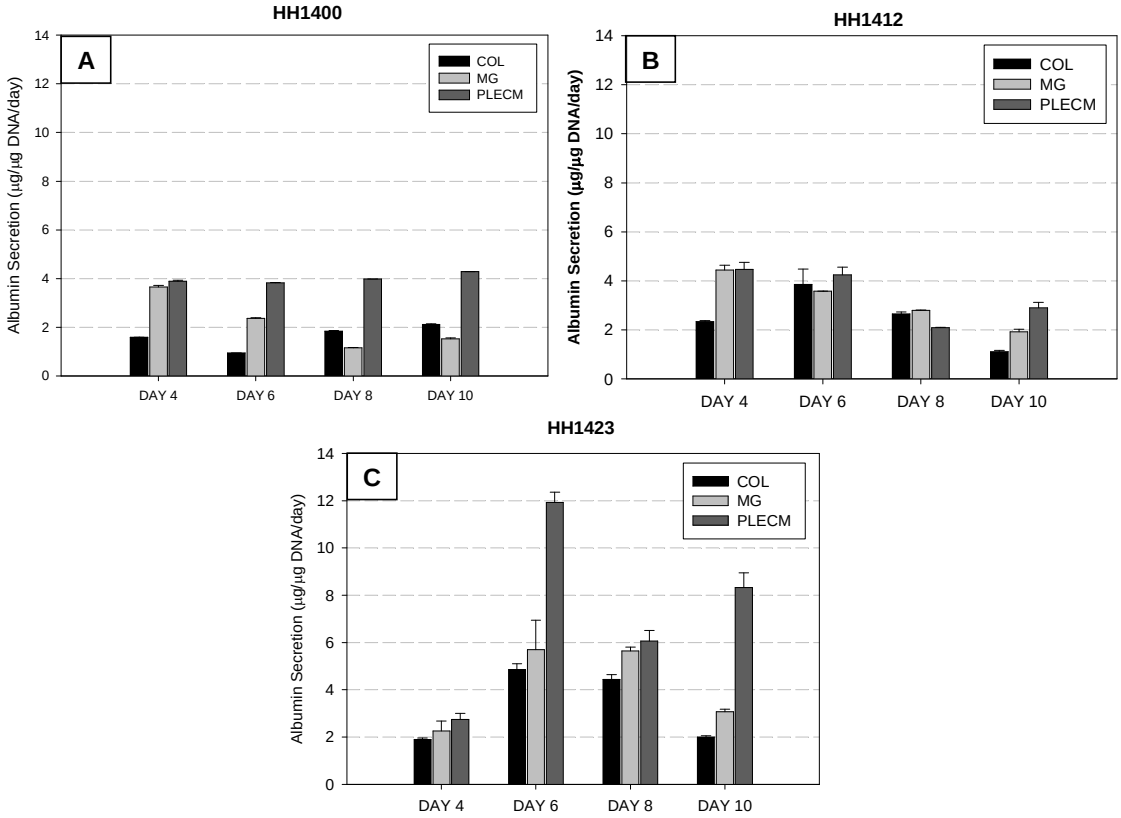

Figure 35. Effect of ECM sandwich configuration on albumin secretion of PHH cultured on type-1 collagen or either in a MG or PLECM sandwich at days four, six, eight and ten. Values represent mean±SD.

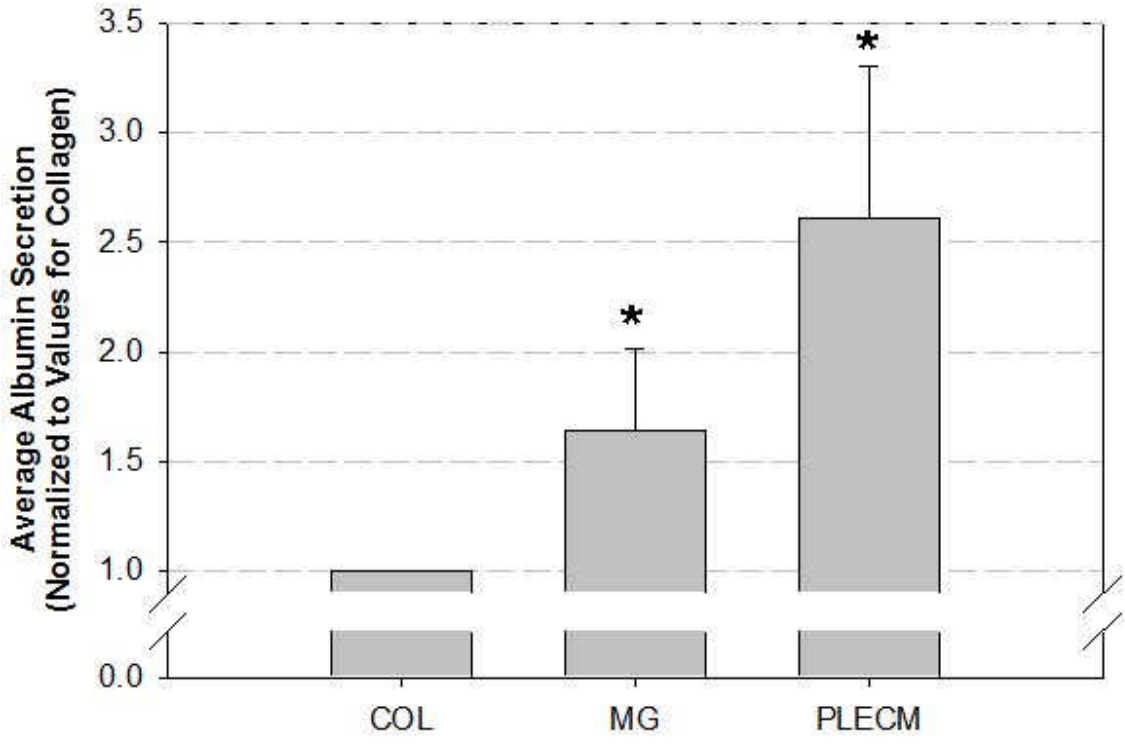

Figure 36. Effect of ECM sandwich configuration on average albumin secretion of PHH cultured in either MG or PLECM sandwich. Data from each culture condition was normalized to average albumin secretion of PHH cultured on type-1 collagen. Values represent mean±SD of three livers. * indicates statistically significant compared to PHH cultured on type-1 collagen (COL) ($p<0.05$).

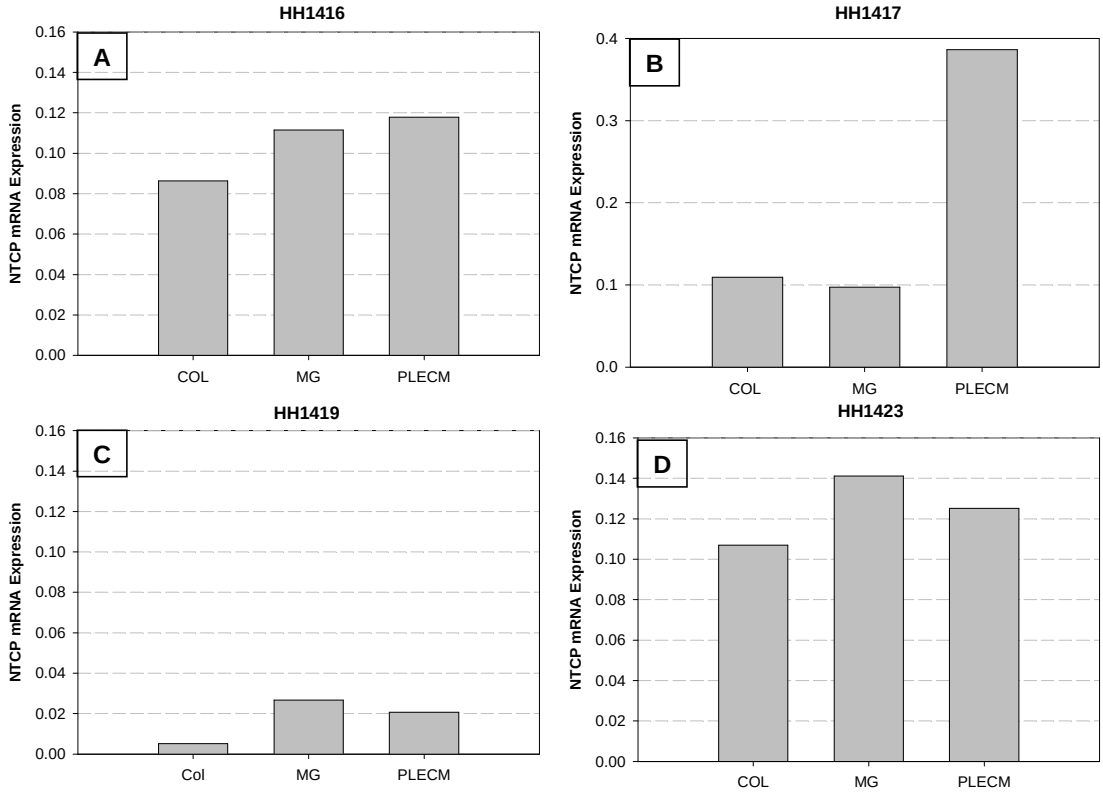

Figure 37. Effect of ECM sandwich configuration on NTCP mRNA expression of PHH cultured on type-1 collagen or either in a MG or PLECM sandwich at day five. All data normalized to cyclophilin. Values represent mean±SD.

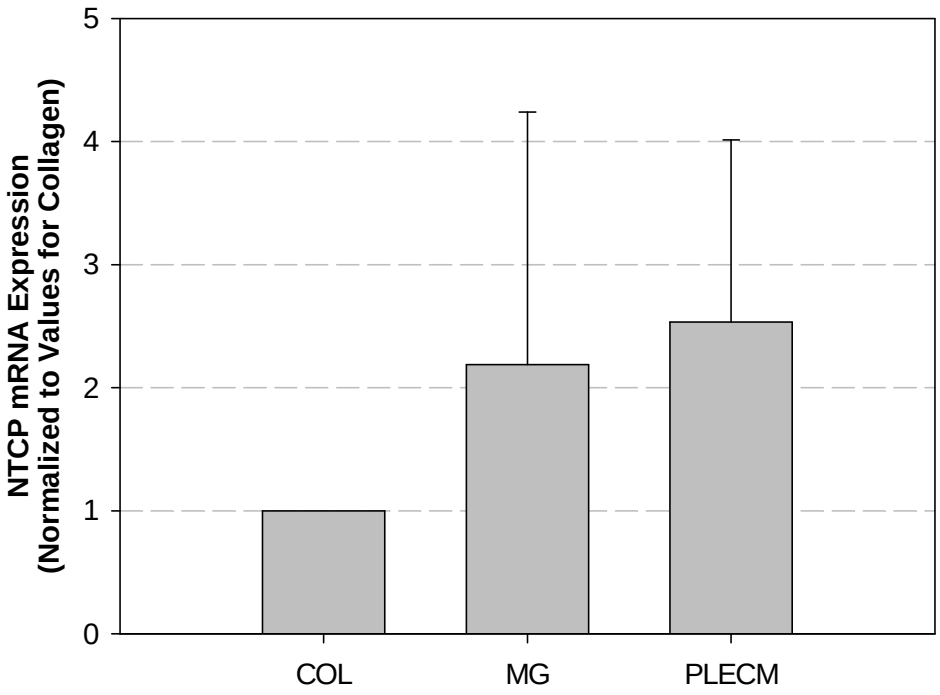

Figure 38. Effect of ECM sandwich configuration on NTCP mRNA expression of PHH cultured on type-1 collagen or either in a MG or PLECM sandwich at day five. Data from each culture condition was normalized to NTCP mRNA expression of PHH cultured on type-1 collagen. Values represent mean±SD of four livers.

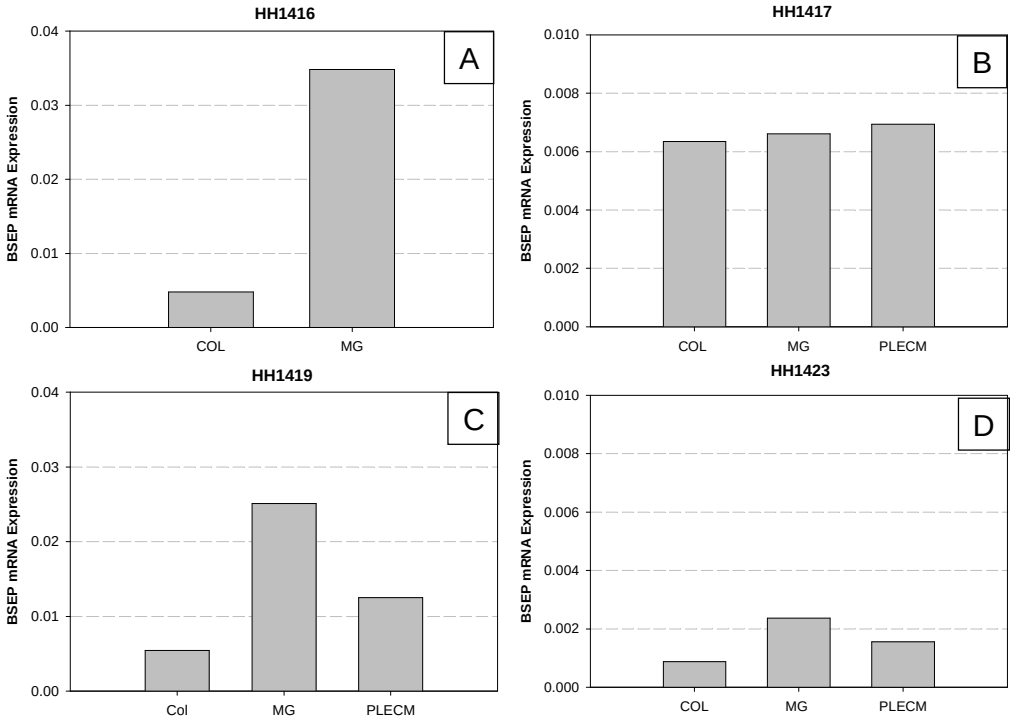

Figure 39. Effect of ECM sandwich configuration on BSEP mRNA expression of PHH cultured on type-1 collagen or either in a MG or PLECM sandwich at day five. All data normalized to cyclophilin. Values represent mean±SD.

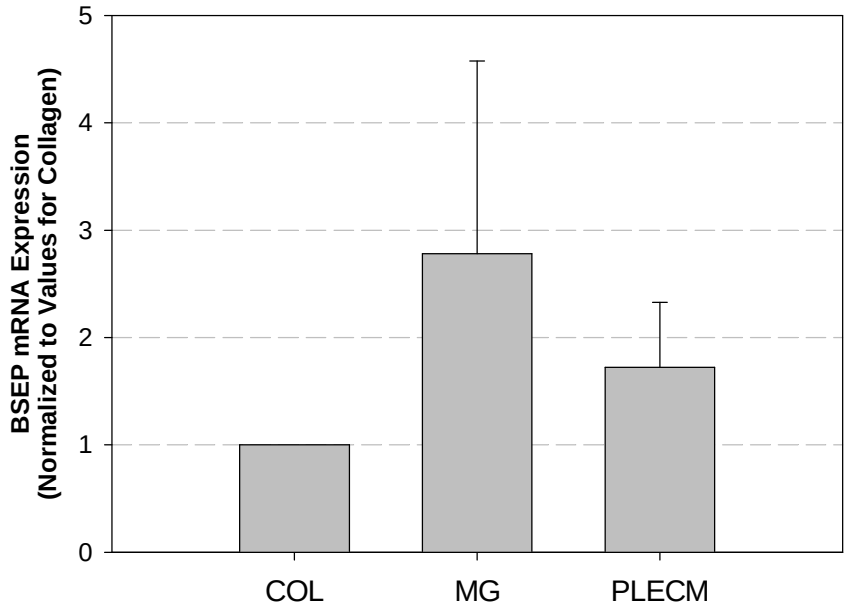

Figure 40. Effect of ECM sandwich configuration on BSEP mRNA expression of PHH cultured on type-1 collagen or either in a MG or PLECM sandwich at day five. Data from each culture condition was normalized to BSEP mRNA expression of PHH cultured on type-1 collagen. Values represent mean±SD of four livers.

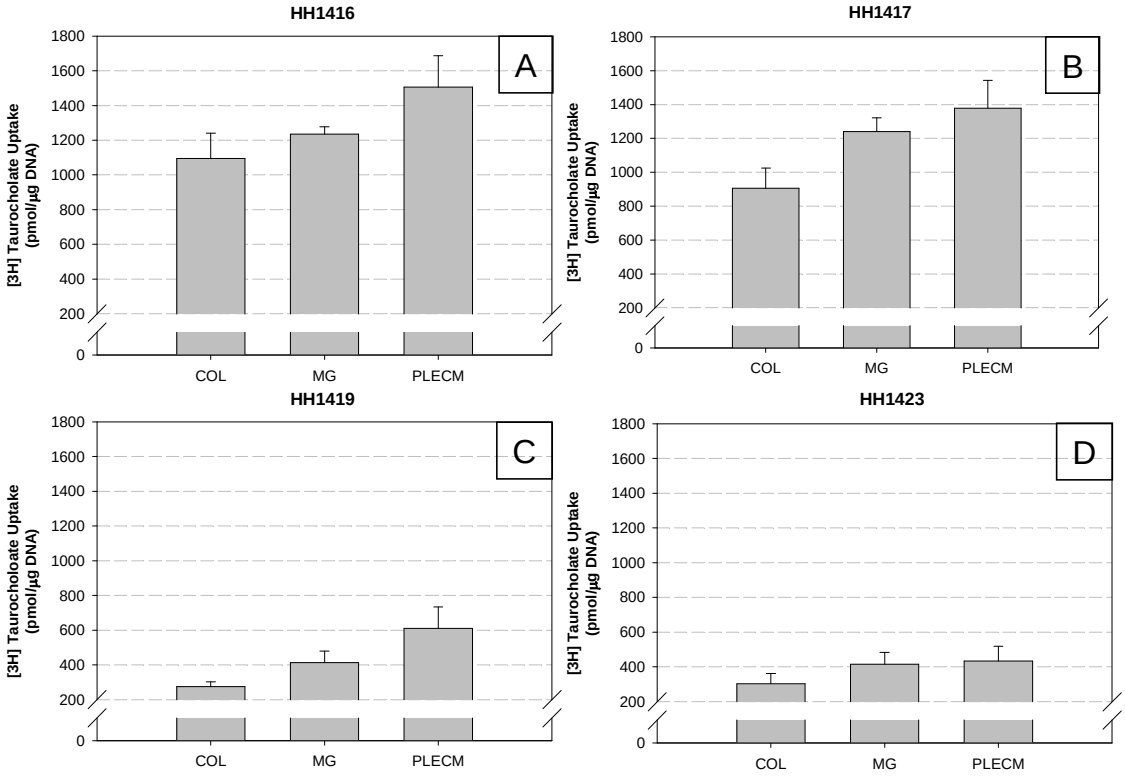

Figure 41. Effect of ECM sandwich configuration on [3H] Taurocholate uptake of PHH cultured on type-1 collagen, or either in a MG or PLECM sandwich at day five. Values represent mean±SD.

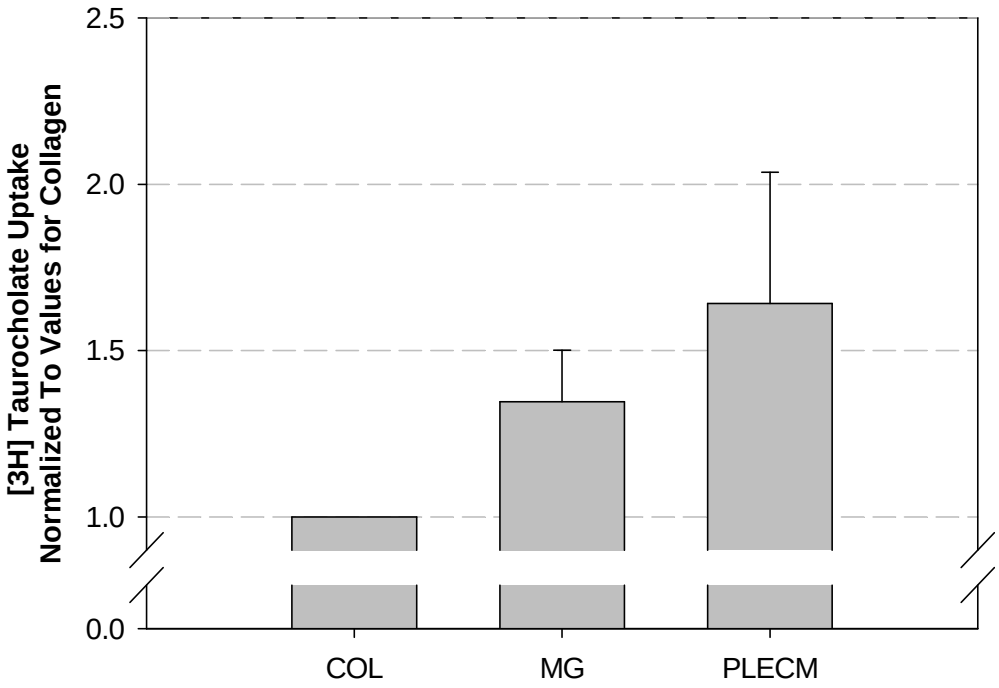

Figure 42. Effect of ECM sandwich configuration on [3H] Taurocholate uptake of PHH cultured on type-1 collagen, or either in a MG or PLECM sandwich at day five. Data from each culture condition was normalized to [3H] taurocholate uptake of PHH cultured on type-1 collagen. Values represent mean±SD of four livers.

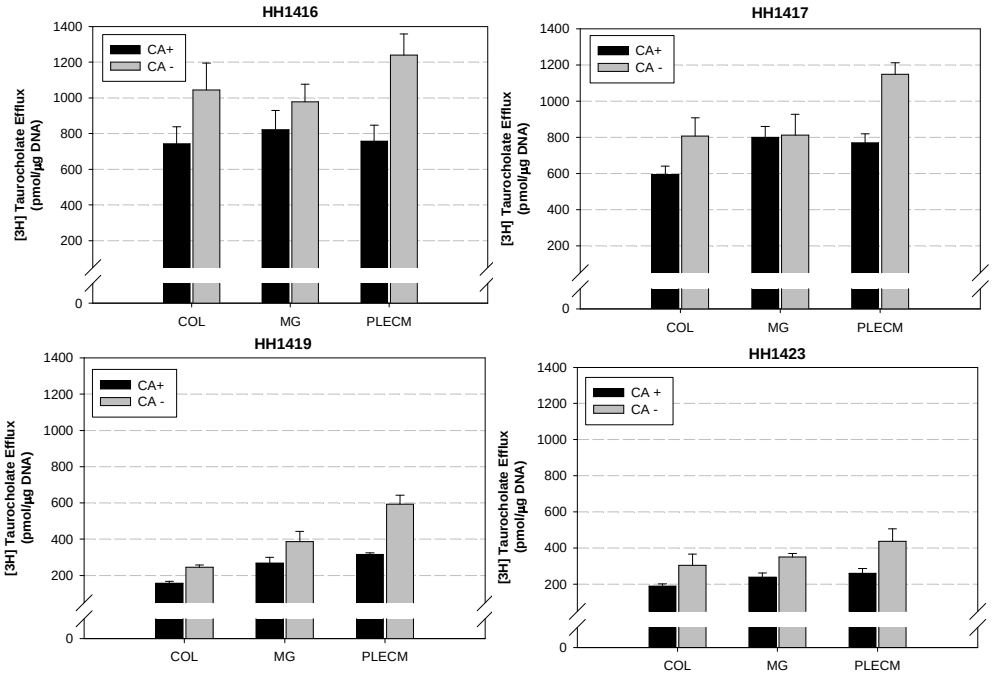

Figure 43. Effect of ECM sandwich configuration on [3H] Taurocholate efflux of PHH cultured on type-1 collagen, or either in a MG or PLECM sandwich at day five. Values represent mean±SD. CA+ indicates PHH were cultured with cations and CA- indicates PHH were cultured without cations.

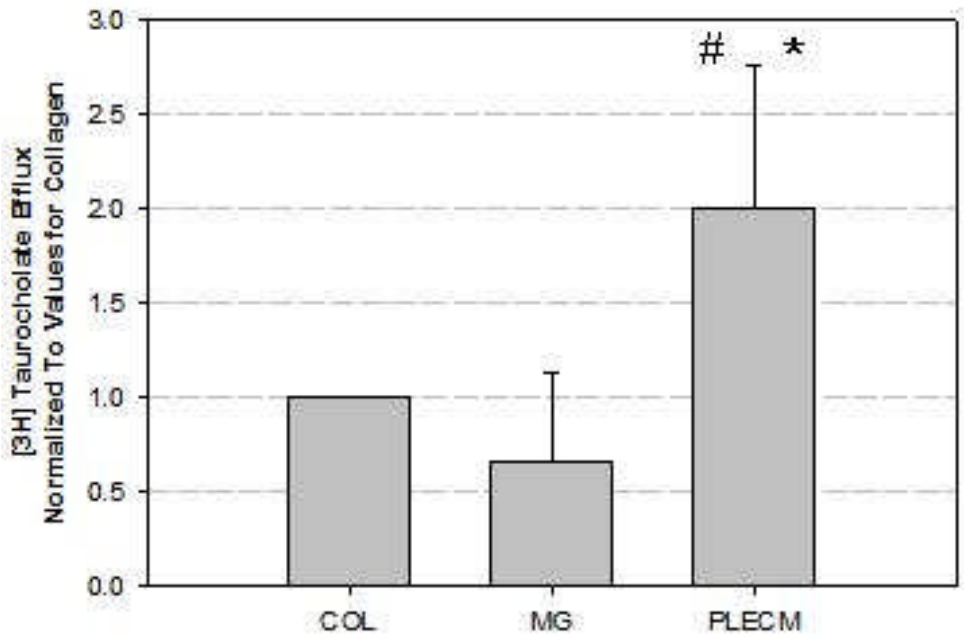

Figure 44. Effect of ECM sandwich configuration on [3H] Taurocholate efflux of PHH cultured on type-1 collagen, or either in a MG or PLECM sandwich on day five. Data from each culture condition was normalized to [3H] taurocholate efflux of PHH cultured on type-1 collagen. Values represent mean±SD of four livers. # represents statistically significant compared to MG ($p<0.05$) and * represents statistically significant compared to type-1 collagen.

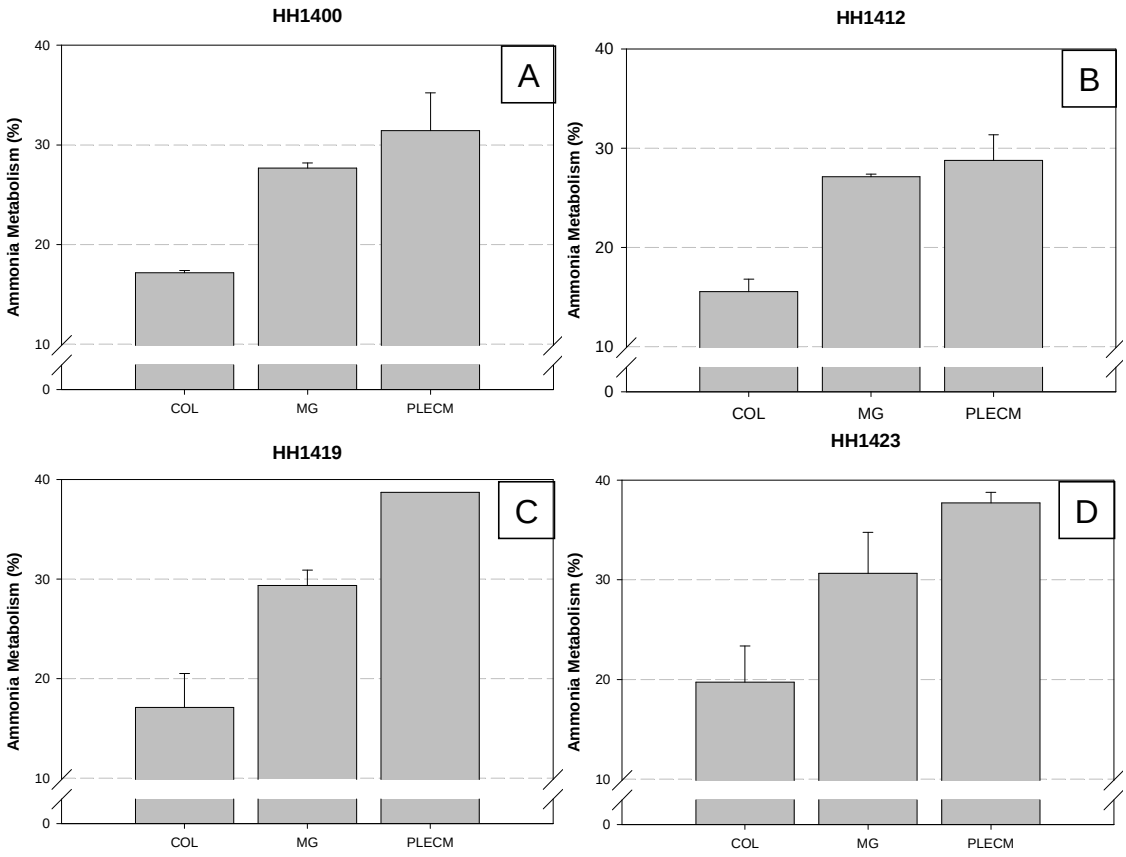

Figure 45. Effect of ECM sandwich configuration on percentage of ammonia metabolism by PHH cultured on type-1 collagen, or in MG or PLECM sandwich on day five. Values represent mean±SD.

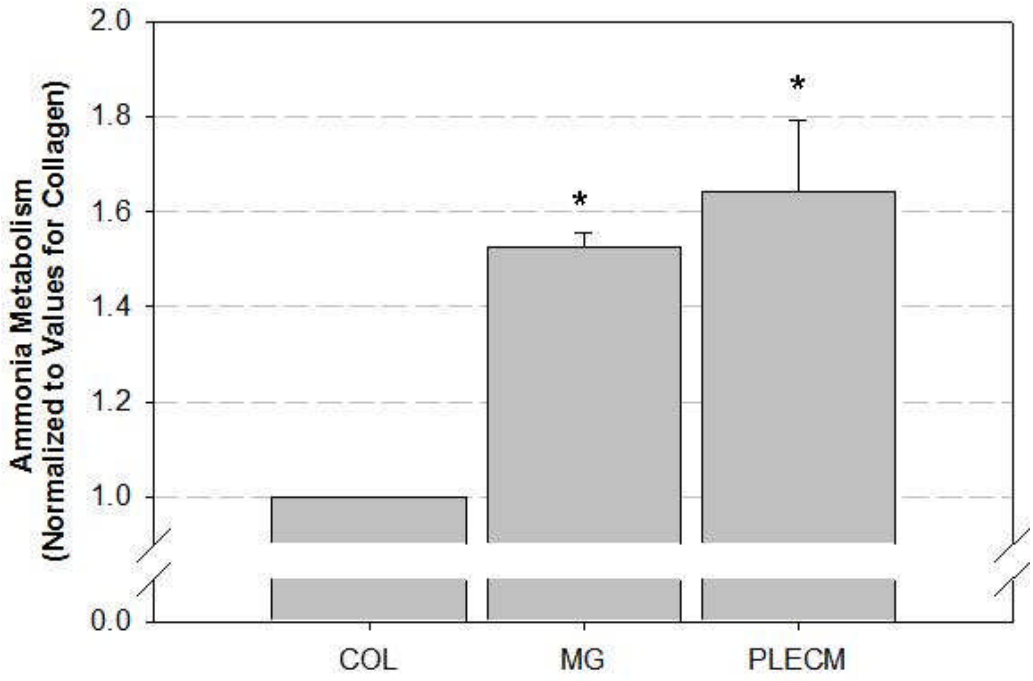

Figure 46. Effect of ECM sandwich configuration on ammonia metabolism of PHH cultured on type-1 collagen, or either in a MG or PLECM sandwich on day five. Data from each group was normalized to ammonia metabolism of PHH cultured on type-1 collagen. Values represent mean±SD of four livers. * represents statistically significant compared to collagen.

APPENDIX A

MAINTAINENCE OF HEPATIC SINUSOIDAL ENDOTHELIAL CELL PHENOTYPE IN VITRO BY ORGAN-SPECIFIC EXTRACELLULAR MATRIX SCAFFOLDS

The effect of tissue-specific ECM scaffolds on maintainence of SEC phenotype *in vitro* was evaluated. The porcine ECM scaffolds used for culture of hepatic SEC were derived from small intestine (SIS-ECM), urinary bladder (UBM-ECM), or liver (LECM). Either SEC alone or a co-culture of SEC plus hepatocytes were cultured on the ECM.

A.1 INTRODUCTION

Sinusoidal endothelial cells (SEC) are difficult to culture *in vitro*. SEC are highly specialized endothelial cells characterized by the presence of fenestrations organized into sieve plates, which permit the selective passage of proteins and metabolites. Differentiated SEC have sieve plates, express anti-rat hepatic sinusoidal endothelial cells mouse IgG monoclonal antibody (SE-1) [137-139], and do not express CD31. CD31 is a marker of both macro- and microvascular endothelial cells and is expressed by dedifferentiating SEC [140].

SEC derived from GFP-expressing rats were cultured on ECM derived from either porcine small intestinal submucosa (SIS-ECM), urinary bladder (UBM-ECM), or liver (LECM) for seven days. Either SEC alone or a co-culture of SEC plus PHH were cultured on the ECM.

The effect of the ECM substrate upon SEC dedifferentiation was evaluated by scanning electron microscopy (SEM) (presence or absence of fenestrations and sieve plates) and confocal microscopy (expression of SE-1 and CD31).

A.2 METHODS

A.2.1 Overview of Experimental Design

Rat derived liver SEC were cultured alone or were co-cultured with rat derived hepatocytes for one, three or seven days on one of five different substrates: collagen type I, untreated glass slides, ECM derived from liver (L-ECM), ECM derived from urinary bladder (UBM-ECM), or ECM derived from small intestinal submucosa (SIS-ECM). The effect of the ECM substrate upon SEC differentiation was evaluated by: (1) scanning electron microscopy (SEM) to view the presence of fenestrations and sieve plates and (2) confocal microscopy for expression of SE-1, a marker of SEC differentiation [137-139], and (3) confocal microscopy for CD31, a marker of hepatic SEC dedifferentiation [140].

A.2.2 Isolation and Preparation of ECM

The liver, urinary bladder, and small intestine were harvested from market weight pigs (~110-130kg) immediately after euthanasia. The tissues were rinsed with tap water and frozen until used.

The methods used to isolate liver ECM (L-ECM) have been previously described [28, 44]. Briefly, each liver lobe was cut into 5 mm slices with a rotating blade and subjected to three separate thirty-minute washes in deionized water with mechanical agitation on an orbital shaker.

The sections were then gently massaged to aid in cell lysis and soaked in 0.02% trypsin/0.05% EDTA (Gibco; Carlsbad, CA) at 37° C for one hour. The tissue was then rinsed in deionized water and the massaging was repeated followed by mechanical agitation of the liver sections in 3% Triton X-100 (Spectrum; Gardena, CA). The rinsing and massaging process was repeated until all visible remnants of cellular material were removed. The tissue sections were then mechanically agitated in 4% sodium deoxycholic acid (Spectrum) for one hour followed by extensive rinsing in water. The remaining decellularized connective tissue matrix was referred to as L-ECM [28].

A detailed description of the isolation and preparation of UBM-ECM has been previously described [44, 141]. The urothelial cell layer was removed from porcine urinary bladder by immersion in deionized water on a mechanical shaker for 60 minutes. The tunica serosa, tunica muscularis externa, tunica submucosa and most of the muscularis mucosa were removed from the urinary bladder tissue by manual scraping. The remaining layers, which consisted primarily of basement membrane and tunica (lamina) propria, were referred to as UBM-ECM.

The preparation of SIS-ECM has also been previously described [44, 102, 142]. The luminal portion of the tunica mucosa, including the majority of the lamina propria, was removed, and the entirety of the serosa and tunica muscularis externa were removed by manual scraping. The remaining tunica submucosa, muscularis mucosa and stratum compactum of the lamina propria was referred to as SIS-ECM.

After processing, all tissues were then immersed in a solution of 0.1% peracetic acid followed by repeated rinses in water or phosphate buffered saline at pH 7.4. The resulting decellularized and disinfected ECM was terminally sterilized with ethylene oxide [105].

A.2.3 Isolation and culture of hepatocytes and SEC

Transgenic adult Sprague-Dawley rats carrying the enhanced green fluorescence protein (EGFP) gene were used as the source of all cells in this study [143]. The procedures were approved by the Institutional Animal Care and Use Committee at the University of Pittsburgh and were conducted in accordance with the guidelines of the National Institutes of Health for the humane care of research animals. The rats weighed approximately 200 g at time of sacrifice for cell harvest.

Hepatocytes and nonparenchymal cells (NPC), which include SEC, were isolated by two-stage collagenase perfusion as previously described [144]. After removal of undigested tissues, hepatocytes were separated from NPC by filtration differential centrifugation [145].

To purify SEC from NPC, SEC were isolated by magnetite beads coated with a charged 50 nm cationic, polyethyleniemine-coated colloidal, a specific antibody against rat SEC membrane surface antigen (Chemicell, Berlin, Germany) [146]. The isolated SEC were resuspended in EGM-2 media (Clonetics BulletKit).

Typically, 200 to 300 million hepatocytes were isolated with 85 to 95% viability as assessed by exclusion of trypan blue dye. Hepatocytes were then cultured in hepatocyte growth medium (HGM). Basal HGM (Dulbecco's Modified Eagle Medium (DMEM) medium, HEPES, glutamine, and antibiotics (Gibco; Carlsbad, CA) supplemented with bovine albumin (2.0 g/L), glucose (2.25 g/L), galactose (2.0 g/L), ornithine (0.1 g/L), proline (0.030 g/L), nicotinamide (0.305 g/L), $ZnCl_2$ (0.544 g/L), $ZnSO_4$:$7H_20$ (0.750 g/L), $CuSO_4$:$5H_20$ (0.20 g/L), $MnSO_4$ (0.025 g/L), glutamine (5 mmol/L), and dexamethasome (10^{-7} mol/L) (Sigma Chemical Company; St. Louis, MO) was mixed and sterile filtered through a 0.22 μm low-protein-binding filter system, stored at 4° C, and used within four weeks. Insulin, transferrin and selenium were added to the

basal HGM just before use, for a final concentration of 5 µg/ml Insulin, 5 ng/ml transferrin, and 5 ng/ml selenium [147].

All experiments involved the culture of either SEC only or a co-culture of SEC plus hepatocytes upon the following substrates: untreated glass coverslips (Fisher Scientific; Pittsburgh, PA), collagen type I (BD Biosciences; Bedford, MA), the luminal surface of SIS-ECM (i.e. stratum compactum surface), the luminal surface of UBM-ECM (i.e. basement membrane surface) or L-ECM. For cells cultured on ECM substrates, untreated polystyrene 6 well microplates were used (Evergreen Scientific; Los Angeles, CA). The seeding density for the co-culture experiments was $0.7x10^6$ hepatocytes:$1x10^6$ SEC/cm^2. The SEC only group were seeded at $1x10^6$ SEC/cm^2 in Clonetics EBM-2 medium with EGM-2 supplements (Cambrex, E.Rutherford, NJ), while the SEC and hepatocyte co-culture media formulation was 50% HGM/50% EGM-2. As a control to determine the effects of the co-culture media on SEC phenotype, SEC were also cultured without hepatocytes on the three different ECM in 50% HGM/50% EGM-2. Cells were seeded at $1x10^6$ cells/cm^2 of substrate surface area and cells were examined using scanning electron microscopy at one, three and seven days after seeding.

A.2.4 Scanning Electron Microscopy.

Samples were fixed overnight with 2.5% glutaraldehyde in phosphate buffered saline (PBS). After three PBS washes, tissue was dehydrated through a graded series of ethanol washes followed by critical point drying using an Emscope CPD 750. Samples were sputter coated with a 7-nm layer of gold-palladium (Cressington 108 sputter coater) and visualized at a voltage of 12 kV using a JEM 6335F field emission gun SEM (JEOL, Peabody, MA).

For each experimental group, three samples were examined at each time point (days one, three, and seven). Cells were randomly selected for imaging by starting at a preselected point in the lower left quadrant of the 1 cm^2 sample and moving to subsequent preselected areas in a clockwise manner taking approximately 12 photomicrographs for each sample. Representative images were selected for inclusion in this report.

A.2.5 Immunofluorescence for SE-1 and CD31

Hepatocytes cultured on ECM scaffolds were fixed in 2% paraformaldehyde in PBS at room temperature for 10 minutes. Fixed samples were washed 3 times in PBS and permeabilized in 0.1% Triton-X for 20 minutes at room temperature. Following cell permeabilization, samples were washed 3 times with bovine 0.5% serum albumin (BSA) in PBS and were then blocked with 2% BSA in PBS for 1 hour. Following 3 washes in 0.5% BSA in PBS, samples were incubated for 1 hr at room temperature: mouse anti-rat CD31 (1:250 in 0.5% BSA; Serotec, Raleigh, NC) or SE-1 (1:100 in 0.5% BSA; Immuno-Biological Laboratories, Minneapolis, MN). Following 3 washes with BSA in PBS, samples were incubated at room temperature for 1 hour with goat anti-mouse Cy3 conjugated secondary (1:1000 in 0.5% BSA; JacksonImmunoResearch, West Grove, PA). After incubation in the secondary antibody, samples were then placed in PBS and incubated with Hoeschts dye (bizBenzamide, 1 mg/mL in PBS) for 30 seconds to stain nuclear DNA. Finally, the samples were washed 3 times in PBS and stored at 4°C for a maximum of 24 hours before imaging. Experiments were performed in triplicate. Samples were imaged using an inverted Olympus Fluoview 1000 microscope (Olympus). Representative images were selected for inclusion in this report.

A.3 SEM RESULTS

A.3.1 Culture of Sinusoidal Endothelial Cells on ECM Substrates

After one day of culture on SIS-ECM, no sieve plates were present on SEC. Only a few fenestrations were present as well as large holes at day one (Figure 47A). Large holes were present and no fenestrations were present at day three (figure not shown) and day seven (Figure 47B).

When SEC were cultured on UBM-ECM, there were few sieve plates and fenestrations at day one (Figure 47C), large holes were present at day three (Figure 47D) and after seven days of culture, a confluent monolayer of dedifferentiated SEC containing no fenestrations or sieve plates was observed (not shown).

After one and three days of culture on LECM, the SEC had fenestrations that were organized into sieve plates, characteristic of differentiated SEC (Figures 48A&B). Large holes and no fenestrations were present at day seven (Figure 48C).

A.3.2 Co-culture of Sinusoidal Endothelial Cells and Hepatocytes on ECM substrates

While the SEC co-cultured with hepatocytes on SIS-ECM (Figure 49A) and UBM-ECM (Figure 49C) maintained fenestrations that were organized in sieve plates for at least one day, the appearance of sieve plates was not as frequent when compared to the SEC co-cultured with hepatocytes on LECM. After three days (Figures not shown) and seven days of culture, no fenestrations were present on SEC co-cultured with hepatocytes on either SIS-ECM (Figure 49B) or UBM-ECM (Figure 49D).

At all time points, the SEC co-cultured with hepatocytes on LECM maintained the greatest amount of fenestrations and these fenestrations were organized in characteristic sieve plates. At day one, many sieve plates were present (Figure 49E). At three days, sieve plates were still present only in those SEC that were co-cultured with hepatocytes upon the LECM substrate (not shown) and by seven days, only the SEC co-cultured with hepatocytes on LECM maintained a fenestrated phenotype (Figure 49F).

When SEC only were cultured on either type-1 collagen, UBM-ECM, or SIS-ECM, SEC showed signs of dedifferentiation after only one day. In contrast, SEC only cultured on LECM maintained their differentiated phenotype for at least three days, indicated by the presence of many fenestrations on SEC surface. When SEC were co-cultured with hepatocytes on any of the ECM scaffolds, the SEC maintained a near normal fenestrated phenotype for at least one day. However, SEM revealed that the shape, size, frequency and organization of the fenestrations varied greatly depending on ECM source. At all time points, SEC co-cultured with hepatocytes on LECM maintained the greatest degree of differentiation.

A.4 CONFOCAL MICROSCOPY RESULTS

A.4.1 Culture of Sinusoidal Endothelial Cells on ECM substrates

After one day of culture, SE-1 was minimally expressed in SEC cultured on SIS-ECM (Figure 50A) and UBM-ECM (Figure 50B), and SE-1 was expressed most intensely in the SEC cultured on LECM (Figure 50C). After three days of culture, SE-1 was minimally expressed in SEC cultured on SIS-ECM (Figure 51A) and UBM-ECM (Figure 51B), compared to SEC on LECM (Figure 51C).

On day one, SEC cultured on SIS-ECM (Figure 52A) and UBM-ECM (Figure 52B) had CD31 expression localized in the cytoplasm of SEC with some expression of CD31 at cell-cell junctions, findings consistent with dedifferentiation. In contrast, SEC cultured on LECM for one day (Figure 52C) expressed minimal amounts of CD31 in the cytoplasm and expressed no CD31 at the cell surface.

After three days of culture on SIS-ECM (Figure 53A) and UBM-ECM (Figure 53B), SEC had extensive expression of CD31 at the cell-cell junctions, indicative of SEC dedifferentiation. After three days of culture on LECM (Figure 53C), SEC expressed CD31 in the cytoplasm and at some cell-cell junctions. At day seven of culture, SEC on LECM expressed both SE-1 (Figure 54A) and CD31 (Figure 54B).

A.5 CONCLUSIONS

The effect of organ-specific ECM scaffolds on maintainence of SEC phenotype was evaluated. Hepatic SEC maintained their differentiated state the longest when cultured on ECM derived from the liver compared to ECM derived from either the UBM-ECM or the SIS-ECM. SEC cultured on LECM had markedly increased fenestrations, increased expression of SE-1 and decreased expression of CD31 compared with SEC cultured on SIS-ECM or UBM-ECM. The present study suggests liver-derived ECM provides a unique set of tissue-specific signals that contribute to the maintenance of a site-specific, fenestrated phenotype for hepatic SEC.

As the field of tissue engineering and regenerative medicine moves toward the replacement of more complex tissues and three-dimensional organs, it is likely that more specialized scaffolds will be needed to support multiple, functional cell phenotypes in site-

specific, unique three-dimensional arrangements. The findings of the present study suggest that tissue-specific ECM substrates can help maintain appropriate cell phenotype.

A.6 SUMMARY

The biochemical composition of ECM varies throughout the body and is dependent on the resident cells of the organ to tailor the ECM so that it supports the needs of the highly specialized cell populations residing within a tissue or organ. For example, cardiac fibroblasts produce a highly specialized ECM that supports the structural and functional requirements of heart. In this study, we showed that after decellularization, the ECM retains its tissue-specificity.

The results of the tissue-specific ECM study laid the foundation of this dissertation. Since the above study showed an tissue-specific effect on cell phenotype, the question was asked “Do ECM scaffolds have a species-specific effect on cell phenotype?” In other words, would an ECM scaffold derived from a human liver better maintain the phenotype of cells derived from human liver compared to an ECM scaffold derived from porcine liver?

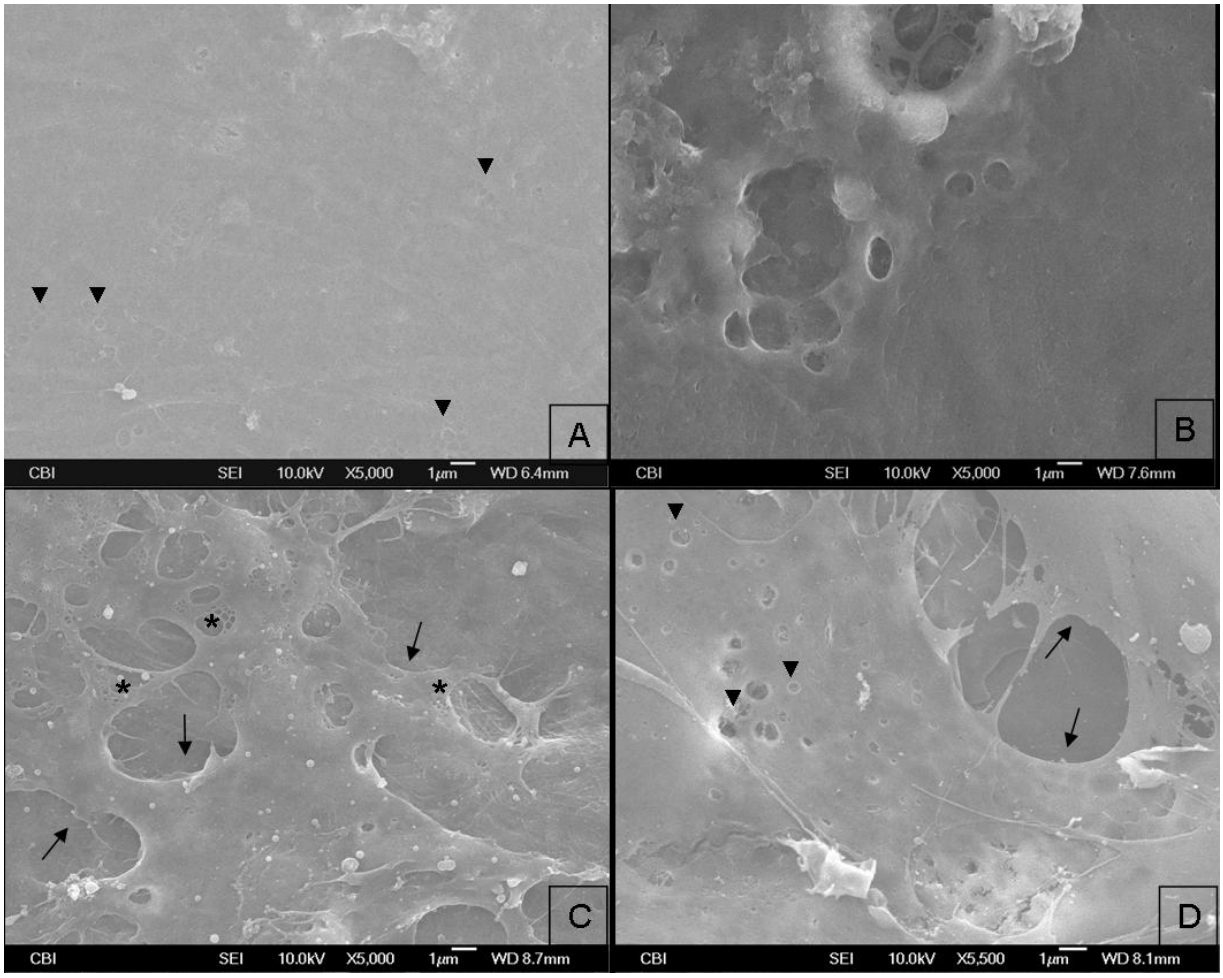

Figure 47. SEM of SEC cultured on SIS-ECM at day 1 (A) and at day 7 (B) and on UBM-ECM at (C) day one and at (D) day three (5000x). Arrows indicate cell boundaries ▼ indicate representative fenestrations, * indicate representative sieve plates.

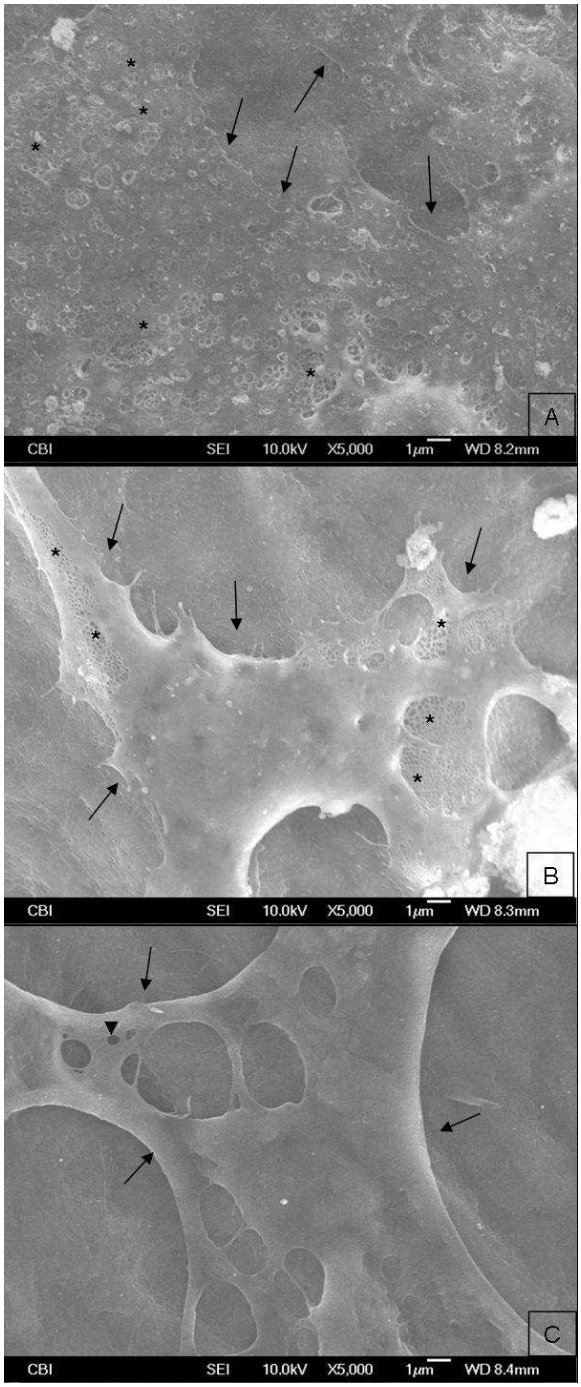

Figure 48. SEM of SEC cultured on LECM at (A) day one, (B) day three and (C) day seven (5000x). Arrows indicate cell boundaries. ▼ indicate representative fenestrations and * indicate representative sieve plates.

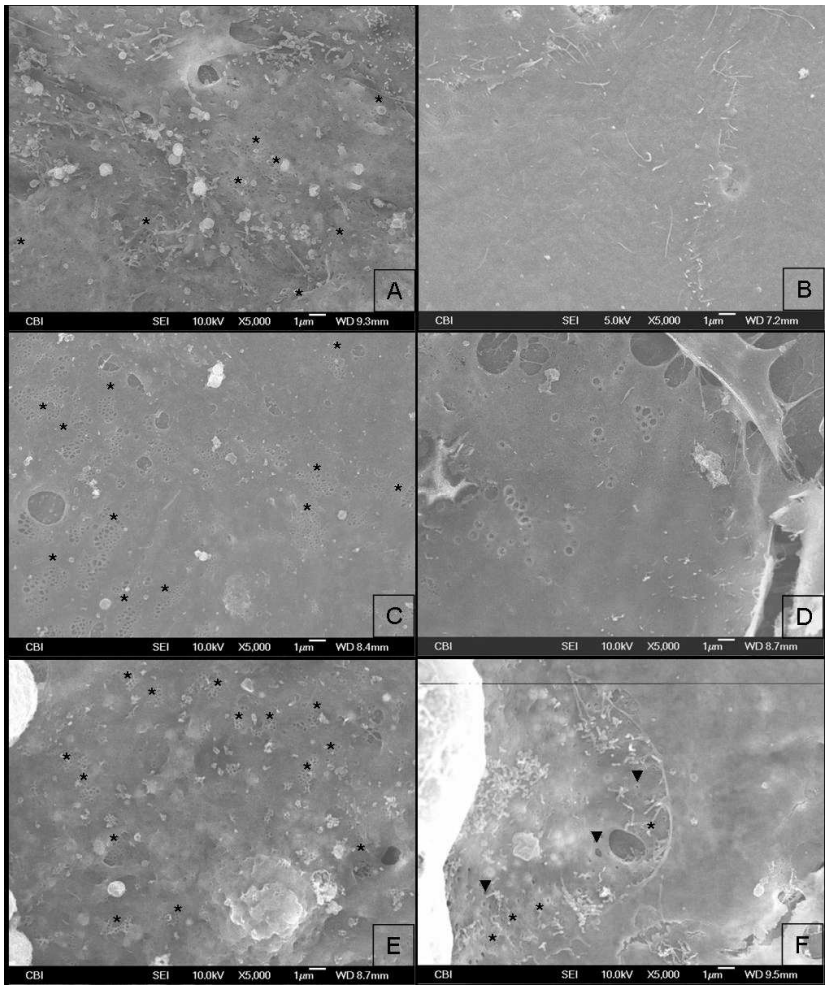

Figure 49. SEM of SEC co-cultured with hepatocytes on SIS-ECM at (A) day one and (B) day seven. SEM of SEC and hepatocytes on UBM-ECM at (C) day one and at (D) day seven. SEM of SEC and hepatocytes on LECM at (E) day one and (F) day seven (5000x). Arrows indicate cell boundaries, ▼ indicate representative fenestrations, and * indicate representative sieve plates.

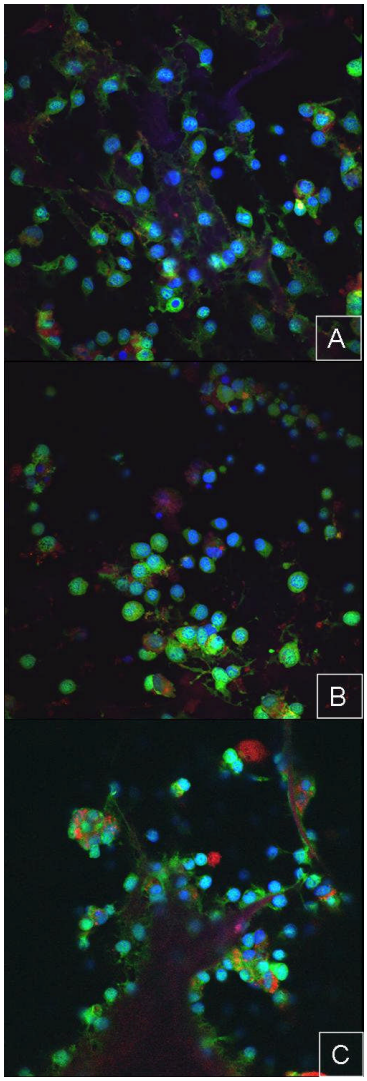

Figure 50. Expression of SE-1 at day one. Confocal microscopy images of SEC cultured on (A) SIS-ECM, (B) UBM-ECM, and (C) LECM at day one (400x). Red indicates expression of SE-1, green indicates green fluorescent protein (GFP), and blue indicates nuclear stain. Yellow is co-localization of red and green. Purple results from the autofluorescence of the ECM scaffold.

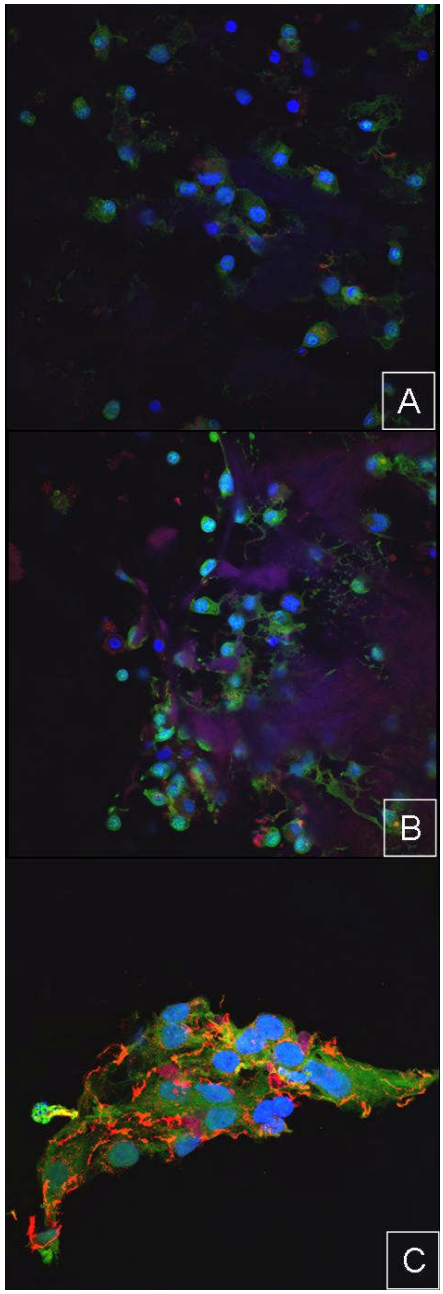

Figure 51. Expression of SE-1 at day three. Confocal microscopy images of SEC cultured on (A) SIS-ECM (400x), (B) UBM-ECM (400x) and (C) LECM (600x) scaffolds at day three. Red indicates expression of SE-1, green indicates expression of GFP, and blue indicates nuclear stain. Yellow is co-localization of red and green.

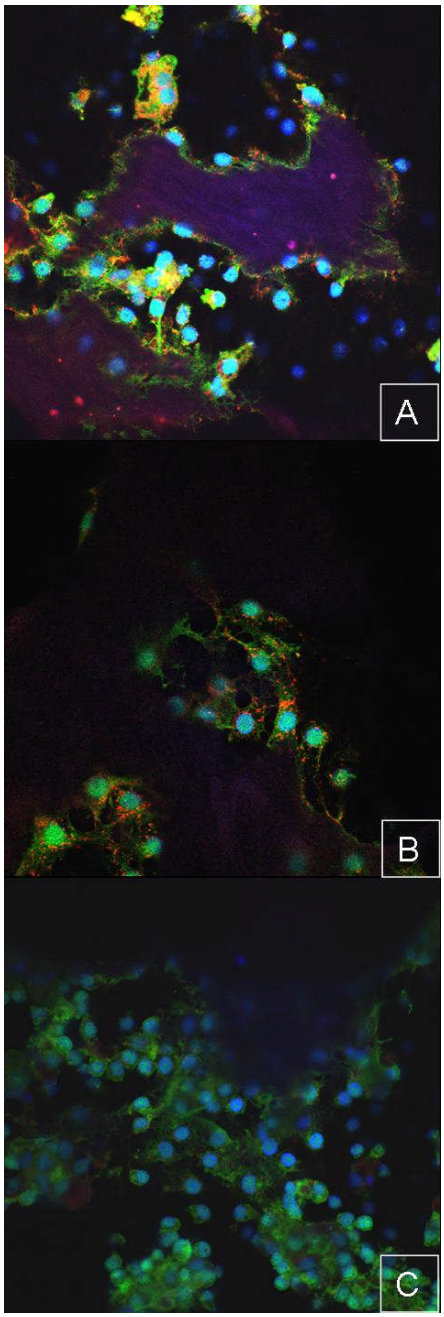

Figure 52. Expression of CD31 at day one. Confocal microscopy images of SEC cultured on (A) SIS-ECM, (B) UBM-ECM and (C) LECM at day one (400x). Red indicates expression of CD-31, green indicates expression of GFP, and blue indicates nuclear stain. Yellow is co-localization of red and green.

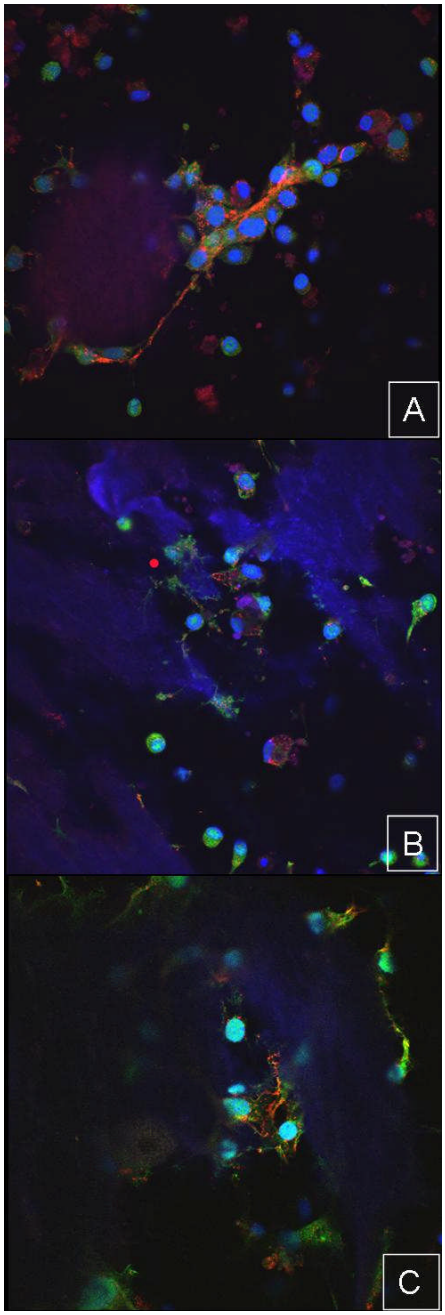

Figure 53. Expression of CD31 at day three. Confocal microscopy images of SEC cultured on (A) SIS-ECM, (B) UBM-ECM, and (C) LECM at day three (400x). Red indicates expression of CD-31, green indicates expression of GFP, and blue indicates nuclear stain. Yellow is co-localization of red and green.

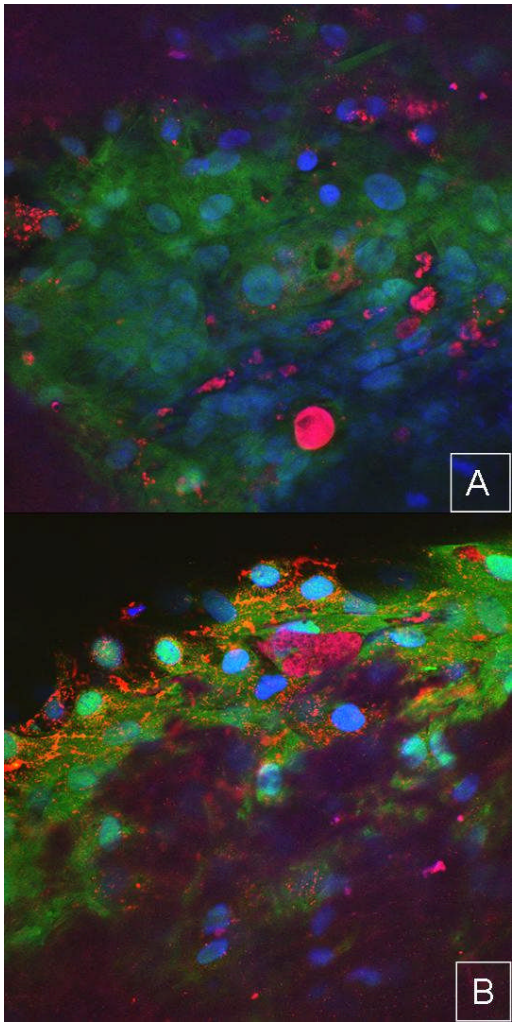

Figure 54. Expression of SE-1 and CD31 at day seven. Confocal microscopy images of SEC cultured on LECM scaffolds expressing (A) SE-1 and (B) CD31 at day 7 (600x). Red indicates expression of (A) SE-1 or (B) CD31, green indicates expression of GFP, and blue indicates nuclear stain. Yellow is co-localization of red and green.

APPENDIX B

DECELLULARIZATION OF WHOLE ORGAN SCAFFOLDS

B.1 INTRODUCTION

Tissue engineering and regenerative medicine efforts to reconstruct functional tissue have been limited to skin, lower urinary tract, and musculoskeletal tissues. More complex organs such as the heart, kidney, liver, and pancreas have had limited success due to the inability of existing substrate materials to support proliferation and differentiation of specialized cells such as cardiomyocyte, hepatocytes, pancreatic exocrine and endocrine cells, and the various ductular epithelial cells of the kidney.

Tissue-specific extracellular matrix (ECM) biological scaffolds have been shown to support the viability of functional, differentiated hepatocyte *in* vitro [28, 148]. In these studies, the ECM scaffolds used were limited to a two-dimensional form and the native liver architecture and vasculature was not preserved. Use of an intact, whole organ ECM, which maintains the three-dimensionality of the native liver, could provide a more optimal hepatocyte culture environment compared to hepatocytes cultured on the sheet or gel form of LECM.

The objective of the present study was to isolate a three-dimensional form of liver ECM and to evaluate the ability of the intact, three-dimensional form to maintain primary hepatocyte-

specific functions *in vitro*. The project is predicated upon the hypothesis that the scaffold or substrate upon which primary human hepatocytes are seeded is a critical determinant of cell phenotype and function.

B.2 METHODS

B.2.1 Development of Whole Organ Perfusion Bioreactor

In this closed looped system, a peristaltic pump transports the perfusate from the media reservoir into the intact rat liver at a rate of 20 ml/min (Figure 55).

B.2.2 Decellularization of Whole Intact Rat Liver

Adult Sprague-Dawley rats were used for isolation of hepatocytes and weighed approximately 200 g at time of sacrifice. The procedures were approved by the Institutional Animal Care and Use Committee at the University of Pittsburgh and were conducted in accordance with the guidelines of the National Institutes of Health for the humane care of research animals.

Livers were perfused using a decellularization solution to remove existing cellular components. For delivery of solutions to the rat liver, a catheter was inserted into the inferior vena cava below the liver. The inferior vena cava above the liver was tied off. The rat liver was perfused with deionized water overnight. The solution was changed at least three times. The rat liver was then perfused with a solution containing 0.02% trypsin/0.05% EDTA at 37° C for one

hour. The liver was then perfused with deionized water for 2 hours. Following perfusion with the deionized water, the liver was perfused overnight with sterile PBS. The next day, the liver was perfused with deionized water for 1 hour followed by perfusion with a 3% Triton X-100 for one hour. The liver was then perfused overnight with PBS. The next perfusate contained 4% sodium deoxycholic acid for one hour followed by rinsing in water a minimal of three times. The rat liver was then perfused overnight with PBS followed by perfusion with 0.1% peracetic acid followed for 2 hours. After decellularization, the intact rat liver ECM was perfused with at pH 7.4 overnight (Figure 56A). The phosphate buffered saline solution was changed a minimum of three times. All solutions were sterile filtered with a 0.22 μm filter prior to use.

B.2.3 Hepatocyte Isolation and Culture

Adult Sprague-Dawley rats were used for isolation of hepatocytes and weighed approximately 200 g at time of sacrifice. The procedures were approved by the Institutional Animal Care and Use Committee at the University of Pittsburgh and were conducted in accordance with the guidelines of the National Institutes of Health for the humane care of research animals.

Hepatocytes were isolated by two-stage collagenase perfusion as previously described [144]. After removal of undigested tissues, hepatocytes were separated from NPC by filtration differential centrifugation [145].

Typically, 200 to 300 million hepatocytes were isolated with 85 to 95% viability as assessed by exclusion of trypan blue dye. Hepatocytes were then cultured in hepatocyte growth medium (HGM). Basal HGM (Dulbecco's Modified Eagle Medium (DMEM) medium, HEPES, glutamine, and antibiotics (Gibco; Carlsbad, CA) supplemented with bovine albumin (2.0 g/L),

glucose (2.25 g/L), galactose (2.0 g/L), ornithine (0.1 g/L), proline (0.030 g/L), nicotinamide (0.305 g/L), $ZnCl_2$ (0.544 g/L), $ZnSO_4$:$7H_20$ (0.750 g/L), $CuSO_4$:$5H_20$ (0.20 g/L), $MnSO_4$ (0.025 g/L), glutamine (5 mmol/L), and dexamethasome (10^{-7} mol/L) (Sigma Chemical Company; St. Louis, MO) was mixed and sterile filtered through a 0.22 μm low-protein-binding filter system, stored at 4° C, and used within four weeks. Insulin, transferrin and selenium were added to the basal HGM just before use, for a final concentration of 5 μg/ml Insulin, 5 ng/ml transferrin, and 5 ng/ml selenium [147].

Hepatocytes were injected into the perfusion system for delivery to the acellular rat liver by 22-gauge syringe with a flow rate of 2 ml/min. Approximately 140 million hepatocytes were perfused into the rat liver and were cultured for 72 hours (Figure 56B).

B.2.4 Hematoxylin and Eosin Staining

Hematoxylin and eosin staining was performed on native rat liver and acellular, intact rat liver.

B.2.5 Scanning Electron Microscopy

Samples were fixed overnight with 2.5% glutaraldehyde in phosphate buffered saline (PBS). After three PBS washes, tissue was dehydrated through a graded series of ethanol washes followed by critical point drying using an Emscope CPD 750. Samples were sputter coated with a 7-nm layer of gold-palladium (Cressington 108 sputter coater) and visualized at a voltage of 12 kV using a JEM 6335F field emission gun SEM (JEOL, Peabody, MA).

For each experimental group, three samples were examined. Cells were randomly selected for imaging by starting at a preselected point in the lower left quadrant of the 1 cm^2 sample and moving to subsequent preselected areas in a clockwise manner taking approximately 12 photomicrographs for each sample. Representative images were selected for inclusion in this report.

B.2.6 Immunofluorescence

Hepatocytes cultured within intact LECM were fixed in 2% paraformaldehyde in PBS at room temperature for 10 minutes. Fixed samples were washed three times in PBS and permeabilized in 0.1% Triton-X for 20 minutes at room temperature. Following cell permeabilization, samples were washed three times PBS and then were incubated for 1 hr at room temperature with rhodamine phalloidin (F-actin) (1:250 in 0.5% BSA; Molecular Probes, Carlsbad, CA). Samples were washed three times in PBS and then incubated with Hoeschts dye in PBS (bizBenzamide, 1 mg/mL in PBS) for 30 seconds to stain nuclear DNA. Finally, the samples were washed three times in PBS and stored at 4°C for a maximum of 24 hours before imaging. Experiments were performed in triplicate. Samples were imaged using an inverted Olympus Fluoview 1000 microscope (Olympus). Representative images were selected for inclusion in this report.

B.3 RESULTS

Histological examination of native rat liver showed typical morphology of native rat liver (Figure 57A). Hematoxylin and eosin staining of acellular rat liver ECM confirmed the absence of intact cellular components (Figure 57B). Histological examination of intact, rat liver ECM seeded with rat hepatocytes showed the presences of hepatocytes (Figure 57C).

SEM images of native rat liver revealed a fibrous structure interspersed with cell (Figure 58A). SEM images of acellular whole organ rat liver ECM confirmed the absence of cells and revealed a fibrous structure similar to native liver tissue ultrastructure (Figure 58B). SEM images of whole organ rat liver ECM seeded with rat hepatocytes revealed the presence of hepatocytes cultured within the ECM (Figure 58C).

Factin and nuclear staining revealed that the hepatocytes remained within the vasculature of the decellularized, whole organ rat liver ECM. (Figure 59).

B.4 SUMMARY

Preliminary results show that whole rat liver decellularization can be achieved and that three-dimensional rat liver ECM is an extremely complex scaffold that is similar to that of the native hepatic architecture.

A common regenerative medicine strategy for tissue and organ reconstruction involves the seeding of a scaffold with cells harvested from the tissues or organs of interest, followed by eventual placement of the cell-scaffold combination to the intended *in vivo* location. Isolation of an acellular, three-dimensional form of liver ECM that could be reseeded with allogeneic cells

and implanted into a patient would represent a major advancement in tissue engineering and regenerative medicine.

B.5 FUTURE DIRECTIONS

Hepatocyte functionality will be evaluated by measurement of albumin secretion, ammonia and urea metabolism, CYP450 3A4 and CYP1A1/1A2 inducibility and activity, bile salt export pump activity (BSEP) and expression of connexin 32. The following mRNA levels will be measured: cyclophilin, albumin, CYP3A4, CYP1A1, CYP1A2, and connexin 32, BSEP and NTCP. All data will be normalized to total DNA content. Hepatocytes will be cultured for at least one week.

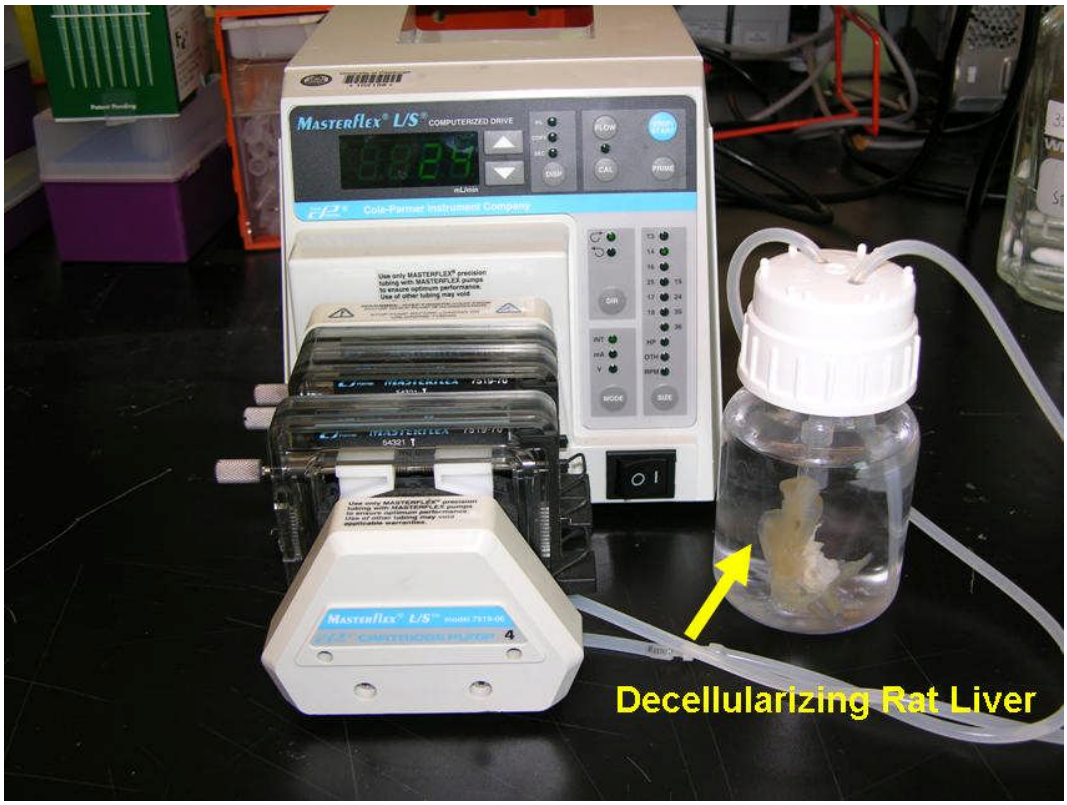

Figure 55. Schematic of perfusion bioreactor.

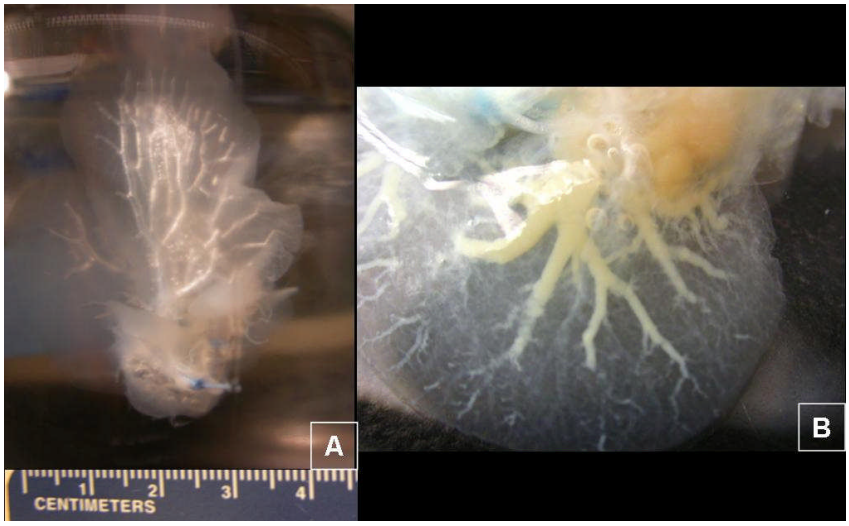

Figure 56. (A) Image of acellular, intact rat liver ECM. (B) Image of intact rat liver ECM seeded with rat hepatocytes.

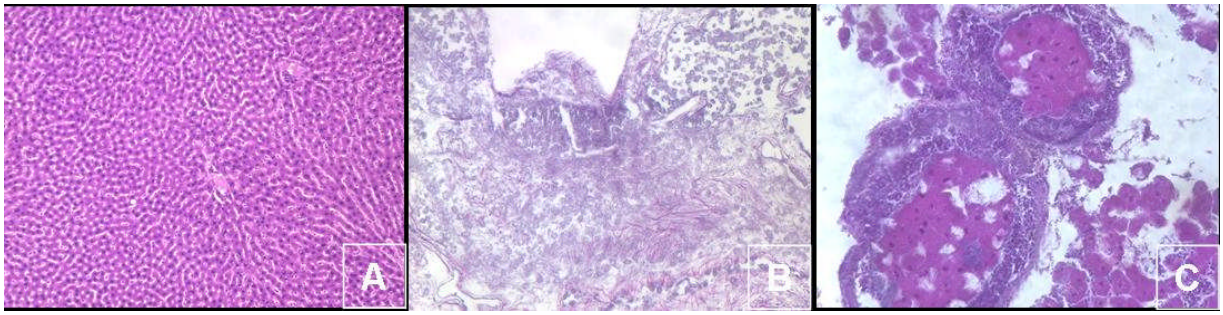

Figure 57. Hematoxylin and eosin staining of (A) native rat liver (200x), (B) acellular, intact rat liver ECM (200x), and (C) intact rat liver ECM seeded with rat hepatocytes (400x).

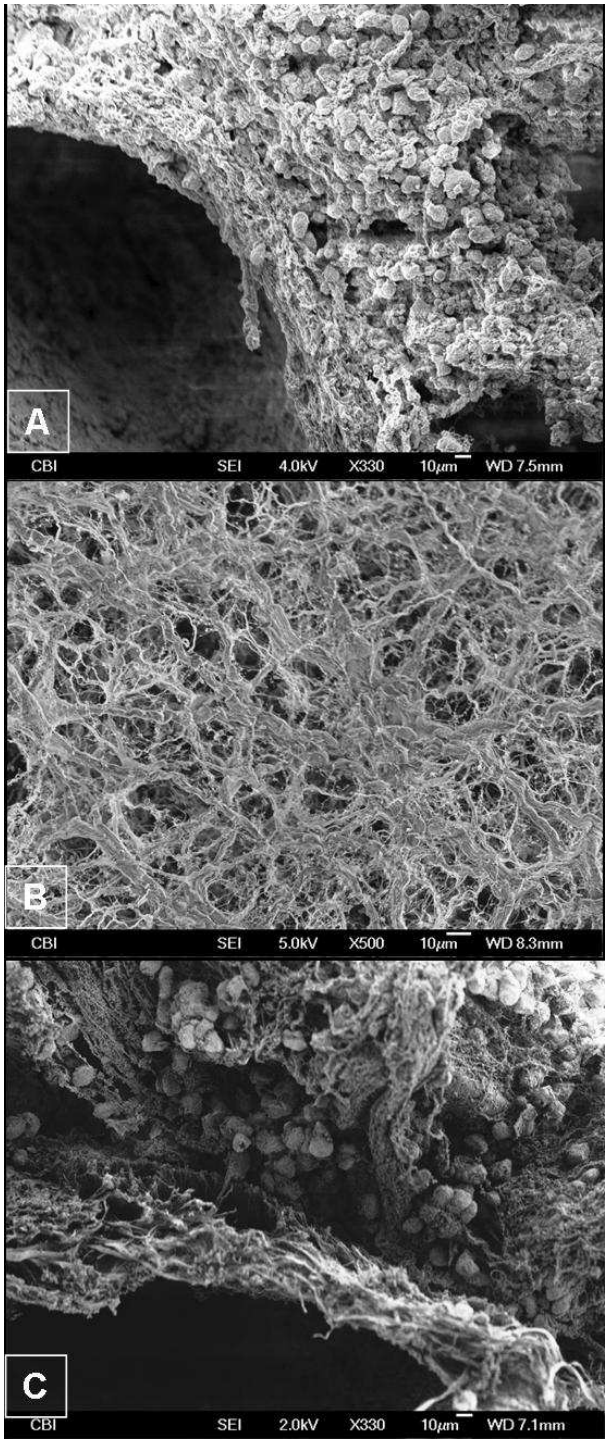

Figure 58. Scanning electron micrograph of (A) native rat liver (330x), (B) acellular rat liver ECM (500x), (C) intact rat liver ECM seeded with rat hepatocytes (330x).

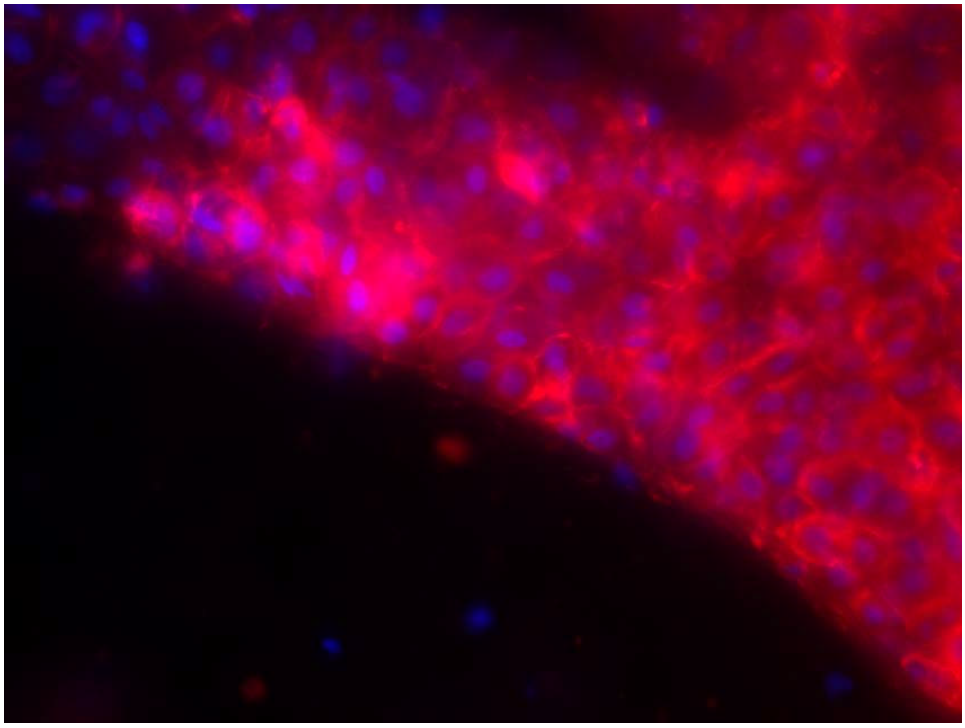

Figure 59. F-actin localization (red) and nuclear staining (blue) of rat hepatocytes seeded within whole organ rat liver ECM.

BIBLIOGRAPHY

1. Blouin, A., R.P. Bolender, and E.R. Weibel, Distribution of organelles and membranes between hepatocytes and nonhepatocytes in the rat liver parenchyma. A stereological study. J Cell Biol, 1977. **72**(2): p. 441-55.

2. Saxena R, Zucker SD, and C. JM, in *The Liver*, Z. D and B. T, Editors. 2002, WB Saunders: Philadelphia. p. 1-30.

3. Martinez-Hernandez, A. and P.S. Amenta, *The hepatic extracellular matrix. I. Components and distribution in normal liver.* Virchows Arch A Pathol Anat Histopathol, 1993. **423**(1): p. 1-11.

4. *Center for Disease Control*, C.F.D. Control, Editor: Atlanta, GA.

5. [cited; Available from: http://www.optn.org/data/.

6. Shakil, A.O., et al., Acute liver failure: clinical features, outcome analysis, and applicability of prognostic criteria. Liver Transpl, 2000. **6**(2): p. 163-9.

7. Strom, S.C. and E.C.S. Ellis, *Hepatocyte Transplantation*, in *Principles of Regenerative Medicine*, A. Atala, et al., Editors. 2008, Elsevier: Burlington, MA. p. 912-27.

8. Allen, J.W. and S.N. Bhatia, *Engineering liver therapies for the future.* Tissue Eng, 2002. **8**(5): p. 725-37.

9. Buhler, L., et al., *Xenotransplantation--state of the art--update 1999.* Front Biosci, 1999. **4**: p. D416-32.

10. Fisher, R.A. and S.C. Strom, *Human hepatocyte transplantation: worldwide results.* Transplantation, 2006. **82**(4): p. 441-9.

11. Fox, I.J., et al., *Treatment of the Crigler-Najjar syndrome type I with hepatocyte transplantation.* N Engl J Med, 1998. **338**(20): p. 1422-6.

12. Tsang VL, C.A., Cho LM, Jadin KD, Sah RL, DeLong S, West JL,Bhatia SN, *Fabrication of 3D Hepatic Tissues by Additive Photopatterning of Cellular Hydrogels.* Faseb J, 2007. **21**: p. 790-801.

13. Soto-Gutierrez, A., et al., *Construction and transplantation of an engineered hepatic tissue using a polyaminourethane-coated nonwoven polytetrafluoroethylene fabric.* Transplantation, 2007. **83**(2): p. 129-37.

14. Wang, S., et al., *Three-Dimensional Primary Hepatocyte Culture in Synthetic Self-Assembling Peptide Hydrogel.* Tissue Eng, 2008.

15. Kern, A., et al., *Drug metabolism in hepatocyte sandwich cultures of rats and humans.* Biochem Pharmacol, 1997. **54**(7): p. 761-72.

16. Reid, L.M. and D.M. Jefferson, *Culturing hepatocytes and other differentiated cells.* Hepatology, 1984. **4**(3): p. 548-59.

17. Watt, F.M., *Cell culture models of differentiation.* Faseb J, 1991. **5**(3): p. 287-94.

18. Lauffenburger, D.A. and L.G. Griffith, *Who's got pull around here? Cell organization in development and tissue engineering.* Proc Natl Acad Sci U S A, 2001. **98**(8): p. 4282-4.

19. Huang, H., et al., *Enhanced functional maturation of fetal porcine hepatocytes in three-dimensional poly-L-lactic acid scaffolds: a culture condition suitable for engineered liver tissues in large-scale animal studies.* Cell Transplant, 2006. **15**(8-9): p. 799-809.

20. Ranucci, C.S. and P.V. Moghe, *Polymer substrate topography actively regulates the multicellular organization and liver-specific functions of cultured hepatocytes.* Tissue Eng, 1999. **5**(5): p. 407-20.

21. Underhill, G.H., et al., *Assessment of hepatocellular function within PEG hydrogels.* Biomaterials, 2007. **28**(2): p. 256-70.

22. Kim, I.Y., et al., *Chitosan and its derivatives for tissue engineering applications.* Biotechnol Adv, 2008. **26**(1): p. 1-21.

23. Seo, S.J., et al., *Alginate/galactosylated chitosan/heparin scaffold as a new synthetic extracellular matrix for hepatocytes.* Tissue Eng, 2006. **12**(1): p. 33-44.

24. Cheng, N., E. Wauthier, and L.M. Reid, *Mature Human Hepatocytes from Ex Vivo Differentiation of Alginate-Encapsulated Hepatoblasts.* Tissue Eng, 2007.

25. Dvir-Ginzberg, M., et al., *Liver tissue engineering within alginate scaffolds: effects of cell-seeding density on hepatocyte viability, morphology, and function.* Tissue Eng, 2003. **9**(4): p. 757-66.

26. Gross-Steinmeyer, K., et al., *Influence of Matrigel-overlay on constitutive and inducible expression of nine genes encoding drug-metabolizing enzymes in primary human hepatocytes.* Xenobiotica, 2005. **35**(5): p. 419-38.

27. Rojkind, M., et al., *Connective tissue biomatrix: its isolation and utilization for long-term cultures of normal rat hepatocytes.* J Cell Biol, 1980. **87**(1): p. 255-63.

28. Lin, P., et al., *Assessing porcine liver-derived biomatrix for hepatic tissue engineering.* Tissue Eng, 2004. **10**(7-8): p. 1046-53.

29. Mirsadraee, S., et al., *Development and characterization of an acellular human pericardial matrix for tissue engineering.* Tissue Eng, 2006. **12**(4): p. 763-73.

30. Jang, Y.J., et al., *Tutoplast-processed fascia lata for dorsal augmentation in rhinoplasty.* Otolaryngol Head Neck Surg, 2007. **137**(1): p. 88-92.

31. Misra, S., et al., *Results of AlloDerm use in abdominal hernia repair.* Hernia, 2008.

32. Badylak, S.F., *Xenogeneic extracellular matrix as a scaffold for tissue reconstruction.* Transpl Immunol, 2004. **12**(3-4): p. 367-77.

33. Badylak, S.F., *The extracellular matrix as a scaffold for tissue reconstruction.* Semin Cell Dev Biol, 2002. **13**(5): p. 377-83.

34. Sellaro, T.L., et al., *Maintenance of hepatic sinusoidal endothelial cell phenotype in vitro using organ-specific extracellular matrix scaffolds.* Tissue Eng, 2007. **13**(9): p. 2301-10.

35. Zeisberg, M., et al., *De-differentiation of primary human hepatocytes depends on the composition of specialized liver basement membrane.* Mol Cell Biochem, 2006. **283**(1-2): p. 181-9.

36. Lindberg, K. and S.F. Badylak, *Porcine small intestinal submucosa (SIS): a bioscaffold supporting in vitro primary human epidermal cell differentiation and synthesis of basement membrane proteins.* Burns, 2001. **27**(3): p. 254-66.

37. Reid, L.M., et al., Long-term cultures of normal rat hepatocytes on liver biomatrix. Ann N Y Acad Sci, 1980. **349**: p. 70-6.

38. Zhang, Y., et al., *Coculture of bladder urothelial and smooth muscle cells on small intestinal submucosa: potential applications for tissue engineering technology.* J Urol, 2000. **164**(3 Pt 2): p. 928-34; discussion 934-5.

39. Voytik-Harbin, S.L., et al., *Identification of extractable growth factors from small intestinal submucosa.* J Cell Biochem, 1997. **67**(4): p. 478-91.

40. Woods, E.J., et al., *Improved in vitro function of islets using small intestinal submucosa.* Transplant Proc, 2004. **36**(4): p. 1175-7.

41. Streuli, C., *Extracellular matrix remodelling and cellular differentiation.* Curr Opin Cell Biol, 1999. **11**(5): p. 634-40.

42. Aumailley, M. and B. Gayraud, *Structure and biological activity of the extracellular matrix.* J Mol Med, 1998. **76**(3-4): p. 253-65.

43. Wood, r., *Evidence of species differences in the ultrastructure of the hepatic sinusoid.* Z Zellforsch Mikrosk Anat, 1963. **58**: p. 679-92.

44. Brown, B., et al., *The basement membrane component of biologic scaffolds derived from extracellular matrix.* Tissue Eng, 2006. **12**(3): p. 519-26.

45. Sacks, M.S., D.B. Smith, and E.D. Hiester, *A small angle light scattering device for planar connective tissue microstructural analysis.* Ann Biomed Eng, 1997. **25**(4): p. 678-89.

46. Badylak, S.F., et al., *The use of xenogeneic small intestinal submucosa as a biomaterial for Achilles tendon repair in a dog model.* J Biomed Mater Res, 1995. **29**(8): p. 977-85.

47. Hodde, J.P., et al., *Glycosaminoglycan content of small intestinal submucosa: A bioscaffold for tissue replacement.* Tissue Eng, 1996. **2**: p. 209-217.

48. Cahir A. McDevitt, G.M.W.R.M.C., *Transforming growth factor-?1 in a sterilized tissue derived from the pig small intestine submucosa.* Journal of Biomedical Materials Research Part A, 2003. **67A**(2): p. 637-640.

49. Hodde, J.P., D.M. Ernst, and M.C. Hiles, *An investigation of the long-term bioactivity of endogenous growth factor in OASIS Wound Matrix.* J Wound Care, 2005. **14**(1): p. 23-5.

50. Schuppan, D., et al., *Matrix as a modulator of hepatic fibrogenesis.* Semin Liver Dis, 2001. **21**(3): p. 351-72.

51. McGuire, R.F., et al., *Role of extracellular matrix in regulating fenestrations of sinusoidal endothelial cells isolated from normal rat liver.* Hepatology, 1992. **15**(6): p. 989-97.

52. Augustin-Voss, H.G., R.C. Johnson, and B.U. Pauli, *Modulation of endothelial cell surface glycoconjugate expression by organ-derived biomatrices.* Exp Cell Res, 1991. **192**(2): p. 346-51.

53. Bissell, D.M., et al., *Support of cultured hepatocytes by a laminin-rich gel. Evidence for a functionally significant subendothelial matrix in normal rat liver.* J Clin Invest, 1987. **79**(3): p. 801-12.

54. Lin, C.Q. and M.J. Bissell, *Multi-faceted regulation of cell differentiation by extracellular matrix.* Faseb J, 1993. **7**(9): p. 737-43.

55. Bhatia, S.N., et al., *Effect of cell-cell interactions in preservation of cellular phenotype: cocultivation of hepatocytes and nonparenchymal cells.* FASEB J, 1999. **13**(14): p. 1883-900.

56. Michalopoulos, G., et al., *Mutagenesis induced by procarcinogens at the hypoxanthine-guanine phosphoribosyl transferase locus of human fibroblasts cocultured with rat hepatocytes.* Cancer Res, 1981. **41**(5): p. 1873-8.

57. Strom, S., A.D. Kligerman, and G. Michalopoulos, *Comparisons of the effects of chemical carcinogens in mixed cultures of rat hepatocytes and human fibroblasts.* Carcinogenesis, 1981. **2**(8): p. 709-15.

58. Utesch, D., et al., *Differential stabilization of cytochrome P-450 isoenzymes in primary cultures of adult rat liver parenchymal cells.* In Vitro Cell Dev Biol, 1991. **27A**(11): p. 858-63.

59. Morin, O. and C. Normand, *Long-term maintenance of hepatocyte functional activity in co-culture: requirements for sinusoidal endothelial cells and dexamethasone.* J Cell Physiol, 1986. **129**(1): p. 103-10.

60. Goulet, F., C. Normand, and O. Morin, *Cellular interactions promote tissue-specific function, biomatrix deposition and junctional communication of primary cultured hepatocytes.* Hepatology, 1988. **8**(5): p. 1010-8.

61. Fry, J.R. and J.W. Bridges, *A novel mixed hepatocyte-fibroblast culture system and its use as a test for metabolism-mediated cytotoxicity.* Biochem Pharmacol, 1977. **26**(10): p. 969-73.

62. Donato, M.T., J.V. Castell, and M.J. Gomez-Lechon, *Co-cultures of hepatocytes with epithelial-like cell lines: expression of drug-biotransformation activities by hepatocytes.* Cell Biol Toxicol, 1991. **7**(1): p. 1-14.

63. Michalopoulos, G., F. Russell, and C. Biles, *Primary cultures of hepatocytes on human fibroblasts.* In Vitro, 1979. **15**(10): p. 796-806.

64. Mendoza-Figueroa, T., et al., *Intracytoplasmic triglyceride accumulation produced by dexamethasone in adult rat hepatocytes cultivated on 3T3 cells.* Toxicology, 1988. **52**(3): p. 273-86.

65. Michalopoulos, G., et al., *Interaction of chemical carcinogens and drug-metabolizing enzymes in primary cultures of hepatic cells from the rat.* Am J Pathol, 1976. **85**(3): p. 755-72.

66. Hamilton, G.A., et al., *Regulation of cell morphology and cytochrome P450 expression in human hepatocytes by extracellular matrix and cell-cell interactions.* Cell Tissue Res, 2001. **306**(1): p. 85-99.

67. Bissell, D.M., *Cell-matrix interaction and hepatic fibrosis.* Prog Liver Dis, 1990. **9**: p. 143-55.

68. Caron, J.M., *Induction of albumin gene transcription in hepatocytes by extracellular matrix proteins.* Mol Cell Biol, 1990. **10**(3): p. 1239-43.

69. Moghe, P.V., et al., *Culture matrix configuration and composition in the maintenance of hepatocyte polarity and function.* Biomaterials, 1996. **17**(3): p. 373-85.

70. Luttringer, O., et al., *Influence of isolation procedure, extracellular matrix and dexamethasone on the regulation of membrane transporters gene expression in rat hepatocytes.* Biochem Pharmacol, 2002. **64**(11): p. 1637-50.

71. Schuetz, E.G., et al., *Regulation of gene expression in adult rat hepatocytes cultured on a basement membrane matrix.* J Cell Physiol, 1988. **134**(3): p. 309-23.

72. LeCluyse, E.L., et al., *Regeneration and maintenance of bile canalicular networks in collagen-sandwiched hepatocytes.* Toxicol In Vitro, 2000. **14**(2): p. 117-32.

73. Dunn, J.C., R.G. Tompkins, and M.L. Yarmush, *Long-term in vitro function of adult hepatocytes in a collagen sandwich configuration.* Biotechnol Prog, 1991. **7**(3): p. 237-45.

74. LeCluyse, E.L., K.L. Audus, and J.H. Hochman, *Formation of extensive canalicular networks by rat hepatocytes cultured in collagen-sandwich configuration.* Am J Physiol, 1994. **266**(6 Pt 1): p. C1764-74.

75. Silva, J.M., et al., *Refinement of an in vitro cell model for cytochrome P450 induction.* Drug Metab Dispos, 1998. **26**(5): p. 490-6.

76. Sidhu, J.S., F.M. Farin, and C.J. Omiecinski, *Influence of extracellular matrix overlay on phenobarbital-mediated induction of CYP2B1, 2B2, and 3A1 genes in primary adult rat hepatocyte culture.* Arch Biochem Biophys, 1993. **301**(1): p. 103-13.

77. Dvorak, Z., et al., *Colchicine down-regulates cytochrome P450 2B6, 2C8, 2C9, and 3A4 in human hepatocytes by affecting their glucocorticoid receptor-mediated regulation.* Mol Pharmacol, 2003. **64**(1): p. 160-9.

78. Page, J.L., et al., *Gene expression profiling of extracellular matrix as an effector of human hepatocyte phenotype in primary cell culture.* Toxicol Sci, 2007. **97**(2): p. 384-97.

79. Michalopoulos, G.K. and M.C. DeFrances, *Liver regeneration.* Science, 1997. **276**(5309): p. 60-6.

80. Chenard-Neu, M.P., et al., *Auxiliary liver transplantation: regeneration of the native liver and outcome in 30 patients with fulminant hepatic failure--a multicenter European study.* Hepatology, 1996. **23**(5): p. 1119-27.

81. Association, J.o.A.M., *Hepatology: A Textbook of Liver Disease* ed. Iber. Vol. 1 & 2. 2003.

82. Dunn, J.C., et al., *Hepatocyte function and extracellular matrix geometry: long-term culture in a sandwich configuration.* Faseb J, 1989. **3**(2): p. 174-7.

83. Berry, M., *The Hepatocyte Review*. 2000, Boston, London: Kluwer Academic Publishers. 365.

84. Jauregui, H.O., et al., *Attachment and long term survival of adult rat hepatocytes in primary monolayer cultures: comparison of different substrata and tissue culture media formulations.* In Vitro Cell Dev Biol, 1986. **22**(1): p. 13-22.

85. Smith, D.A., *Species differences in metabolism and pharmacokinetics: are we close to an understanding?* Drug Metab Rev, 1991. **23**(3-4): p. 355-73.

86. Jasmund, I., et al., *The influence of medium composition and matrix on long-term cultivation of primary porcine and human hepatocytes.* Biomol Eng, 2007. **24**(1): p. 59-69.

87. Chandra, P., E.L. Lecluyse, and K.L. Brouwer, *Optimization of culture conditions for determining hepatobiliary disposition of taurocholate in sandwich-cultured rat hepatocytes.* In Vitro Cell Dev Biol Anim, 2001. **37**(6): p. 380-5.

88. Stamatoglou, S.C. and R.C. Hughes, *Cell adhesion molecules in liver function and pattern formation.* Faseb J, 1994. **8**(6): p. 420-7.

89. Ben-Ze'ev, A., et al., *Cell-cell and cell-matrix interactions differentially regulate the expression of hepatic and cytoskeletal genes in primary cultures of rat hepatocytes.* Proc Natl Acad Sci U S A, 1988. **85**(7): p. 2161-5.

90. Bader, A., et al., *Use of organotypical cultures of primary hepatocytes to analyse drug biotransformation in man and animals.* Xenobiotica, 1994. **24**(7): p. 623-33.

91. Koebe, H.G., et al., *Collagen gel immobilisation provides a suitable cell matrix for long term human hepatocyte cultures in hybrid reactors.* Int J Artif Organs, 1994. **17**(2): p. 95-106.

92. Tchen R, T.J., Sellaro TL, Jiang H, Badylak SF,Ogilvie JB. *Decellularization of Pancreatic Extracellular Matrix for the Development of a Tissue-Engineered Artificial Pancreas*. in *TERMIS NA 2007 Conference and Exposition*. 2007. Toronto, Canada.

93. Liu Y, et al., *A new tracheal bioartificial organ: evaluation of a tracheal allograft with minimal antigenicity after treatment by detergent.*Asaio 2000. **46**(5): p. 536-539.

94. Jiang H, et al. *Tissue Engineered Adrenal Glands Functions In Vitro.* . in *Tissue Engineering and Regenerative Medicine International Society 2007 Conference and Exposition*. 2007. Toronto, Canada.

95. Wilshaw, S.P., et al., *Production of an acellular amniotic membrane matrix for use in tissue engineering.* Tissue Eng, 2006. **12**(8): p. 2117-29.

96. Hudson, T.W., S.Y. Liu, and C.E. Schmidt, *Engineering an improved acellular nerve graft via optimized chemical processing.* Tissue Eng, 2004. **10**(9-10): p. 1346-58.

97. O'Connor, R.C., R.V. Patel, and G.D. Steinberg, *Successful repair of a ureteroneobladder stricture using porcine small intestine submucosa.* J Urol, 2001. **165**(6 Pt 1): p. 1995.

98. Cartwright, L.M., et al., *Porcine bladder acellular matrix porosity: impact of hyaluronic acid and lyophilization.* J Biomed Mater Res A, 2006. **77**(1): p. 180-4.

99. Freytes, D.O., et al., *Preparation and rheological characterization of a gel form of the porcine urinary bladder matrix.* Biomaterials, 2008.

100. Urita, Y., et al., *Regeneration of the esophagus using gastric acellular matrix: an experimental study in a rat model.* Pediatr Surg Int, 2007. **23**(1): p. 21-6.

101. Ott, H.C., et al., *Perfusion-decellularized matrix: using nature's platform to engineer a bioartificial heart.* Nat Med, 2008. **14**(2): p. 213-21.

102. Badylak, S.F., et al., *Small intestinal submucosa as a large diameter vascular graft in the dog.* J Surg Res, 1989. **47**: p. 74.

103. Wainwright, J., et al. *Whole Organ Decellularization for Creation of a 3D Scaffold for Cell Seeding*. in *5th Symposium on the Use of Biologic Scaffolds for Regenerative Medicine*. 2008. Phoenix, AZ.

104. Gilbert, T.W., T.L. Sellaro, and S.F. Badylak, *Decellularization of tissues and organs.* Biomaterials, 2006. **27**(19): p. 3675-83.

105. Brown, S.A., et al., *Effects of different disinfection and sterilization methods on tensile strength of materials used for single-use devices.* Biomed Instrum Technol, 2002. **36**(1): p. 23-7.

106. Strom, S.C., et al., *Use of human hepatocytes to study P450 gene induction.* Methods Enzymol, 1996. **272**: p. 388-401.

107. Kostrubsky, V.E., et al., *The use of human hepatocyte cultures to study the induction of cytochrome P-450.* Drug Metab Dispos, 1999. **27**(8): p. 887-94.

108. Krovat, B.C., J.H. Tracy, and C.J. Omiecinski, *Fingerprinting of cytochrome P450 and microsomal epoxide hydrolase gene expression in human blood cells.* Toxicol Sci, 2000. **55**(2): p. 352-60.

109. Gibson, G.G., et al., *Receptor-dependent transcriptional activation of cytochrome P4503A genes: induction mechanisms, species differences and interindividual variation in man.* Xenobiotica, 2002. **32**(3): p. 165-206.

110. Xu, L., et al., *2,3,7,8 Tetrachlorodibenzo-p-dioxin induction of cytochrome P4501A in cultured rat and human hepatocytes.* Chem Biol Interact, 2000. **124**(3): p. 173-89.

111. *The Organ Procurement and Transplantation Network*. 2008 [cited; Available from: http://www.optn.org/latestData/rptData.asp.

112. Fiegel, H.C., et al., *Review: Hepatic Tissue Engineering.* J Cell Mol Med, 2007.

113. Borenstein, J.T., et al., *Microfabrication of three-dimensional engineered scaffolds.* Tissue Eng, 2007. **13**(8): p. 1837-44.

114. Ohashi, K., et al., *Engineering functional two- and three-dimensional liver systems in vivo using hepatic tissue sheets.* Nat Med, 2007. **13**(7): p. 880-5.

115. LeCluyse, E., et al., *Expression and regulation of cytochrome P450 enzymes in primary cultures of human hepatocytes.* J Biochem Mol Toxicol, 2000. **14**(4): p. 177-88.

116. Kostrubsky, V.E., et al., *Evaluation of hepatotoxic potential of drugs by inhibition of bile-acid transport in cultured primary human hepatocytes and intact rats.* Toxicol Sci, 2003. **76**(1): p. 220-8.

117. Cepko, C.L., *The roles of intrinsic and extrinsic cues and bHLH genes in the determination of retinal cell fates.* Curr Opin Neurobiol, 1999. **9**(1): p. 37-46.

118. Jadhav, A.P., H.A. Mason, and C.L. Cepko, *Notch 1 inhibits photoreceptor production in the developing mammalian retina.* Development, 2006. **133**(5): p. 913-23.

119. Kleinman, H.K., et al., *Isolation and characterization of type IV procollagen, laminin, and heparan sulfate proteoglycan from the EHS sarcoma.* Biochemistry, 1982. **21**(24): p. 6188-93.

120. Futaki, S., et al., *Molecular basis of constitutive production of basement membrane components. Gene expression profiles of Engelbreth-Holm-Swarm tumor and F9 embryonal carcinoma cells.* J Biol Chem, 2003. **278**(50): p. 50691-701.

121. Couchman, J.R., et al., *Perlecan and basement membrane-chondroitin sulfate proteoglycan (bamacan) are two basement membrane chondroitin/dermatan sulfate proteoglycans in the Engelbreth-Holm-Swarm tumor matrix.* J Biol Chem, 1996. **271**(16): p. 9595-602.

122. Kato, S., et al., *Concurrent changes in sinusoidal expression of laminin and affinity of hepatocytes to laminin during rat liver regeneration.* Exp Cell Res, 1992. **198**(1): p. 59-68.

123. Reid, L.M., et al., *Extracellular matrix gradients in the space of Disse: relevance to liver biology.* Hepatology, 1992. **15**(6): p. 1198-203.

124. Hubbell, J.A., *Materials as morphogenetic guides in tissue engineering.* Curr Opin Biotechnol, 2003. **14**(5): p. 551-8.

125. Dow, J.A., et al., *Novel methods for the guidance and monitoring of single cells and simple networks in culture.* J Cell Sci Suppl, 1987. **8**: p. 55-79.

126. Clark, P., et al., *Topographical control of cell behaviour: II. Multiple grooved substrata.* Development, 1990. **108**(4): p. 635-44.

127. Clark, P., et al., *Topographical control of cell behaviour. I. Simple step cues.* Development, 1987. **99**(3): p. 439-48.

128. den Braber, E.T., et al., *Quantitative analysis of cell proliferation and orientation on substrata with uniform parallel surface micro-grooves.* Biomaterials, 1996. **17**(11): p. 1093-9.

129. Chehroudi, B., et al., *Computer-assisted three-dimensional reconstruction of epithelial cells attached to percutaneous implants.* J Biomed Mater Res, 1995. **29**(3): p. 371-9.

130. Zeltinger, J., et al., *Effect of pore size and void fraction on cellular adhesion, proliferation, and matrix deposition.* Tissue Eng, 2001. **7**(5): p. 557-72.

131. Brown, B.N., et al. *Surface Characterization of Biologic Scaffolds Composed of Extracellular Matrix* in *The Annual Hilton Head Workshop - Regenerative Medicine: Advancing to Next Generation Therapies.* March 2008. Hilton Head, SC.

132. Turner WS, S.E., McClelland R,, Wauthier E, Chen W, Reid LM, *Human Hepatoblast Phenotype Maintained by Hyaluronan Hydrogels.* Journal of Biomedical Materials Research Part B: Applied Biomaterials, 2006: p. 156-168.

133. Soto-Gutierrez, A., et al., *Differentiation of mouse embryonic stem cells to hepatocyte-like cells by co-culture with human liver nonparenchymal cell lines.* Nat Protoc, 2007. **2**(2): p. 347-56.

134. Cho, C.H., et al., *Homogeneous differentiation of hepatocyte-like cells from embryonic stem cells: applications for the treatment of liver failure.* FASEB J, 2008. **22**(3): p. 898-909.

135. Fox, I.J. and S.C. Strom, *To be or not to be: generation of hepatocytes from cells outside the liver.* Gastroenterology, 2008. **134**(3): p. 878-81.

136. Brill, S., et al., *The role of fetal and adult hepatocyte extracellular matrix in the regulation of tissue-specific gene expression in fetal and adult hepatocytes.* Eur J Cell Biol, 2002. **81**(1): p. 43-50.

137. Ohmura, T., et al., *Establishment of a novel monoclonal antibody, SE-1, which specifically reacts with rat hepatic sinusoidal endothelial cells.* J Histochem Cytochem, 1993. **41**(8): p. 1253-7.

138. Xu, B., et al., *Capillarization of hepatic sinusoid by liver endothelial cell-reactive autoantibodies in patients with cirrhosis and chronic hepatitis.* Am J Pathol, 2003. **163**(4): p. 1275-89.

139. Morita, M., et al., *Analysis of the sinusoidal endothelial cell organization during the developmental stage of the fetal rat liver using a sinusoidal endothelial cell specific antibody, SE-1.* Cell Struct Funct, 1998. **23**(6): p. 341-8.

140. DeLeve, L.D., et al., *Rat liver sinusoidal endothelial cell phenotype is maintained by paracrine and autocrine regulation.* Am J Physiol Gastrointest Liver Physiol, 2004. **287**(4): p. G757-63.

141. Freytes, D.O., et al., *Biaxial strength of multilaminated extracellular matrix scaffolds.* Biomaterials, 2004. **25**(12): p. 2353-61.

142. Badylak, S.F., et al., *Marrow-derived cells populate scaffolds composed of xenogeneic extracellular matrix.* Exp Hematol, 2001. **29**(11): p. 1310-8.

143. Okabe, M., et al., *'Green mice' as a source of ubiquitous green cells.* FEBS Lett, 1997. **407**(3): p. 313-9.

144. Seglen, P.O., *Preparation of isolated rat liver cells.* Methods Cell Biol, 1976. **13**: p. 29-83.

145. Ross, M.A., et al., *Spatiotemporal expression of angiogenesis growth factor receptors during the revascularization of regenerating rat liver.* Hepatology, 2001. **34**(6): p. 1135-48.

146. Stolz, D.B., et al., *Cationic colloidal silica membrane perturbation as a means of examining changes at the sinusoidal surface during liver regeneration.* Am J Pathol, 1999. **155**(5): p. 1487-98.

147. Michalopoulos, G.K., et al., *Hepatocytes undergo phenotypic transformation to biliary epithelium in organoid cultures.* Hepatology, 2002. **36**(2): p. 278-83.

148. Sellaro, T., et al., *Maintainence of Human Hepatocyte-Specific Function In Vitro By Tissue-Specific Extracellular Matrix Biological Scaffolds.* Submitted to Tissue Eng, 2008.